ANL-6928

Argonne National Laboratory

CONSOLIDATION AND FABRICATION TECHNIQUES FOR VANADIUM-20 w/o TITANIUM (TV-20)

by

W. R. Burt, Jr., W. C. Kramer,
R. D. McGowan, F. J. Karasek,
and R. M. Mayfield

LEGAL NOTICE

Printed in USA. Price $3.00. Available from the Clearinghouse for Federal Scientific and Technical Information, National Bureau of Standards, U. S. Department of Commerce, Springfield, Virginia

ANL-6928
Metals, Ceramics,
and Materials
(TID-4500, 41st Ed.)
AEC Research and
Development Report

ARGONNE NATIONAL LABORATORY
9700 South Cass Avenue
Argonne, Illinois 60440

CONSOLIDATION AND FABRICATION TECHNIQUES FOR VANADIUM-20 w/o TITANIUM (TV-20)

by

W. R. Burt, Jr., W. C. Kramer,
R. D. McGowan, F. J. Karasek,
and R. M. Mayfield

February 1965

Metallurgy Division
Program 1.10.6

Portions of the material in this report have appeared in the following Metallurgy Division Annual Report:

ANL-6868 (1963) pp. 92-98

Operated by The University of Chicago
under
Contract W-31-109-eng-38
with the
U. S. Atomic Energy Commission

TABLE OF CONTENTS

TABLE OF CONTENTS

LIST OF FIGURES

LIST OF FIGURES

LIST OF FIGURES

LIST OF TABLES

CONSOLIDATION AND FABRICATION TECHNIQUES FOR VANADIUM-20 w/o TITANIUM (TV-20)

by

W. R. Burt, Jr., W. C. Kramer,
R. D. McGowan, F. J. Karasek,
and R. M. Mayfield

ABSTRACT

Methods are presented covering a recently developed technology for the consolidation and fabrication of bar, rod, sheet, and high-quality, small-diameter (<5-mm), thin-wall (<0.5-mm) tubing of a V-20w/oTi (TV-20) alloy. Consolidation included electron-beam (EB) melting of compacted vanadium chip and titanium sponge drip rods, followed by arc-melting of the EB ingot. The arc-cast ingots were broken down by extrusion. Sheet-bar and tube-blanks were produced by a re-extrusion process. Cold rolling of bar, rod, and sheet products was accomplished with little difficulty. Tube-blanks were cold-finished by swaging and drawing. The alloy showed a pronounced tendency to gall during drawing through carbide dies. This and other processing problems were overcome, and high-quality tubing was produced in the desired quantities. Additional evaluation of the alloy included annealing and other heat-treatment studies and pertinent, room-temperature, mechanical-property tests. Industrial participation in the program has been encouraged, and early results are reported.

I. INTRODUCTION

For several years there has been an increasing need for information concerning the possible use of vanadium or vanadium alloys as materials for fast-reactor fuel-element cladding or jacketing. While considerable effort has been devoted to studies of the properties of vanadium and certain of its alloys,[1] evaluation of such materials as substitutes for stainless steel in fast reactors was first reported by Smith and Van Thyne in 1957.[2]

The fast-reactor service demands imposed upon the cladding (and other structural components) are rigorous, and not easily satisfied by just any metal or alloy that happens to be popular at the moment. The material should possess adequate high-temperature properties (including strength and integrity), good thermal conductivity, compatibility with nuclear fuels

and with liquid-metal coolants, and stability under irradiation, just to mention a few of the requirements. Finally, and perhaps of greatest importance (although most often neglected or overlooked) the material must be fabricable into the desired shapes, i.e., high-quality, small-diameter, thin-wall tubing and/or related structures.

Further studies of vanadium alloys were reactivated at ANL in early 1963 - stimulated in part by the work of Okrent,[3] which indicated the relative importance of vanadium-base alloys for large, fast, power reactors. Sufficient although limited quantities of vanadium-titanium alloys of various compositions were first produced to gain some early insight into such characteristics as compatibility with fuel and coolant, mechanical properties, and fabricability. The material was in all cases not the best from the standpoint of controlled alloy content and impurities; despite this, the early results were encouraging.[4,5,6]

The above considerations prompted a further and more complete evaluation of selected vanadium-titanium alloys of carefully controlled quality and composition. It became necessary, therefore, to provide the wrought materials desired for further tests of mechanical properties, fuel compatibility, sodium corrosion, and irradiation behavior. Tubing fabrication techniques had to be established for the alloy in order to provide high-quality tubing for irradiation testing and to insure availability of TV-20 tubing should it appear attractive for large-scale usage.

This report presents the details of a fully integrated consolidation and fabrication program having, as its end result, the delivery of high-quality TV-20 bar, rod, sheet, and tubing for further testing for reactor service conditions by others. While the fabrication of bar, rod, and sheet was relatively easy and conventional methods were employed, consolidation and fabrication of the alloy into finished high-quality tubing required both conventional and developmental techniques.

Whether or not these products survive the rigors of testing for ultimate reactor service is outside the scope of this report. Naturally, our hope is that the alloy will weather the storm; however, should it fail in some area, then perhaps the alloy will serve as a first-generation base reference that can be altered, perhaps by a ternary addition, to overcome the possible shortcomings - this remains to be seen.

Before actual consolidation and fabrication operations are detailed, data obtained in preliminary alloy studies are presented. Fabrication and product evaluation details follow, organized generally in the way in which the processing was accomplished, i.e., consolidation, primary fabrication, and secondary fabrication. Data obtained as an adjunct to the main course of work are included in the appendices. Industrial participation in the program has been stimulated, and the early results, which are quite encouraging, are reported.

II. PRELIMINARY ALLOY STUDIES

The results of a small-scale alloy fabricability study, carried out in early 1963, are summarized in Table I. The alloy ingredients were consolidated into buttons by arc-melting precleaned materials. Most of the alloys* were jacketed in either mild steel or Type 304 stainless steel to prevent contamination during hot rolling. The rolling practice was similar to that reported for foil production.(7)

Table I

FABRICABILITY EVALUATION OF SELECTED NIOBIUM, VANADIUM, AND ZIRCONIUM ALLOYS

(Not commercially available)

Alloy Composition (Numerals Indicate w/o)	Hardness as Cast	Hot Rolling Temp, °C	Hardness after Hot Breakdown	Cold Reduction	Hardness after Cold Reduction	Remarks
Nb-5Mo(1)	NA(2)	1000	NA	~25%	93 R_B	Some difficulty in cold working.
Nb-5Mo(1)	NA	850	NA	10% initially 30% after anneal	20-24 R_C	1125°C anneal dropped hardness to 91 R_B.
Nb-10Ti(1)	74-80 R_B	850	75-77 R_B	40% anneal then 50%	95 R_B	Works well.
Nb-10V	20-21 R_C	950	20-23 R_C	Not Attempted		(4)
Nb-20V	28-31 R_C	1000 to 1150	-	-	-	(3)
Nb-39V-1Ti	25-27 R_C	1000 to 1150	-	-	-	(3)
Nb-9Ti-8V	96 R_B	850 to 1150	-	-	-	(3)
Nb-9Ti-3Mo(1)	75-79 R_B	850	92 R_B	60%	98 R_B	Works well.
Nb-15Ti-6V	87-90 R_B	950	87-91 R_B	50%	26-28 R_C	To be annealed before further cold working. Works well.
Nb-18Ti-4V(1)	85-90 R_B	650	90 R_B	68%	22-25 R_C	Works well.
V-10Ti (TV-10)(1)	NA	850 (Air)	NA	50%	95 R_B	Works well.
V-20Ti (TV-20)(1)	NA	850-900 (Air)	NA	50%	27 R_C	Works well.
V-40Ti	24-26 R_C	1050	20-24 R_C	Not attempted	-	(4)
V-5Mo	94 R_B	950	88 R_B	-	-	Unable to cold-work without cracking.
V-50Mo	28-36 R_C	1050 to 1150	-	-	-	(3)
V-20 Nb-5Ti	30 R_C	1000 to 1150	-	-	-	(3)
65V-35Nb (AS-514)	28 R_C	850 to 1150	-	-	-	(3)
56Zr-28V-16Ti (AS-537)	41-43 R_C	1000	43 R_C	-	-	(3) 1125°C anneal dropped hardness to 35 R_C.

(1) Alloy coupons supplied to Engineering Corrosion Group for sodium compatability evaluation.
(2) Not available.
(3) Breakdown by hot rolling unsuccessful at temperatures indicated (Furnace limitation: 1150°C).
(4) Further hot rolling at higher temperature or high-temperature anneal required.

*The alloys were generally of the solid-solution type, devoid of intentional additions of dispersions and/or precipitation-hardening elements.

The most fabricable binary alloys were Nb-10w/oTi, V-10w/oTi, and V-20w/oTi; the more easily workable ternaries were Nb-9w/oTi-3w/oMo, Nb-18w/oTi-4w/oV, and Nb-15w/oTi-6w/oV, on the basis of the methods and temperatures employed. Regarding the vanadium-titanium alloys, interstitial analysis of the 0.81-mm-thick coupon stock yielded values averaging about 850 ppm oxygen and 500 ppm carbon for the V-10w/oTi and 800 ppm oxygen and 450 ppm carbon for the V-20w/oTi alloy.

The ease of workability of the vanadium-titanium alloys generally confirmed the earlier results reported by Smith and Van Thyne[2] even though different fabrication techniques were employed in the preliminary alloy studies, and even though the interstitial contents of the final product were not given in the earlier report by Smith and Van Thyne, which was ANL-sponsored work conducted at IITRI (formerly Armour Research Foundation).

As indicated by Note (1) at the bottom of Table I, certain alloy coupons were submitted to the Engineering Corrosion Group for sodium compatibility evaluation at 650°C. The results indicated, in part, "that the vanadium-titanium alloys experienced a rate of weight loss less by about an order of magnitude than that apparently typical of niobium-base alloys exposed under similar conditions."[4]

The encouraging sodium-compatibility results on the vanadium-titanium alloys strengthened belief in the practicability of an alloy "scale-up" effort to provide the larger quantities of alloy stock needed for further evaluation studies.

However, before any alloy "scale-up" was started, the previous fabricability results were confirmed and the effects of various titanium and oxygen contents were determined in specimens made by using arc-button-melting procedures essentially the same as before, but with close enough control for the results to be meaningful and useful to the scale-up effort that was to follow.

Accordingly, some vanadium-titanium alloys were made from vanadium containing approximately 200 ppm of oxygen and some from vanadium containing approximately 1300 ppm of oxygen. The carbon, nitrogen, and hydrogen were nearly the same in either case (~400, ~250, and ~20 ppm, respectively). The titanium was from plate stock having an interstitial content of ~100 ppm carbon, ~250 ppm oxygen, ~20 ppm nitrogen, and ~10 ppm hydrogen.

The nominal titanium content of the alloys was 0, 3, 5, and from 5 to 30 w/o in 5-w/o increments. The overall melt weighed 60 to 70 g, but the initial alloy charge mixture was divided into two batches weighing 30 to 35 g each.

A single batch was charged into a rectangular copper mold of a small nonconsumable-arc furnace. The system was thereupon evacuated, purged three times with argon gas, and then evacuated and back-filled with a helium-argon gas mixture to a slightly positive pressure. The charge was melted into a small button, which was then cooled, flipped over, and remelted. After a similar double melting of the second batch of the alloy lot, both buttons were broken up by cold rolling and recleaned, and both batches were recharged together into the furnace. Double melting again was used, with the final cast button measuring approximately 1.2 x 3.8 x 3.8 cm (0.5 x 1.5 x 1.5 in.). Multiple melting and the combining of two buttons made from half-size batches were necessary to obtain full-size buttons of adequate homogeneity. Each alloy lot was processed in the same manner.

The arc-cast buttons were individually jacketed in Type-304 stainless steel for hot rolling. A coating of alumina was flame-sprayed on the jacket interior to prevent any interaction, or bonding, between the button and the jacket. The jacketed alloys were hot-rolled with reductions of 10% per pass and to a total reduction of approximately 75%, or to a final thickness of about 0.32 cm (0.125 in.). Hot-rolling temperatures ranged from 850 to 950°C, the higher temperatures being used for the higher titanium-content alloys. After the rolling, the alloys were removed from their stainless-steel jackets, cleaned, and visually inspected. The alloys were then cold-rolled to a total reduction of 50 to 60% - to a thickness of 0.16 cm (0.063 in.) - with initial 5% reductions increased to 10% per pass after some cold-work had been achieved. At this stage, the cold-rolled sheets were vacuum-annealed. The vanadium sheet was annealed for 2 hr at 800°C, while the titanium alloy sheet was annealed for 1 hr at 900°C. After annealing, the sheet stock was again cold-rolled to the final 0.08-cm (0.031-in.) thickness (~50% reduction).

Hardness values for the annealed and cold-rolled sheet, 0.16 and 0.08-cm thickness, respectively, are plotted as a function of titanium and oxygen content* in Figure 1. The hardness of unalloyed vanadium is markedly affected by oxygen content; this effect is diminished with titanium additions up to about 7 to 8 w/o. The hardness decrease in vanadium with small additions of titanium has been previously observed and reported, including possible explanations.[8] Subsequent hardness increases with increasing titanium content are credited to solid-solution hardening. Above 10 w/o titanium, the alloys showed a significant but uniformly small sensitivity to differences in oxygen content of approximately 1000 ppm.

*The oxygen content shown in Figure 1 is estimated to be somewhat higher than that of the starting material. While chemical analyses were not obtained, it was assumed that some increase in oxygen would occur in the multiple-arc melting operation, which was the same for all the alloys.

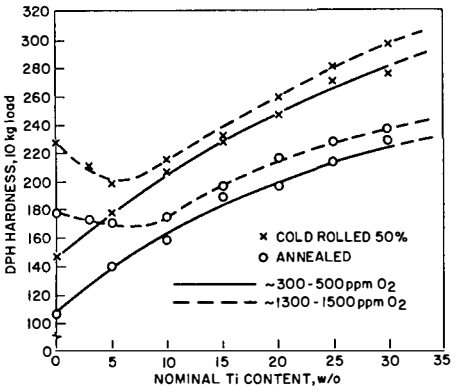

Figure 1

Hardness Data for Rolled and Annealed Vanadium-Titanium Sheet as Function of Titanium and Oxygen Content

The cold reduction produced a significant increase in hardness (work-hardening) for the vanadium and all the alloys. It appears to be a uniform increase for all the ranges of titanium content; however, there is slight (perhaps insignificant) evidence that at titanium contents above 20 w/o, higher hardnesses may be expected. Additional studies will be required to clarify this observation.

All the alloys were fabricated into high-quality sheet, the alloy containing 25 and 30 w/o titanium being the most difficult to fabricate. These latter two alloys might prove difficult to fabricate into high-quality, small-diameter, thin-wall tubing. The higher oxygen content did not affect fabricability measurably, although again the higher the titanium content the more difficult the fabrication. For vanadium alloys containing 10 w/o or more of titanium, an increase in oxygen content of 1000 ppm appears to be equivalent in its effect on fabricability to about a 5-w/o increase in titanium content.

On the basis of preliminary data from the sodium corrosion evaluation of the various vanadium-titanium alloys, it appeared that the corrosion resistance of the alloy increased with increasing titanium content. It was determined that at least 10 w/o titanium would be necessary to provide acceptable corrosion behavior. Presumably, the TV-20 alloy would possess adequate strength, adequate sodium-corrosion resistance, and sufficient fabricability to insure production of the desired products, including tubing. Vanadium alloys of lesser titanium content, although not investigated so extensively, are believed to be fabricable by methods essentially similar to those required for TV-20 alloy, but the fabrication characteristics and hardness of the 25- and 30-w/o titanium alloys foretold potential difficulties in producing high-quality, small-diameter, thin-wall tubing of these higher titanium alloys.

The enhanced interest in TV-20 as a fast-reactor cladding material, that followed this early work with the alloy, increased demands for wrought products, particularly tubing, for continuing irradiation, compatibility, and property-evaluation studies. The alloy "scale-up" from small arc-melted buttons to sizeable production ingots and the successful fabrication into the desired products are described in the following sections of this report.

III. CONSOLIDATION

The consolidation of the V-20w/oTi (TV-20) alloy was accomplished at ANL by means of electron-beam (EB) and arc-melting (AM). The melting points of both elements are above 1600°C (2912°F), and it is highly improbable that they could be more easily consolidated by other means.

A. Equipment

The NRC electron-beam furnace pictured in Figure 2, and shown schematically in Figure 3, has a rated power output of 60 kW derived from a maximum beam current of 3 Amp and an accelerating potential of 20,000 V. A single gun supplies the electron beam, which can be focused to melt either particulates Syntron-fed from a hopper, or a solid drip rod. The water-cooled copper molds are of a bottomless design so that when melting is in progress the ingot can be retracted downward. The furnace

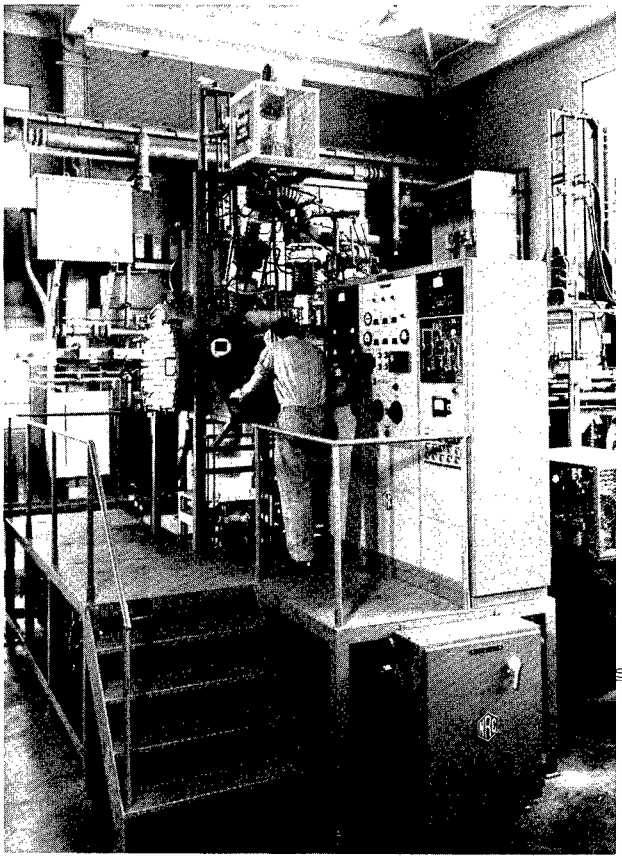

106-7335

Figure 2. Photograph of 60-kW NRC Electron-beam Melting Furnace

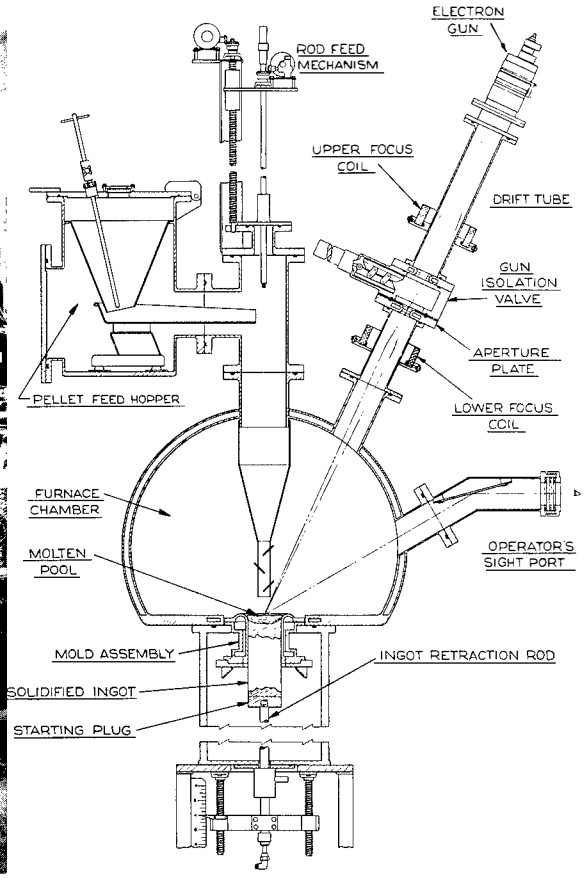

106-7362

Figure 3. Schematic Drawing of 60-kW NRC Electron-beam Melting Furnace, Showing Particulate Feed Funnel in Position in Place of Drip Rod

chamber vacuum system maintains pressures of 10^{-5} to 10^{-7} Torr during melting. A second vacuum system maintains about the same pressure in the gun chamber, which is separated from the furnace chamber by an aperture plate. The remote gun and separate evacuation systems have proven to be very desirable features. Gun power interruptions are infrequent during melting of gassy products, and a minimum of gun maintenance is required.

The NRC (Model 2721A) arc furnace shown in Figure 4, and schematically represented in Figure 5, has a power supply providing up to 4200 Amp for continuous consumable or nonconsumable melting. Particulate charge material is Syntron-fed as indicated. During consumable-electrode melting, the evacuation system maintains vacuums of approximately 10^{-3} Torr. During nonconsumable melting, the furnace chamber is maintained at a pressure of 250 Torr (argon gas), so that an arc can be sustained between the tungsten tip of the nonconsumable electrode and the molten pool in the mold. The water-cooled copper molds are wrapped with magnetic stirring coils for use in promoting arc stability and a refined ingot grain structure.

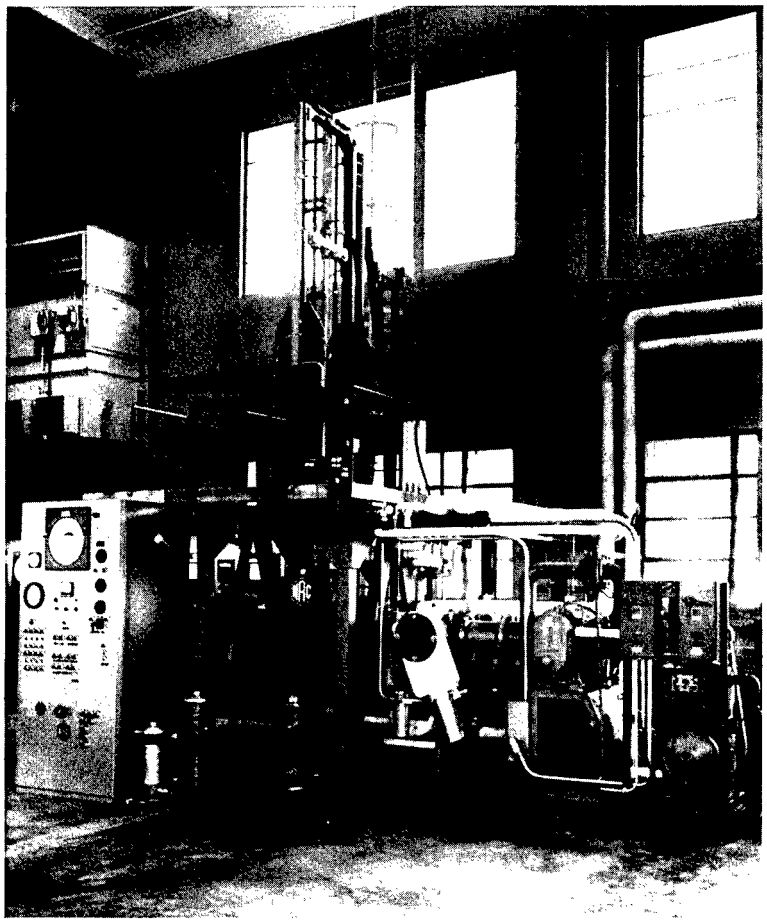

106-7045

Figure 4. Photograph of NRC (Model 2721A) Arc-melting Furnace

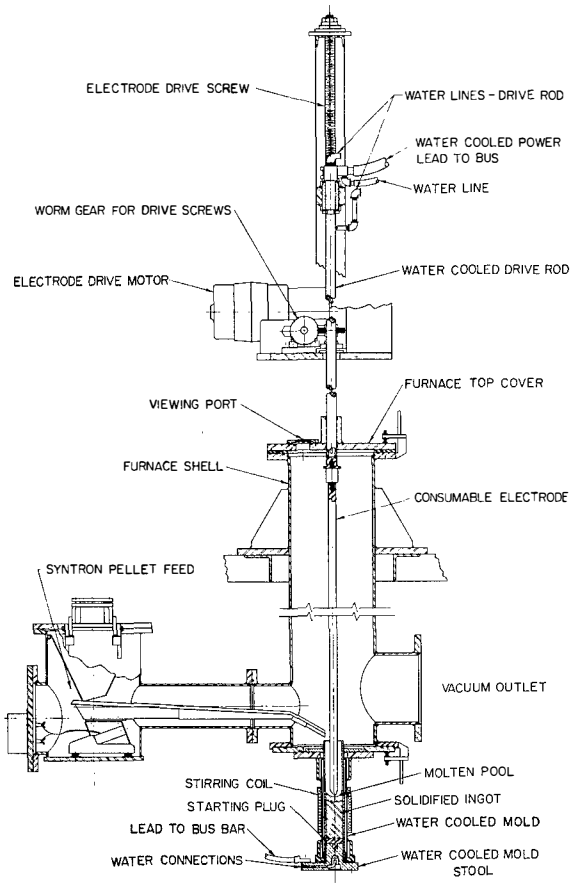

106-7787

Figure 5. Schematic Drawing of NRC (Model 2721A) Arc-melting Furnace

B. Raw Materials

Based upon the results of the preliminary studies on the V-20 w/oTi (TV-20) alloy (see Figure 1), the presumption was that no fabrication problems would be anticipated if the total interstitial-element content of the alloy was held to low levels. Therefore, in choosing potential vanadium and titanium raw materials, only those containing a minimum of interstitial contaminants (C, O, N, and H) were considered in order to minimize possible effects on fabricability.

The purest vanadium commercially available in large quantities at the outset of the program was in the form of -3 +20 mesh (U. S. standard sieve series) chips from the Union Carbide Corp. of Niagara Falls, New York, at a cost of approximately \$81/kg (\$37/lb).

Titanium of equal or higher purity was readily available and was procured as -3 +14 mesh sponge from E. I. DuPont de Nemours and Co. at \$5.20/kg (\$2.40/lb). Limited quantities of 0.64-cm (0.25-in.)-thick titanium plate from the Chicago Development Corp. were used in some of the early consolidation operations. The typical interstitial element analyses (C, O, N, and H) for each of these materials are given in Table II.

Table II

INTERSTITIAL AND MINOR ELEMENT CONTENT OF RAW MATERIALS

Material	Interstitial Element Content, Range in ppm				
	Carbon	Oxygen	Nitrogen	Hydrogen	Total
Vanadium Chips (Union Carbide)	400-450	200-500	100-500	0-10	700-1500
Titanium Sponge (DuPont)	30-300	60-400	20-45	5-45	115-790
Titanium Plate (Chicago Dev. Corp.)	100	250	20	10	380(1)

(1) Range not determined.

Table II (Contd.)

Amount Present, w/o	Minor Element Content	
	Vanadium Chips (Union Carbide)	Titanium Sponge (DuPont)
<2.0	P*	
<0.4	Zn	
<0.2	Mo,* Ta, W	
<0.1	As, Co, Hg, Ni, Si,* Nb	As, Ca,* Hg, Ni,* P
<0.05	Zr	
<0.02	Ba, Ca, K	
0.01	Fe, [Na]	Fe
0.01-0.001	Mg, Mn	Mg, Si
<0.01	Ag, Al, B, Bi, Cr, Cu, Pb, Sb, Sn, Ti	Ag, Al, B, Be, Bi, Co, Cr, Cu, Li, Mn, Mo, Pb, Sb, Sn, V, Zr
<0.001	Be, Li, Sr	

Symbols: *Interference.
[] Accuracy uncertain.

C. Process Development

An alloy content of 20 ± 1 w/o titanium with an interstitial content of ≤1000 ppm (C, O, N, and H) was set as the target parameter. In addition, a fine equiaxed grain structure was desired, with the consolidated product being of sound integrity. The methods used to obtain these objectives are discussed in the following paragraphs.

1. Melting of Particulate Charge Material

Particulate charge materials were melted in both the EB and arc furnaces in an attempt to evaluate these means of consolidation. Vanadium chips were charged by vibratory (Syntron) feeding in both furnaces. Small ingots of vanadium were obtained by both EB and arc melting, and some of this consolidated product was used in further testing and process development. The method, however, was generally considered unsatisfactory because of a lack of suitable feed control. That is, the rate at which the particles are fed from the hopper can vary in a random manner that greatly complicates the melting operation

Attempts to alloy by vibratory feeding were even more unsatisfactory because of the differences in density, particle shape, and size of the two raw materials, combined with the more or less unpredictable feed rate. If the two materials could be preblended so that each pellet contained the desired alloy content (V-20w/oTi), there might be some promise for this method. The preblending technique was not attempted by particulate feeding, but was incorporated into a successful procedure that is discussed later.

Despite the failure by particulate feeding, early melting practice in both furnaces clearly delineated the differences in control

available for developmental procedures of this type. The constant visual observation of the proceedings in EB-melting permits extensive control, while in arc melting one is essentially blind as to the behavior during melting save for certain electrical indications. Viewing the arc pattern provides little solace so far as overall control is concerned.

For the above reasons, first melting for alloying was thereafter carried out in the EB furnace. There were advantages in this procedure, aside from the ease of operation: the vacuum during melting ($<10^{-5}$ Torr) would insure that no contamination of the ingot would occur through pickup of interstitials during melting. By the same token, it was realized that vanadium and titanium would also vaporize with a possible preferential loss of titanium.

While the purity of vanadium can be improved by a series of EB melting operations (see Appendix A), such operations are time-consuming, can result in large losses in vanadium, and can accordingly increase the cost of the product; therefore no special purification of the raw material was performed.

Because of the above-mentioned metal losses occurring during purification experiments, EB melting rates were held as high as possible, consistent with a satisfactory product. It was noted early, however, that gross porosity was evident in a single melted EB ingot. This was clearly noted from X-ray radiographs of the ingot; ultrasonic testing was not required.

2. Melting of Preconsolidated Charge Material

The second alloying technique involved the use of vanadium chips and titanium plate. Before alloying, vanadium chips were consolidated into 6.8-cm (2.8-in.)-diameter ingots (AM5 and 6) by nonconsumable arc melting, followed by remelting into 3.8-cm (1.5-in.)-diameter ingots in the EB furnace. In contrast to particulate feeding, the drip-rod method clearly indicated a much improved control, largely because the material dropping into the molten pool generally was molten rather than in the form of solid chips.

An EB-melted vanadium ingot was wrapped with titanium sheet (rolled from the plate stock starting material) and EB drip-melted into a 3.8-cm (1.5-in.)-diameter ingot. To promote homogeneity, the TV-20 alloy was triple-melted (EB8). Analysis showed the ingot to vary in titanium content from top to bottom to such an extent that improvement was considered necessary. There was still some porosity in EB8 after the three remelts, but much less porosity than that found after a single EB melt.

The third alloying method was based on the use of vanadium chips and titanium plate, somewhat as in the second method. Before alloying, the vanadium chips were consolidated into a 3.8-cm (1.5-in.)-diameter ingot by

electron-beam melting. Strips of titanium, sheared from the rolled plate, were tack-welded along the length of the vanadium ingot to produce a composite drip-rod for alloying in the EB furnace. Four strips were used, representing 20% of the total drip-rod weight.

Chemical analysis of the alloy ingot (EB14R5) produced in this manner indicated that this ingot also was depleted in titanium at the top, and rich in titanium at the bottom, as before in the case of the wrap-around ingot (EB8). As seen in Table III, the titanium increased from 13.3 w/o at the top to 18.7 w/o near the bottom of the ingot. This variance in titanium content was also observed through hardness measurements taken along a milled flat on the ingot surface (Table III).

Table III

HARDNESS READINGS AND CHEMICAL ANALYSES AT SELECTED LOCATIONS ALONG TWO ELECTRON-BEAM-CAST VANADIUM-20 w/o TITANIUM (TV-20) INGOTS

Ingot EB14R5 Cast from (Vanadium Ingot)-(Titanium Plate) Drip-Rod			Ingot EB19 Cast from (Vanadium Chip)-(Titanium Sponge) Briquet Drip-Rod		
Distance from Ingot Bottom (cm)	Hardness (DPH)	Analysis (w/o Ti)	Distance from Ingot Bottom (cm)	Hardness (DPH)	Analysis (w/o Ti)
1.3	228	18.7	1.3	199	19.4
2.5	224		2.5	202	
3.8	213		3.8	199	
5.0	216		5.0	205	
6.3	218		6.3	215	
7.5	202		7.5	202	
8.8	192	16.9	8.8	207	
10.0	188		10.0	199	
11.3	182		11.3	209	
12.5	189		12.5	212	
13.8	186		13.8	213	
15.0	189		15.0	205	
16.3	181	13.3	16.3	207	
			17.5	197	
			18.8	215	
			20.0	193	19.9
Hardness range = 181-227			Hardness range = 193-215		
Mean hardness = 201			Mean hardness = 205		

The variance in titanium content resulted from the method of drip-rod preparation (both wrap-around and welded strips) and subsequent drip-rod "melt-off" characteristics of the electron beam. As the beam is inclined at an angle of 25° from the vertical, the beam initially points the end of the drip-rod, melting the outer material first. More titanium than desired is melted in initially pointing the rod.

A balanced melting rate between the vanadium and titanium was never achieved in the ingot by either of these methods. As a result, these methods of EB drip-rod melting were abandoned and a technique yielding the target homogeneity was sought.

3. Melting of Precompacted Particulate Charge Material

The fourth alloying method involved compaction of vanadium chips and titanium sponge into a suitable EB drip-rod. Batches of 100 g were weighed out (80 g of vanadium, 20 g of titanium) and individually pressed at 6,900 kg/cm^2 (49 tsi) into 3.2-cm (1.25-in.)-diameter x 2.5-cm (1-in.)-long briquets. The raw materials, blended mixture, and a pressed briquet are shown in Figure 6. A series of briquets were welded together in an inert-atmosphere glovebox to form a drip-rod 50 to 75 cm (20 to 30 in.) in length. Figure 7 shows the individual briquets and a completed drip-rod.

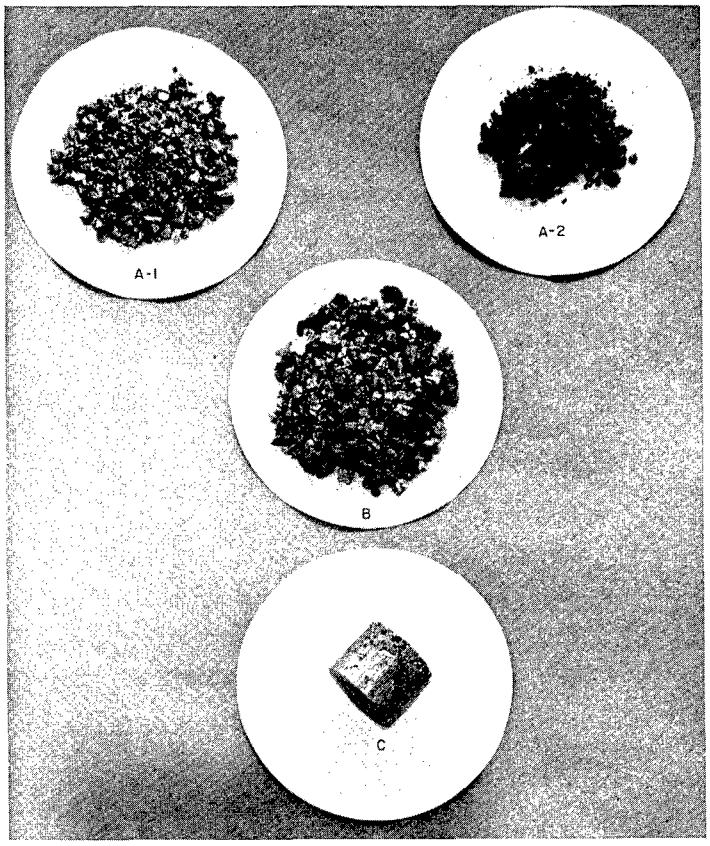

106-7656

Figure 6

Vanadium Chips (A-1) and Titanium Sponge (A-2) after Blending (B) and Pressing into Briquet Form (C)

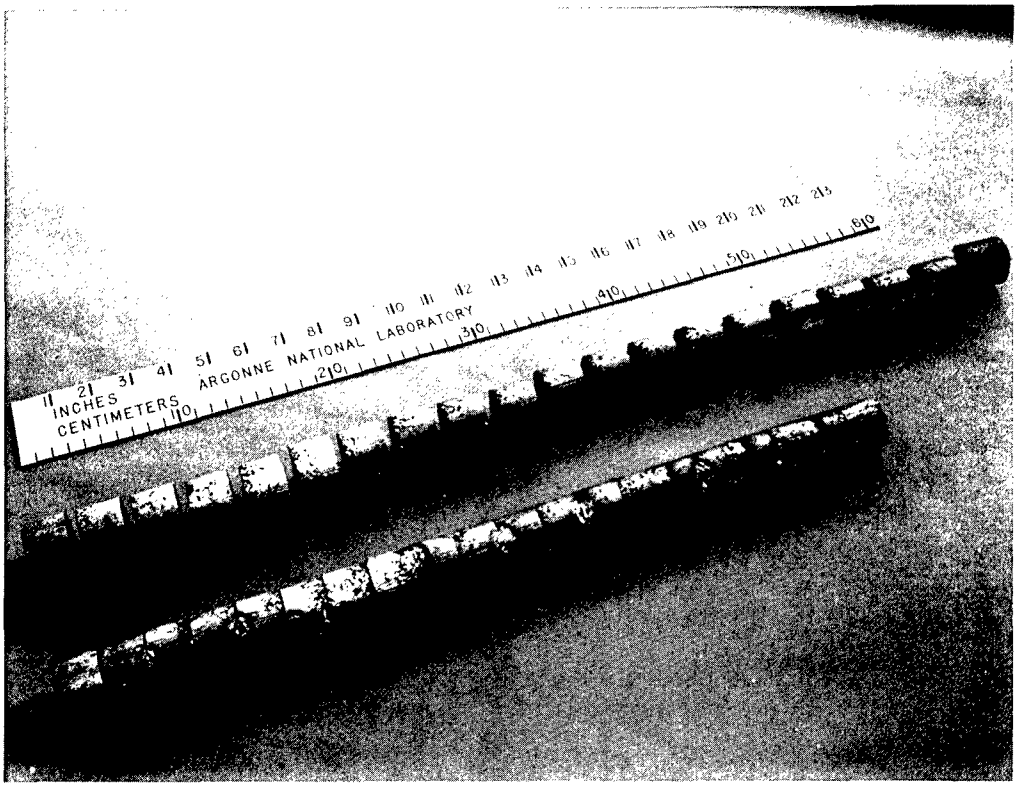

106-7654

Figure 7. A Series of Vanadium-Titanium Pressed Briquets before and after Welding to Form a Drip Rod for Electron-beam Melting

Three developmental EB castings were made by the briquet-drip-rod method. EB15 and 16 were 3.8 cm (1.5 in.) in diameter, while EB19 was 5.8 cm (2.3 in.) in diameter. Chemical analyses of all the ingots revealed that the titanium content was within (or very near to) the 20 ± 1 w/o limit. The chemical analysis results for EB19 (top and bottom) are presented in Table III. The DPH values (measured as for ingot EB14R5 in Section 2 above) were indicative of a random distribution of titanium within a fairly narrow range.*

Figure 8 shows a transverse macrostructure of the EB19 cast ingot. The presence of unalloyed vanadium particles probably resulted from pieces of solid briquet material occasionally falling from the end of the drip-rod into the molten pool during the melting operation. This could result from insufficient mechanical bond in the TV briquet. Apparently the molten pool solidified before the fallen pieces became molten.

*While variation in hardness values in an ingot can be affected by cooling rate and other factors besides titanium content, readings along the length of a given ingot have proven to be of some value in locating areas in which the titanium content differs significantly from the mean.

Transverse Section

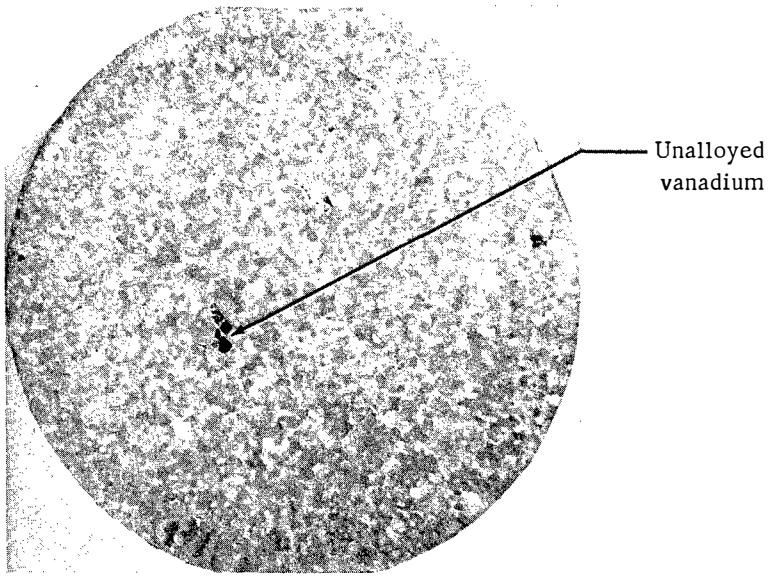

Macro 38491 1.3X

Figure 8. Macrostructure of Electron-beam-cast Vanadium-20 w/o Titanium Ingot (EB19)

A change in EB melting practice was used to minimize the problem. If pieces of solid metal were seen to fall into the molten pool, the drip-rod was retracted to stop further melting for about 30 to 60 sec. During this time, the solid pieces could dissolve completely. While the probability of finding unalloyed solids in the EB ingot was reduced, one cannot say that true homogeneity would exist after a single melting operation of this type. Further, there was no indication that the change in EB melting practice eliminated porosity or improved the surface quality.

At this stage of development, an arc-melting operation was counted on to improve alloy homogeneity, ingot soundness, and surface quality. The pressure in the arc furnace (10^{-3} Torr) might result in some interstitial contamination of the alloy, but the degree of vacuum was not enough to cause significant vaporization of materials. By melting once in each furnace, the advantages of both techniques could be utilized without compounding the disadvantages of either method.

The above premise was tested by combining EB ingots 15 and 16 into a consumable electrode and arc-melting into a 9.7-cm (3.8-in.)-diameter mold (AM20). The arc-melted surface was considerably improved. Chemistry results at three locations showed good homogeneity. Minor porosity was found only within the outer annular band of ingot material and appeared to be entirely within the directionally-oriented grains. This minor porosity might be expected since rapid cooling of outer ingot surface by transfer of heat to the water-cooled copper mold causes entrapment of gases within solidifying metal in this region.

X-ray radiographs of the ingot showed no porosity, but an ultrasonic inspection was not conducted. The ingot was sectioned longitudinally and the surfaces macroetched. A uniform grain structure was revealed with no further evidence of porosity.

D. Alloy Scale-up by EB and Arc Melting

The "scale-up" phase of the program was undertaken after a proven consolidation method had been established. It remained, however, to coordinate quantity and ingot sizes with the demands for TV-20 wrought products. Of equal importance was matching the final arc-melted ingot size with extrusion operations that were to follow.

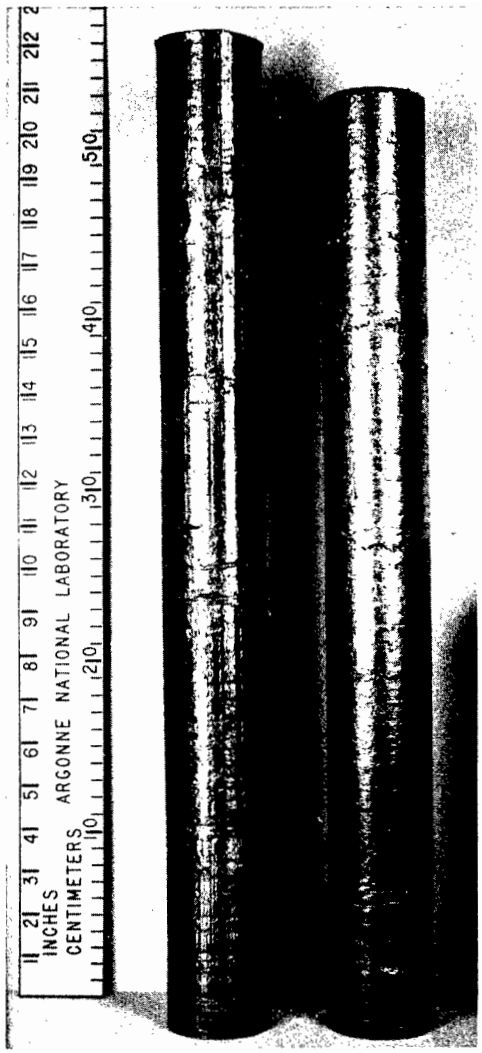

Micro 38372 0.2X

Figure 9. Electron-beam-melted Ingots of TV-20

It was clear that a double-melting technique was required to produce a final ingot of suitable alloy homogeneity and soundness.

Early extrusion studies (see page 34) also were indicating that a double-extrusion technique would be required to obtain an extruded product suitable for secondary fabrication. These two requirements were satisfied by the following consolidation procedures.

For producing the large ingots required for further fabrication, six briqueted and welded 76-cm (30-in.)-long drip-rods were EB-melted to produce two 5.8-cm (2.3-in.)-diameter x 51- to 56-cm (20- to 22-in.)-long EB-melted ingots. Throughout the EB-melting period, a melt chamber pressure of $<10^{-5}$ Torr was maintained. A power setting of about 26 to 30 kW (approximately half of rated capacity) was used to effect a melting rate of approximately 60 g/min (0.13 lb/min). With this melt rate, a yield of about 95% was typical. Vaporization losses vary inversely with melting rate, other factors being equal. Typical ingots are shown in Figure 9. The casting surface was generally good, although no real effort was made

to control surface quality or to avoid internal porosity. The main purpose of EB melting was to provide alloy electrode stock for arc melting.

Initially, the two EB ingots to be used as a consumable electrode for arc melting were machined and screwed together. Welding the ingots together under an inert gas was found to be a faster and more economical method. A typical consumable electrode was about 100 cm (40 in.) long and weighed about 16 kg (35 lb). No difficulty was encountered in consumable-arc melting of the electron-beam ingots into a 9.7-cm (3.8-in.)-diameter, high-quality, arc-cast ingot. A melting rate of 1 kg/min was achieved by using straight polarity (consumable electrode negative) and 90 kW (3,000 Amp and 30 V) of power. The furnace chamber pressure throughout melting was 10^{-2} to 10^{-3} Torr. A stirring coil setting of 1.5 to 3 Amp aided arc collimation and grain refinement. The melting power was reduced in successive steps toward the end of the melt cycle. This procedure ("hot-topping") promoted gradual solidification and minimized the cavity ("pipe") that generally forms at the ingot top. Essentially no charge material was lost during melting.

The arc-cast ingots were radiographed upon removal from the arc-furnace mold. They were then cropped at each end to remove the starting plug from the bottom and the secondary pipe (approximately 5 cm [1.9 in.] long) near the top. Cropped ingots were 27 to 33 cm (11 to 13 in.) long and weighed 12 to 14 kg (26 to 31 lb). A typical cropped ingot is shown in Figure 10. In general, ingot surface quality was excellent and markedly improved over that obtained in the electron-beam furnace. Ingot hardness measured approximately 208 DPH.

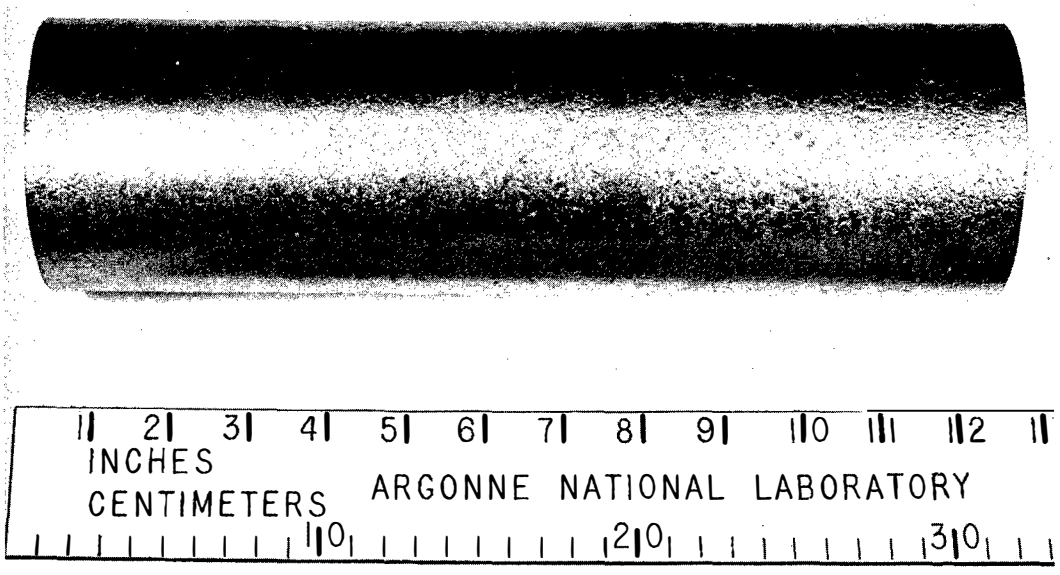

Micro 38425 0.4X

Figure 10. Arc-cast Ingot of TV-20 (AM21)

E. Ingot Evaluation

1. ANL-produced Ingots

Evaluation of the arc-cast ingots included visual, radiographic, and ultrasonic inspection, macro- and microstructural examination, and chemical analysis.

No defects normally were found in radiographs of the ingots, except for the secondary piping near the ingot top as previously mentioned. Samples for macro- and microstructural examination were taken from the end cropping.

The transverse macrostructure of arc-cast ingot No. AM21, as shown in Figure 11, was typical of all three of the 9.7-cm (3.8-in.)-diameter ingots produced at ANL. Some radially-oriented solidification was evident in an annular band adjacent to the outer edge (circumference) of the ingot, the remainder of the section exhibiting a typical fine, equiaxed, grain structure. Minor porosity in the ingots was found only within the outer annular band of ingot material and appeared to be entirely within the directionally-oriented grains, as mentioned earlier. Machining of the ingots from 9.7 cm (3.8 in.) to the extrusion billet diameter of 9.0 cm (3.5 in.) did not completely remove this band of material containing pinhead-size porosity.

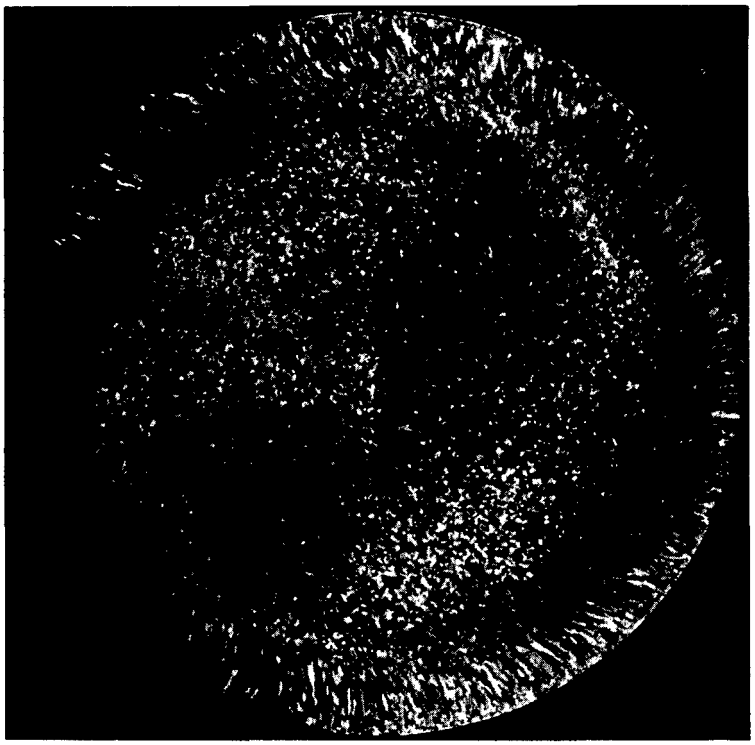

Macro 38446 1X

Etchant: 5% $AgNO_3$, 2% HF (swab)

Figure 11. Transverse Macrostructure of TV-20 Arc-cast Ingot (AM21)

An ultrasonic through-transmission inspection of the machined billets gave no indication of the presence of internal cracks, pores, or inclusions. The minor porosity existing near the billet surface was subsequently removed in conditioning the surface of the bar after primary extrusion of the ingot, as will be discussed later.

The as-cast microstructure of TV-20 (AM21) is shown in Figure 12. The matrix is β solid solution (vanadium-titanium), but the precipitate phase has not been fully identified. (Additional information concerning possible identity of the precipitate phase is included in Appendix A.)

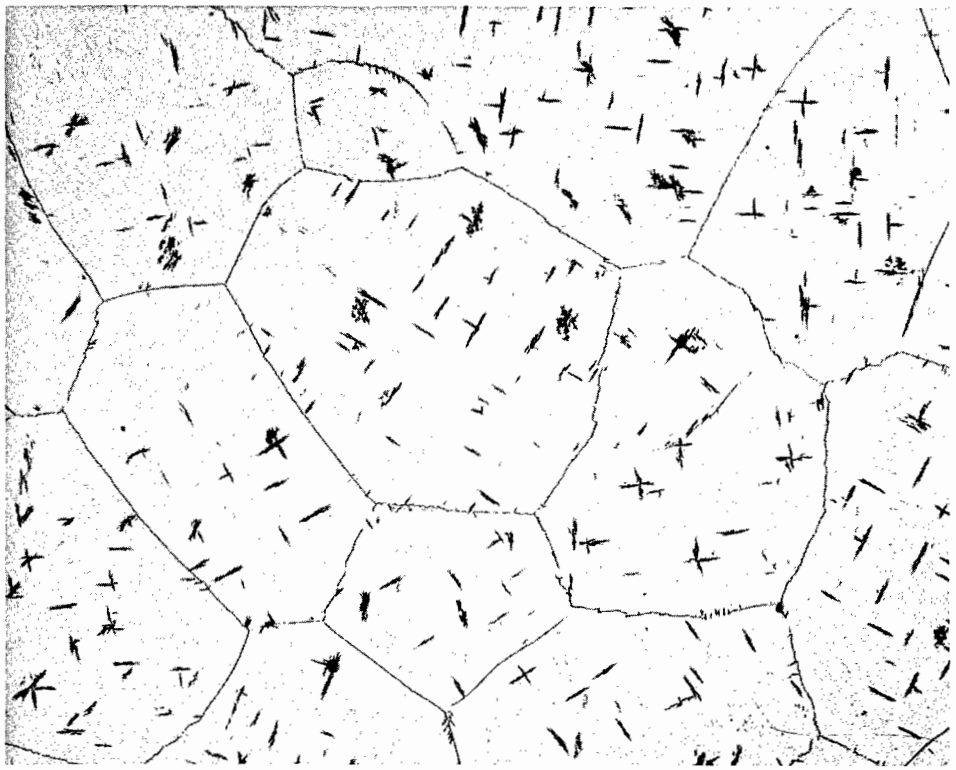

Micro 38584 100X

Etchant: 10% KOH, 10% $K_3Fe(CN)_6$

Figure 12. Microstructure of Transverse Section from TV-20 Arc-cast Ingot (AM21)

Chemistry samples were collected during the process of machining the ingots to the primary extrusion billet diameter. Titanium and interstitial-element analyses results for three TV-20 ingots are presented in Table IV. In general, the target alloy content (20 ± 1 w/o titanium) was achieved in each of the ingots. The total interstitial contents are only slightly above the target maximum of 1,000 ppm. The analytical results on AM21 indicate that some preferential loss of titanium may have occurred during processing. Consequently 21 w/o of titanium was blended into the briquet mixtures used to prepare drip-rods for subsequent ingots.

Table IV

ALLOY AND INTERSTITIAL ELEMENT
ANALYSES FROM THREE TV-20 ARC-CAST INGOTS

Ingot Number and Position	Element Analyses					
	Titanium (w/o)	Carbon (ppm)	Oxygen (ppm)	Nitrogen (ppm)	Hydrogen (ppm)	Total[3] (ppm)
AM21[1] Top	20.2[4]	387	360	270	1	1018
Middle	18.7					
Bottom	19.2					
AM25[2] Top	20.0	342	395	379	20	1136
Middle	19.9					
Bottom	19.4					
AM28[2] Top	20.8	289	420	291	50	1050
Middle	21.1					
Bottom	20.1					

(1) 20 w/o titanium in EB melt charge briquets.
(2) 21 w/o titanium in EB melt charge briquets.
(3) For interstitial content of raw materials, see Table II.
(4) A hardness traverse taken at 1.3-cm (0.5-in.) intervals along the ingot length gave DPH readings ranging from 198 to 215, the mean value being 208. (Compare with Table III.)

Analyses on chip and sponge raw materials may vary somewhat during a single batch or lot, and a variation may be expected in analytical results, owing to sample preparation, surface cleanliness, and the actual technique, per se (see Appendix B). For these reasons, it is not precisely known just how much increase in interstitial content is due to the actual processing and melting operations.

2. Commercially-procured Ingots

In addition to the ingots produced at ANL, three ingots were procured from Union Carbide Corporation (purchase order 445046). The ingots, 10.2-cm (4-in.) diameter x 20.3- to 25.4-cm (8- to-10 in.) long, were produced by essentially the same process as that described above for ANL-produced ingots (i.e., compacted drip-rods were electron-beam melted, and the alloy ingots produced were subsequently arc-melted to ingots of the final diameter). The two main differences in technique were that longer sections were compacted for drip-rods than the 2.5-cm (1-in.)-long ANL briquets, and electron-beam ingots were quartered longitudinally for use as arc-furnace consumable electrodes, rather than being directly melted as whole EB ingots. The first-mentioned change, made possible by the greater pressing capacity available at Union Carbide, is a desirable one inasmuch as drip-rod preparation is simplified and expedited. The second change, made necessary by the comparatively large minimum EB ingot diameter that Union Carbide could cast, is undesirable in that additional waste material is generated, and processing time is increased.

The ingots were evaluated by means of macrosection examination, radiography, ultrasonic inspection, and chemical analyses. Evaluation results indicated that these ingots were of comparable quality to those produced at ANL. Analytical results are summarized in Table V.

Table V

ALLOY AND INTERSTITIAL ELEMENT ANALYSES FROM THREE TV-20 ARC-CAST INGOTS PROCURED FROM UNION CARBIDE CORPORATION

Ingot Number in Position	Element Analyses					
	Titanium[1] (w/o)	Carbon (ppm)	Oxygen (ppm)	Nitrogen (ppm)	Hydrogen (ppm)	Total (ppm)
761-1 Top	20.7	480	358	138	13	989
Middle	19.7					
Bottom	19.0					
761-2 Top	20.5	370	525	230	5	1130
Middle	19.7					
Bottom	18.8					
761-3 Top	19.3	360	508	82	21	971
Middle	19.8					
Bottom	19.4					

(1) ANL analysis for titanium.

Interstitial element analyses were supplied by Union Carbide.
UC and ANL interstitial element analyses are compared in Appendix B.

IV. PRIMARY FABRICATION BY EXTRUSION

The only method used for hot-working the V-20w/oTi (TV-20) alloy was extrusion. No forging facilities were available at ANL, and the shaped roll passes available were too small or of improper design.

A. Equipment

Two presses were used for extruding the TV-20 alloy: a 318-metric-ton (350-ton) vertical press, and a 1135-metric-ton (1250-ton) horizontal press. The 318-metric-ton (350-ton) vertical press is shown in Figure 13. The press is powered by a water accumulator system and is capable of delivering 272 metric tons (300 tons) at a 38-cm/sec (15-in./sec) extrusion speed. Nominal billet diameters are 5.1 or 6.4 cm (2 or 2.5 in.). (All primary working of the TV-20 alloy was done on a 5.1-cm (2-in.)-diameter billet.) An induction coil powered by a 30-kW Tocco motor-generator unit was used for billet heating. Removal of the hot billet from the induction coil to the start of extrusion could easily be held within 8 to 10 sec.

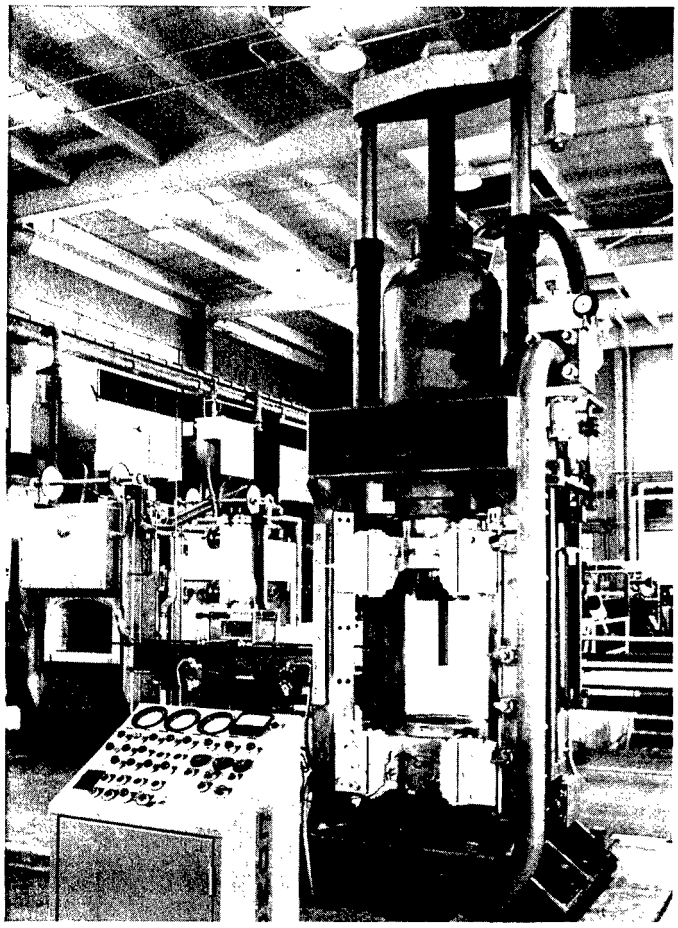

106-7043

Figure 13
Photograph of 318-metric-ton (350-ton) Lombard Vertical Extrusion Press

The die design shown in the tooling arrangement of Figure 14 was occasionally used. Insert dies (located inside the container) were used for the most part to better absorb radial stresses imposed on the die during extrusion and to reduce die costs.

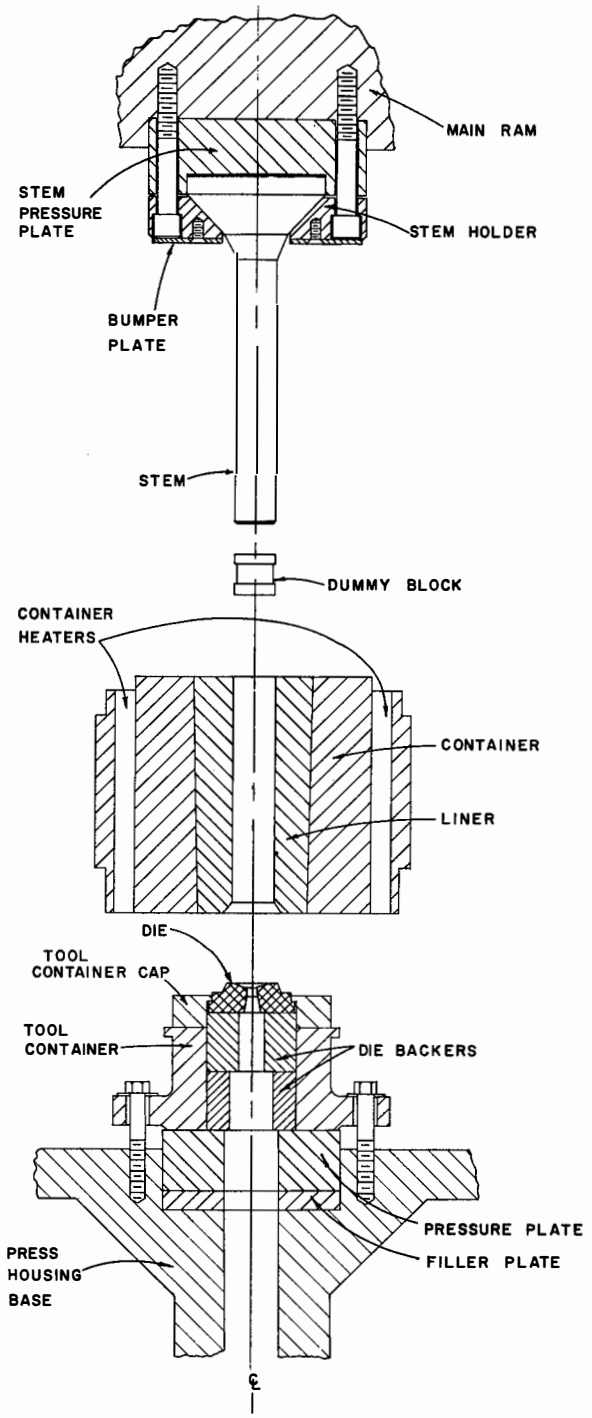

106-7048

Figure 14

Tooling for 318-metric-ton (350-ton) Lombard Vertical Extrusion Press

The 1135-metric-ton (1250-ton) horizontal press is shown in Figure 15, and the tooling arrangement in Figure 16. The press is designed to extrude 10.2- and 15.2-cm (4- and 6-in.)-diameter billets and is capable of delivering a 908-metric-ton (1000-ton) load at an extrusion speed of 25 cm/sec (10 in./sec). Extrusion billets were heated in a large silicon-carbide resistance furnace capable of operation up to 1500°C. A transfer

table from the furnace to the press allowed transfer times of approximately 20 sec. This press is powered by the same water accumulator system used for the smaller (318-metric-ton) press.

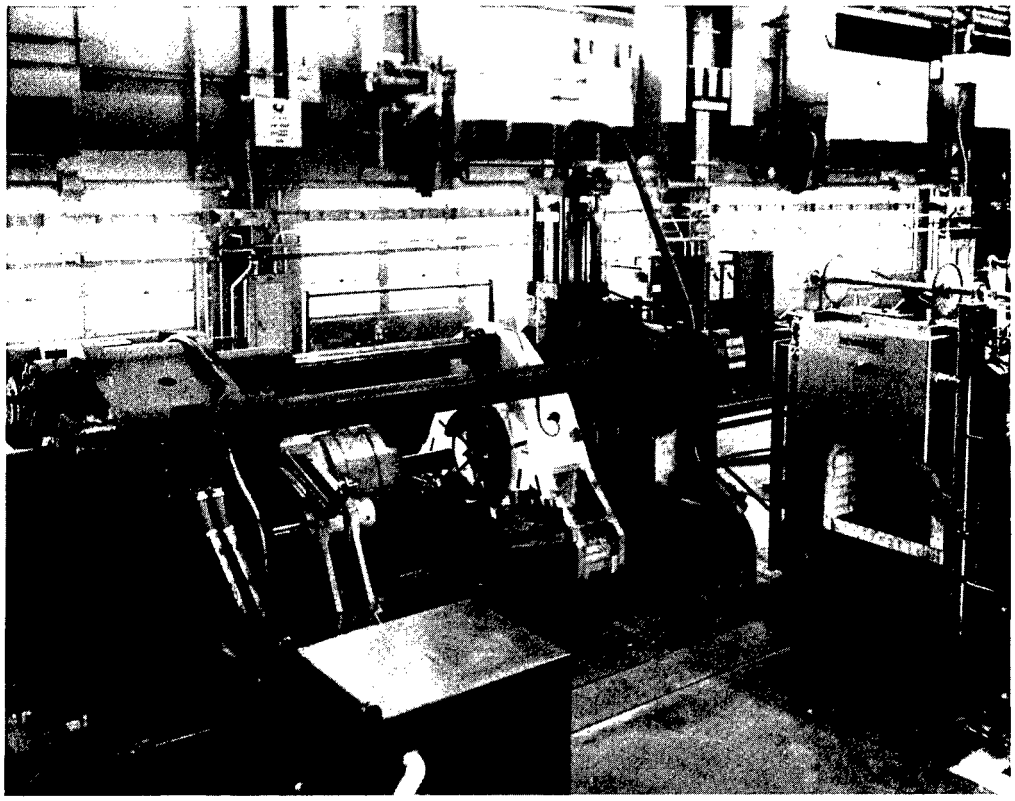

106-7046

Figure 15. Photograph of 1135-metric-ton (1250-ton) Lake Erie Horizontal Extrusion Press

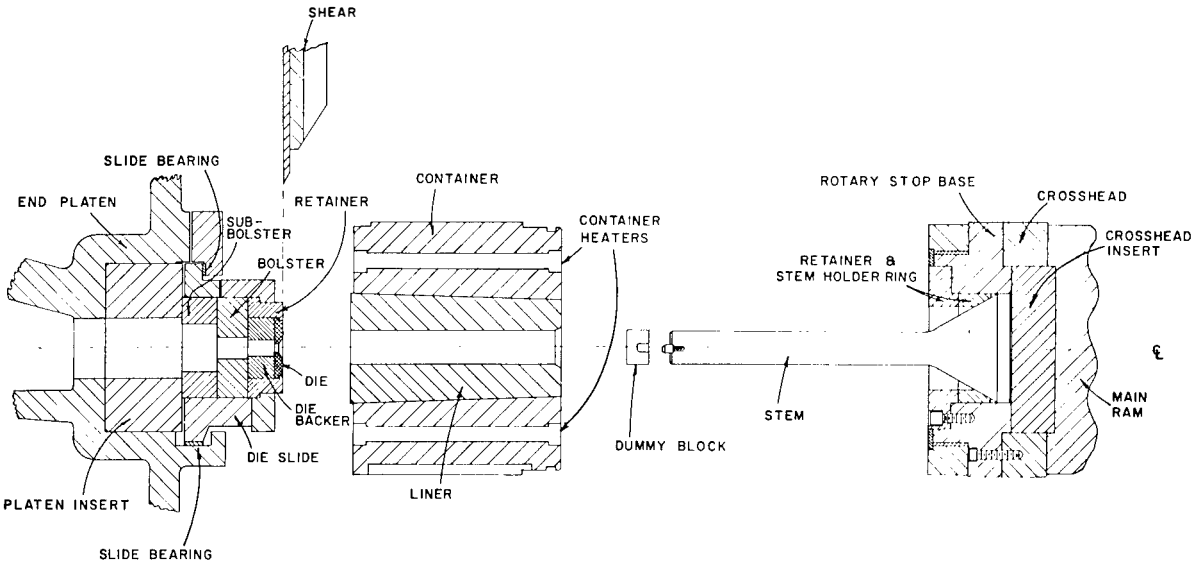

106-7049

Figure 16. Tooling Arrangement for 1135-metric-ton (1250-ton) Lake Erie Horizontal Extrusion Press

B. Process Development

As with all refractory metal and alloys, the vanadium-titanium alloys are susceptible to contamination by interstitial elements at temperatures greater than 300°C. It was reasoned, therefore, that the material should be protected against contamination during heating and extrusion, unless the extruded product is to be heavily conditioned to remove any contaminated surface layers. Based on this consideration, general practice at ANL required "canning" the alloy in Type 304 stainless steel (or mild steel in certain cases) to afford protection against contamination. This technique also permits the billet to be heated in air rather than in a vacuum or an inert atmosphere. Therefore the 3.8-cm (1.5-in.)-diameter EB ingots were machined to 3.4-cm (1.3-in.) diameter by approximately 7.6-cm (3-in.)-long billets, which were canned in Type 304 stainless steel. The components were assembled in an inert-atmosphere glovebox, where the end plug was TIG-welded to seal the can. The overall (composite) billet size was 4.95 cm (1.95 in.) in diameter and approximately 16 cm (6.1 in.) long, with a partial 45° chamfer on the nose end of the billet.

Extrusion temperatures of 1000, 1100, and 1200°C were used in extruding the billets at a 7:1 reduction ratio. At the lowest extrusion temperature of 1000°C, the extrusion pressures required indicated that high reduction ratios could not be achieved. At 1100°C, the extrusion pressures indicated that adequate reduction ratios (approximately 10 to 15:1) could be obtained consistent with acceptable characteristics of the extruded product. The microstructure of the bar extruded at 1100°C showed a fine, recrystallized grain structure with uniform grain size along the complete length of the extrusion. At 1200°C, there was a tendency for a reaction between the alloy and the Type 304 stainless-steel jacket material, thus producing a poor surface on the extruded product. In addition, at this higher temperature, the degree of mismatch between the hardness of the alloy and the stainless-steel jacket resulted in poor control over dimensions. Based on the above considerations, 1100°C was selected as the best extrusion temperature consistent with adequate reduction ratios and quality of the extruded product. (Later, a few production billets were extruded at 1000 or 1200°C to confirm again the best extrusion temperature.)

At all temperatures, rippling of the alloy core occurred as revealed by radiography. This rippling is a common phenomenon in the extrusion of a composite bar whose outer jacket material is markedly softer than the interior core material. To correct this, the diameter of the core alloy was increased, thereby reducing the relative amount of stainless steel present in the can or jacket. When an alloy billet approximately 4.4 cm (1.74 in.) in diameter was used with a Type 304 stainless-steel jacket measuring 4.95-cm OD x 4.45-cm ID (1.95-in. OD x 1.75-in. ID), no rippling was experienced. Accordingly, this design was established as "standard."

All the experimental extrusions revealed a surface having severe longitudinal striations, as shown in Figure 17. By using a double-extrusion technique, a surface quality was produced that minimized or eliminated the need for conditioning before cold finishing of the extruded product. The initial extrusion of an EB- or arc-cast ingot broke up the cast structure and refined the grain size. At this stage, the longitudinal surface striations were removed in conditioning or machining the extruded product into billets for re-extrusion. The second extrusion produced a surface greatly improved over the primary extruded surface, as shown in Figure 17 for the case of a tube-blank.

(a) Surface quality after initial extrusion.

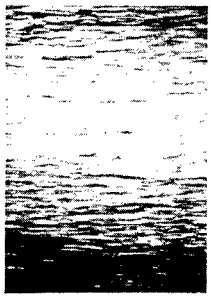

(b) Surface quality after re-extrusion.

Micro 38929 1X

Figure 17. Typical Surface Quality of V-20w/oTi Extrusions after (a) Initial Ingot Breakdown Extrusion and, (b) Re-extrusion into a Tube-blank

It was because of this surface striation characteristic that the starting extrusion billets had to be scaled up to a 9.7-cm (3.8-in.)-diameter ingot (see page 23). These larger ingots would undergo a primary breakdown extrusion to a bar that, after conditioning, would yield a 4.4-cm (1.74-in.)-diameter bar suitable for re-extrusion into tube-blanks, sheet-bar, rod, or other desired shapes.

C. Ingot Breakdown

Arc-cast ingots, 9.7 cm (3.8 in.) in diameter, of V-20w/oTi (TV-20) produced at Argonne National Laboratory (AM21, AM25, and AM28), or procured from the Stellite Division of the Union Carbide Corp., Kokomo, Indiana (UC761-1 and UC761-3), were machined to a nominal diameter of

9.0 cm (3.54 in.) and to a length of 20 to 25 cm (8 to 10 in.) and were canned in Type 304 stainless steel. The stainless steel can measured 10.2-cm OD x 9.0-cm ID (4.0-in. OD x 3.55-in. ID). The nose of the steel can was partially chamfered at a 45° angle. In an inert-gas glovebox, the conditioned ingot was placed in the steel can, and the end plug welded in place. Billets were heated for 2 hr in a "Globar" furnace at the extrusion temperature of 1100°C. (One billet was extruded at 1000°C, but the extrusion pressures required indicated that a higher temperature would be more beneficial for subsequent extrusions.)

After heating, the billets were transferred to the extrusion press and extruded at a speed of approximately 15 cm/sec (6 in./sec) and with a MoS_2-graphite-oil mixture for lubrication. The extrusion dies incorporated a 120° approach angle and were of H-12 tool steel, heat-treated to a 47-50 R_C hardness. A graphite cut-off plug was placed behind the billet to provide complete extrusion of the billet. When necessary, rough straightening was accomplished immediately after extrusion.

After cooling, the bar was radiographed to determine the location of the TV-20 core in the extruded bar. The steel ends were cropped from the extrusion, and the remaining steel jacket was removed by machining. The TV-20 bar was machined to the proper diameter for re-extrusion; in other words, the machining reduced the diameter approximately 0.3 cm (0.125 in.) and thus removed the striated surface caused by the initial extrusion of the ingot. The bar was then sectioned to provide billets for re-extrusion measuring a nominal 4.42 cm (1.74 in.) in diameter and approximately 11.5 to 12.5 cm (4.50 to 5 in.) in length. The nose of the billets were machined to a 120° included angle to fit the cans for re-extrusion. Solid billets were used for re-extrusion into bar and sheet-bar stock. For tube-blank extrusion, a 1.60-cm (0.63-in.)-diameter hole was drilled through the billet before finish-turning the outer surface.

Data on extrusion of arc-cast ingots are presented in Table VI. The extrusion constants derived from pressures required to extrude arc-cast ingots were significantly higher than constants obtained on re-extrusion of the same material undoubtedly, less effective lubrication accounts for part of the required increase in pressure. As found in extrusion of other refractory metals and alloys, however, the initial deformation of a cast structure requires greater effort than later hot-working operations.

Based on the calculated extrusion constants and a limiting stem pressure of 12,600 kg/cm^2 (180,000 psi), the maximum feasible reduction ratio for extrusion of an arc-cast ingot at 1100°C would be about 7:1. This reduction is sufficient to break up the initial cast structure and provide a material that will yield an acceptable surface quality on further extrusion or hot working. The lower extrusion ratio actually used for ingot breakdown (approximately 3.6:1) was based on the need for an extruded bar that

could be machined to 4.42-cm (1.74-in.) diameter. This ratio also was sufficient to break up the initial cast structure so that an acceptable surface would result on re-extrusion. One arc-cast ingot (UC761-1) was extruded at a 6.5:1 extrusion ratio at 1100°C (Extrusion No. 290) to provide stock for cold-rolling bar to 1.2-cm (0.500-in.) diameter and smaller.

Table VI

SUMMARY OF EXTRUSION DATA FOR V-20w/oTi (TV-20) ALLOY[1]

Extrusion Number	Material[2] Source	Nominal Composite Billet Diam, cm	TV-20 Billet Diam, cm	Billet[3] Temp, °C	Reduction Ratio	Extrusion Pressure		Extrusion[4] Constant, kg/cm^2
						Breakthrough, kg/cm^2	Running, kg/cm^2	
Ingot Breakdown: 1135-metric-ton (1250-ton) Horizontal Extrusion Press								
261	AM-21	10.2	8.95	1000	3.6	9,490	8,650	6,820
269	AM-25	10.2	8.95	1100	3.6	8,450	7,730	6,050
289	UC-761-3	10.2	8.95	1100	3.6	NM[5]	NM[5]	NM[5]
290	UC-761-1	10.2	8.95	1100	6.5	11,250	9,630	5,130
303	AM-28	10.2	8.95	1100	3.5	8,930	8,160	6,470
Sheet Bar Extrusion: 318-metric-ton (350-ton) Vertical Extrusion Press								
264	E-261	4.95	4.40	1100	13	11,390	10,470	4,080
280	E-269	4.95	4.42	1100	13	Billet failed to extrude		
281	E-269	4.95	4.42	1200	13	11,390	10,970	4,290
312	E-303	4.95	4.42	1100	13	11,740	10,900	4,250
Tube Blank Extrusion: 318-metric-ton (350-ton) Vertical Extrusion Press								
266	E-261	4.95	4.42 OD 1.60 ID	1100	13	11,740	10,400	4,080
267	E-261	4.95	4.42 OD 1.60 ID	1095	13	11,250	9,700	3,800
268	E-261	4.95	4.42 OD 1.60 ID	1100	16.2	10,900	10,330	3,730
283	E-269	4.95	4.33 OD 1.61 ID	1200	11.2	8,790	8,230	3,270
284	E-269	4.95	4.36 OD 1.60 ID	1200	16.8	10,330	9,210	3,270
286	E-269	4.95	4.35 OD 1.59 ID	1100	12.8	11,530	9,700	3,800
292	E-289	4.95	4.42 OD 1.59 ID	1100	11.7	13,290	10,470	4,250
294	E-289	4.95	4.42 OD 1.59 ID	1100	10.6	10,970	9,490	4,010
295	E-289	4.95	4.42 OD 1.59 ID	1100	11.6	11,670	10,330	4,220
302	E-289	4.95	4.42 OD 1.74 ID	1090	10.5	11,250	10,050	4,290
313	E-303	4.95	4.28 OD 1.59 ID	1100	8.9	11,530	10,610	4,850
314	E-303	4.95	4.42 OD 1.59 ID	1100	11.6	13,220	11,600	4,750
318	E-303	4.95	4.42 OD 1.59 ID	1100	11.5	10,550	9,980	4,570
324	E-303	4.95	4.42 OD 1.60 ID	1100	11.5	9,560	8,860	3,620

(1) All TV-20 billets canned in Type 304 stainless steel for extrusion. Extrusion dies and mandrels of H-12 tool steel at 47-50 R_C. Dies had a 120° approach angle. Lubricant was MoS_2-graphite-oil mixture. Extrusion speeds were between 11 and 16 cm/sec.

(2) AM indicates ANL arc-cast ingot; UC indicates Union Carbide (Haynes Stellite Div.) arc-cast ingot; E indicates breakdown extrusion number.

(3) Billets for ingot breakdown heated for 2 hr in Globar furnace. Billets for sheet-bar and tube-blank extrusions heated by induction (approximately 6 min) and held for 5 min at temperature.

(4) Calculated from $P = K \ln (A_0/A)$, where P is the running extrusion pressure, K is the extrusion constant, and A_0/A is the reduction ratio.

(5) Not measured.

As shown earlier (Figure 17), the surface of a TV-20 bar after ingot breakdown extrusion is characterized by deep longitudinal striations. As also mentioned, these striations were completely removed in conditioning the bar to the 4.42-cm (1.74-in.) diameter for re-extrusion. In some cases, the extreme lead end or nose of the TV-20 bar did not clean up at this diameter. In such cases, the nose was machined until the surface striations were completely removed, and then cold-rolled into bar stock of various sizes. In general, the yield of usable material for re-extrusion was approximately 60% of the weight of the original starting billet. Solid pieces from the lead and tail ends and chips generated in machining can be recycled to improve the yield of recoverable metal.

Samples for metallographic examination from the lead and tail ends of an extruded bar revealed no observable microstructural changes along the length of the bar. Both samples were recrystallized and uniformly fine-grained across the diameter.

Initially, billets for re-extrusion, machined from extruded ingot stock, were nondestructively tested by an ultrasonic through-transmission test. No defects were observed in any of the billets so tested. Since there was no evidence that defects were being initiated in the breakdown extrusion operation, further testing other than visual inspection was eliminated.

D. Re-extrusion of Tube-blanks, Sheet-bar, and Bar

The conditioned billets of extruded V-20w/oTi (TV-20) were re-extruded into bar, sheet-bar, and tube-blanks on the 318-metric-ton (350-ton) vertical extrusion press described earlier. In all cases, the billets were canned in Type 304 stainless steel to prevent contamination during heating and extrusion. The billets, 4.42 cm (1.74 in.) in diameter, were placed in a 5.1-cm-OD x 4.43-cm-ID x approximately 16.5 cm-long (1.95-in.-OD x 1.75-in.-ID x approximately 6.5-in.-long) can. In the case of billets for tube-blank extrusion, an inner liner tube was incorporated into the billet as seen in Figures 18 and 19. This inner liner tube initially varied in size, but eventually standardized to a 1.59-cm-OD x 1.43-cm-ID (0.625-in.-OD x 0.563-in.-ID) size for extrusion over a 1.27-cm (0.500-in.) tool-steel mandrel. As before with billets for ingot extrusion, an inert-atmosphere glovebox was used for assembling the components and making the end-plug closure weld.

Assembled billets were preheated in an induction coil to the extrusion temperature of 1100°C (billets were also extruded at 1000 and 1200°C for comparison purposes). Heating times were approximately 5.5 min with an additional 5-min soak time at the specific billet temperature. The billets were manually transferred from the heating coil to the extrusion press. A transfer time of approximately 10 sec to the initiation of extrusion normally elapsed. As before, lubrication consisted of a MoS_2-graphite-oil mixture.

Extrusion speeds were approximately 10 to 15 cm/sec (4 to 6 in./sec). The dies incorporated a 120° approach angle and were of H-12 tool steel hardened to 47 to 50 R_C. The dies used for sheet-bar extrusion measured 0.63 x 2.54 cm (0.125 x 1.00 in.), the specific die design being shown in Figure 20.

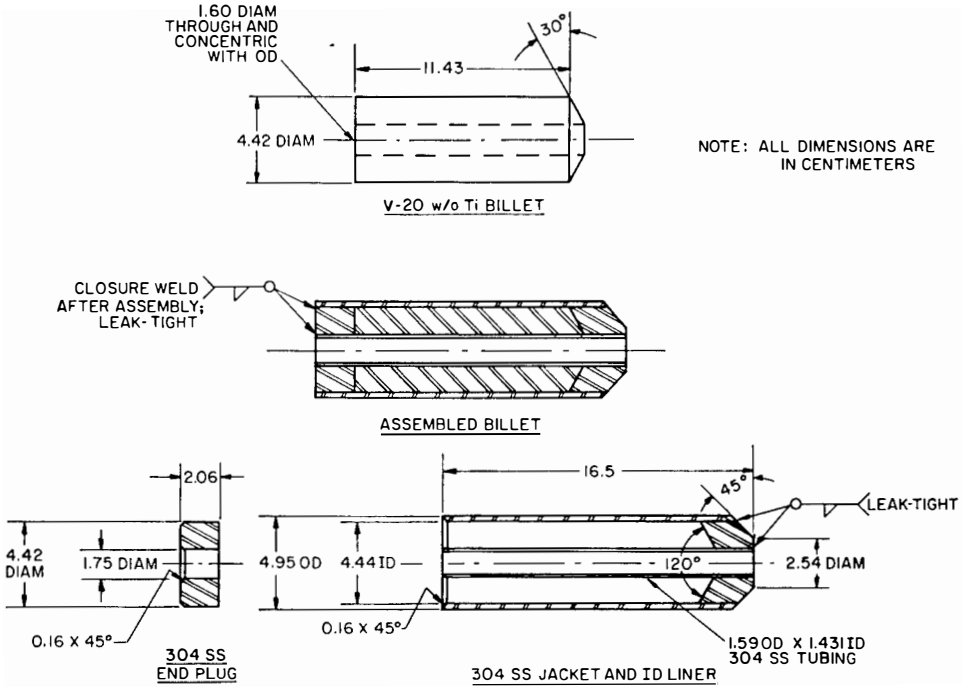

Figure 18. Billet Design for Tube-blank Extrusion

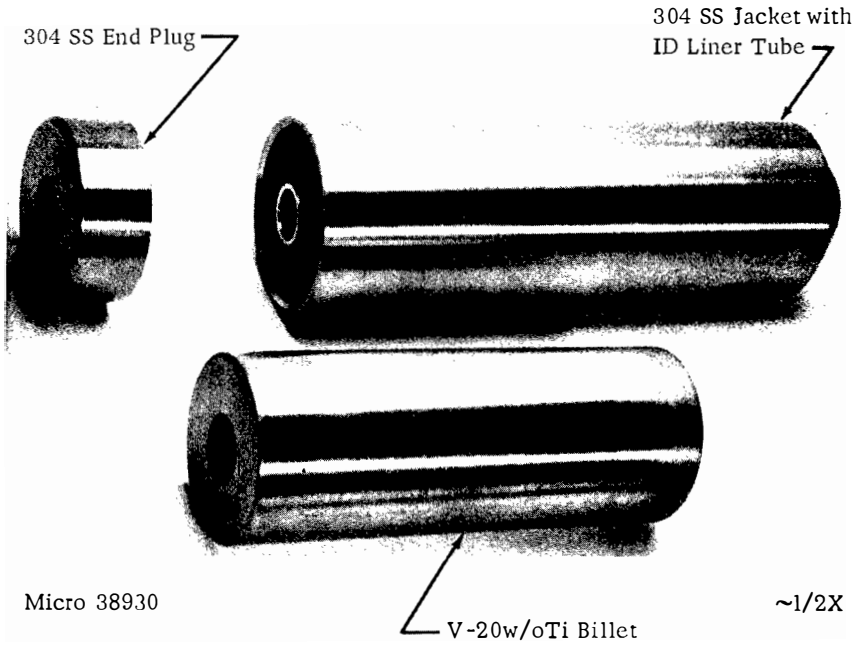

Figure 19. Photograph of Billet Components for Extrusion of V-20w/oTi Tube-blanks

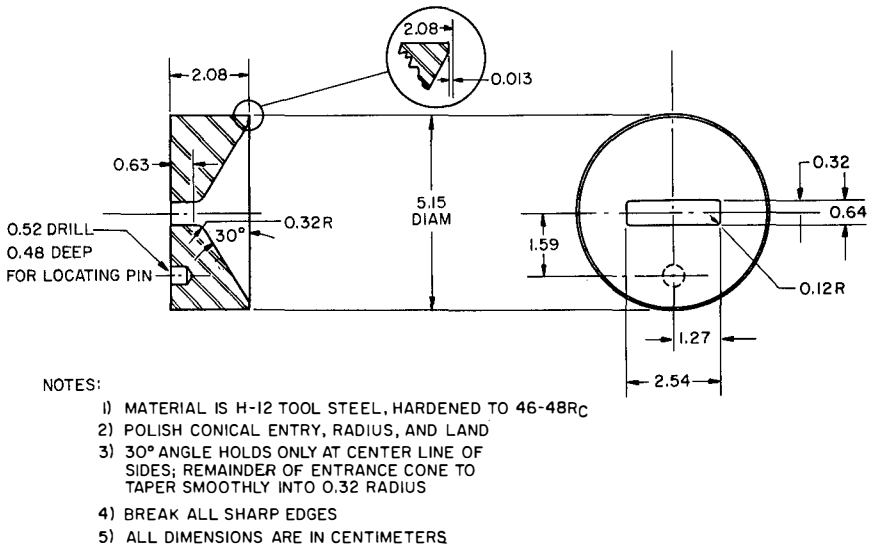

Figure 20. Die Design for Sheet-bar Extrusion

Tube-blanks were extruded over a tool-steel mandrel fabricated from H-12 tool steel and hardened to 46 to 50 R_C. The mandrel sizes were 1.14 or 1.27 cm (0.450 or 0.500 in.) in diameter, the latter size being more common. A floating-mandrel technique was used wherein the mandrel was held in the dummy block and the assembly placed in the billet before extrusion. A graphite-cut-off plug was located between the billet and the dummy block. Initial tube-blank extrusions were effected with a MoS_2-graphite-synthetic oil mixture as a lubricant on the mandrel. However, extruded tube-blanks showed an irregular and rough inner surface that was objectionable for secondary fabrication and difficult to remove by conditioning. Later extrusions were effected with a pre-extrusion application of a glass lubricant to the mandrel. The lubricant, which consisted of a slurry of Corning 7052 glass, water, and "Alignate," was painted on the mandrel and oven-dried. At the billet extrusion temperature of 1100°C, the glass softened enough to act as a lubricant during extrusion. This technique markedly improved the quality of the extruded inner surface and eliminated the need for mechanical conditioning before secondary fabrication. This is highly desirable since internal conditioning of an extruded tube-blank with an ID of $\leq$ 1.3 cm (0.5 in.) can prove both difficult and costly. Since the inner surface of the TV-20 billet was protected by stainless steel, no problems with an alloy/glass reaction were encountered.

After extrusion, the stainless-steel jacket on the external surface of the billet was removed by stripping. (The surface quality obtained on re-extrusion was shown earlier in Figure 17.) At worst, extruded products required only a light belt-sanding to condition the surface before cold-working operations. For tube-blank extrusions, the outer steel jacket was removed in a similar manner, while the inner steel liner [approximately 0.4 mm (0.015 in.) thick at this stage] was removed by pickling in a hot 35 to 50 v/o HCl solution.

Table V shows data obtained upon re-extrusion of TV-20 into sheet-bar and tube-blanks. The re-extrusion constant at 1100°C is approximately 4,100 kg/cm^2 (58,000 psi). This contrasts with a value of 3,700 kg/cm^2 (53,000 psi) for Type 304 stainless steel extruded at 1100°C under similar conditions of lubrication, die design, and extrusion speed. For a limiting stem pressure of 12,600 kg/cm^2 (180,000 psi), this average extrusion constant of TV-20 at 1100°C corresponds to a maximum reduction ratio of approximately 18:1. The variation in the extrusion constant is rather high, and the reasons for this variance are unknown at this time.

Although the tooling dimensions varied for many of the initial tube-blank extrusions, conditions were later standardized to an approximate 11:1 reduction ratio at 1100°C when a 1.27-cm (0.500-in.)-diameter mandrel and an approximate 1.95-cm (0.77-in.)-diameter die are used. After removal of the stainless steel and light conditioning of the surface, the dimensions of extruded tube-blanks were approximately 1.80-cm OD x 1.25-cm ID (0.710-in. OD x 0.490-in. ID), with some 1.93-cm OD x 1.31-cm ID (0.760-in. OD x 0.515-in. ID).

E. Product Evaluation

Although no nondestructive testing was performed on bar or sheet-bar extrusions before secondary fabrication, extruded tube-blanks were inspected thoroughly at the onset of the program. After dejacketing and light vapor-blasting operations, extruded tube-blank surfaces were carefully examined under a low-power microscope, and the inner surface was inspected with a borescope. The tube-blanks were then lightly belt-sanded on the outer surface (if sanding was required) and sent to the Nondestructive Testing Group for an ultrasonic examination. The reject level was set for defects in excess of 10% of the wall thickness. Most extruded tube-blanks were of good quality although, initially, the rough inner surface made it difficult to inspect the tube to the 10% defect level. With the adoption of the glass coating on the mandrel, the inner surface was sufficiently improved to insure reliable nondestructive testing at the required defect level. Short lengths from the lead end and the tail end of the tube blank were generally rejected since the ends were where most of the defects were located and where the "extrusion defect" (nonuniform deformation) occurred.

The typical microstructure of an extruded tube-blank is shown in Figure 21. This is a longitudinal section of a tube-blank extruded at 1100°C and a 13:1 reduction ratio (Extrusion No. 266). The tube-blank has a recrystallized and uniformly fine-grained structure. A minor amount of particles aligned in the extrusion direction as "stringers" can be seen. (These stringers were also present in the microstructure of extruded sheet-bar. They had no directional effect on the properties of finished sheet, as discussed in Appendix D.) No microstructural variations were observed

along its length. Hardness measurements on the as-extruded tube-blank averaged 206 DPH (93 R_B) compared with 208 DPH (94 R_B) for the arc-cast ingot.

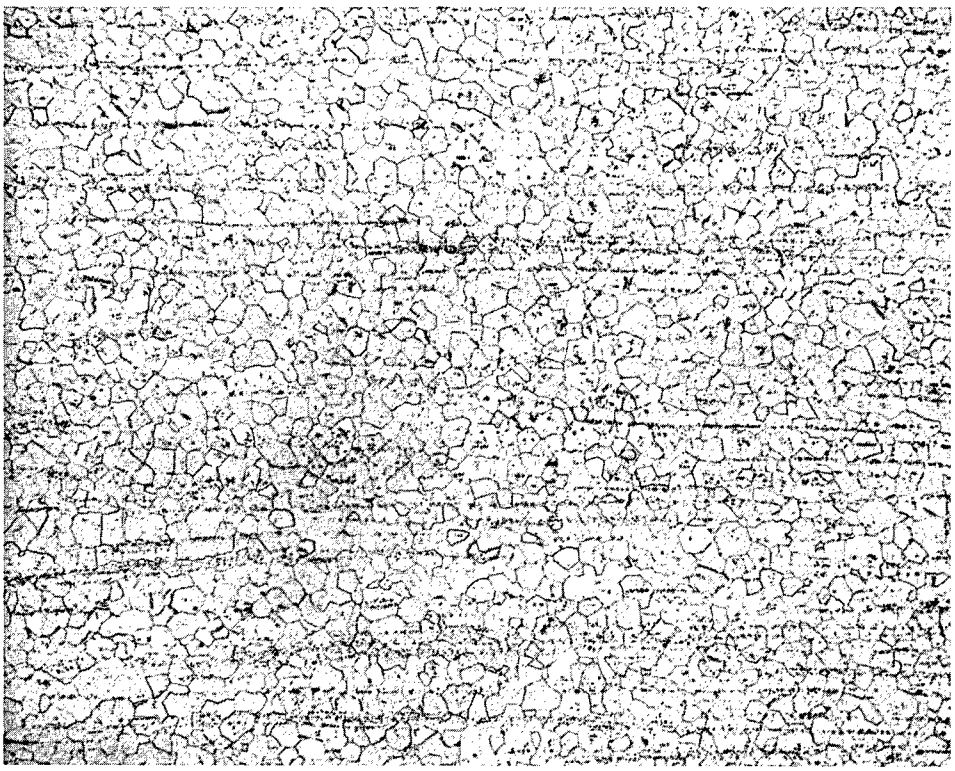

Micro 38746 150X

Etchant: 10% KOH, 10% $K_3Fe(CN)_6$

Figure 21. Longitudinal Microstructure of a V-20w/oTi Tube-blank Extruded at 1100°C and 13:1 Reduction Ratio (Extrusion No. 266)

V. SECONDARY FABRICATION

Bar, rod, and sheet of various thicknesses were fabricated in a fairly conventional manner by cold-rolling extruded bar or sheet-bar products. Tubing fabrication utilized swaging and drawing operations on extruded tube-blanks. Tube sinking was avoided to assure final quality.

A. Equipment

Four rolling mills were used in fabricating bar, rod, and sheet products of V-20w/oTi (TV-20). A 23- x 41-cm (9- x 16-in.), two-high, United mill was used for rolling bar and rod stock. A small, 8- x 13-cm (3- x 5-in.), two-high Stanat mill was used to roll rods smaller than 0.82 cm (0.323 in.) in diameter. The pass sizes and reductions for each of these mills are shown in Table VII. A 43- x 61-cm (17- x 24-in.), two-high, United mill was used for initial cold breakdown of extruded sheet-bar to a 0.15-cm (0.060-in.) thickness. A 15- x 36- x 30-cm (6- x 14- x 12-in.), four-high Bliss mill was used for additional cold-rolling of TV-20 sheet to a 0.04-cm (0.016-in.) thickness.

Table VII

ROD ROLLING SCHEDULES

Roll Pass	Two-high United Mill 23- x 41-cm (9- x 16-in.) Large-roll Passes		Two-high United Mill 23- x 41-cm (9- x 16-in.) Small-roll Passes		Two-high Stanat Mill 9 x 13 cm (3 x 5 in.)	
	Pass Size, cm (in.)	Percent Reduction	Pass Size, cm (in.)	Percent Reduction	Pass Size, cm (in.)	Percent Reduction
1	3.81 (1.500)	12[1]	2.34 (0.920)	15[2]	0.95 (0.375)	4[3]
2	3.56 (1.400)	13	2.16 (0.849)	15	0.86 (0.340)	17
3	3.33 (1.310)	12	1.99 (0.783)	15	0.77 (0.305)	20
4	3.12 (1.230)	12	1.83 (0.722)	15	0.69 (0.270)	22
5	2.93 (1.155)	12	1.69 (0.666)	15	0.61 (0.240)	21
6	2.74 (1.080)	12	1.56 (0.614)	15	0.55 (0.215)	20
7	2.58 (1.015)	12	1.46 (0.575)	12	0.50 (0.195)	17
8	2.54 (1.000)	3	1.37 (0.539)	12	0.44 (0.175)	20
9			1.28 (0.504)	12	0.40 (0.157)	21
10			1.20 (0.473)	12	0.36 (0.140)	21
11			1.12 (0.443)	12	0.32 (0.125)	20
12			1.07 (0.422)	9		
13			1.02 (0.402)	9		
14			0.97 (0.382)	9		
15			0.91 (0.364)	10		
16			0.89 (0.349)	8		
17			0.86 (0.337)	7		
18			0.82 (0.323)	8		

[1]Entering a 4.07-cm (1.6-in.) bar.
[2]Entering a 2.54-cm (1.0-in.) bar.
[3]Entering a 0.97-cm (0.382-in.) bar.

Three Fenn swagers (1F, 2F, and 3F), two hydraulic drawbenches, and a tube straightener were used in the course of tubing fabrication. The draw benches were of 2,270- and 4,550-kg (5,000- and 10,000-lb) capacities. The larger drawbench is shown in Figure 22. The straightener, shown in Figure 23, is capable of handling tubing of 0.3- to 1.3-cm (0.125- to 0.500-in.) diameter.

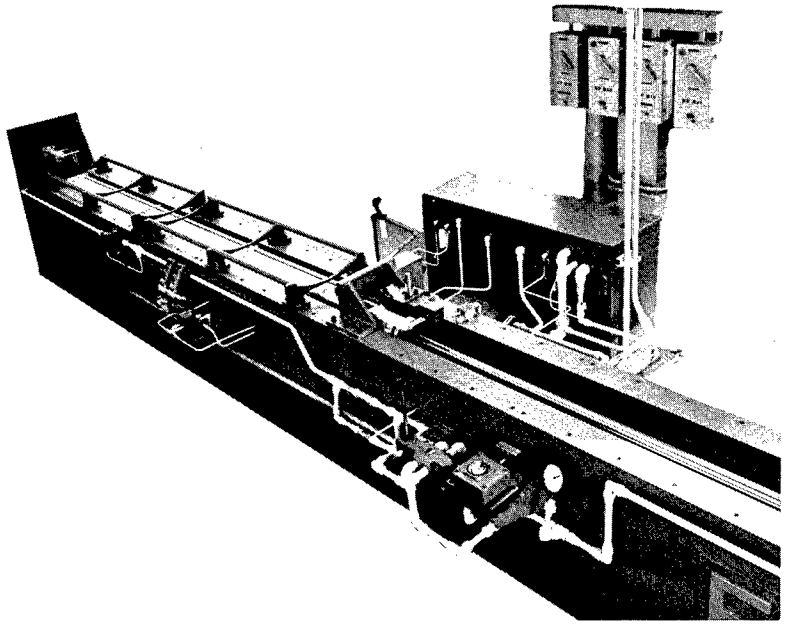

106-7042

Figure 22. Photograph of 4,550-kg (10,000-lb) Fenn Drawbench

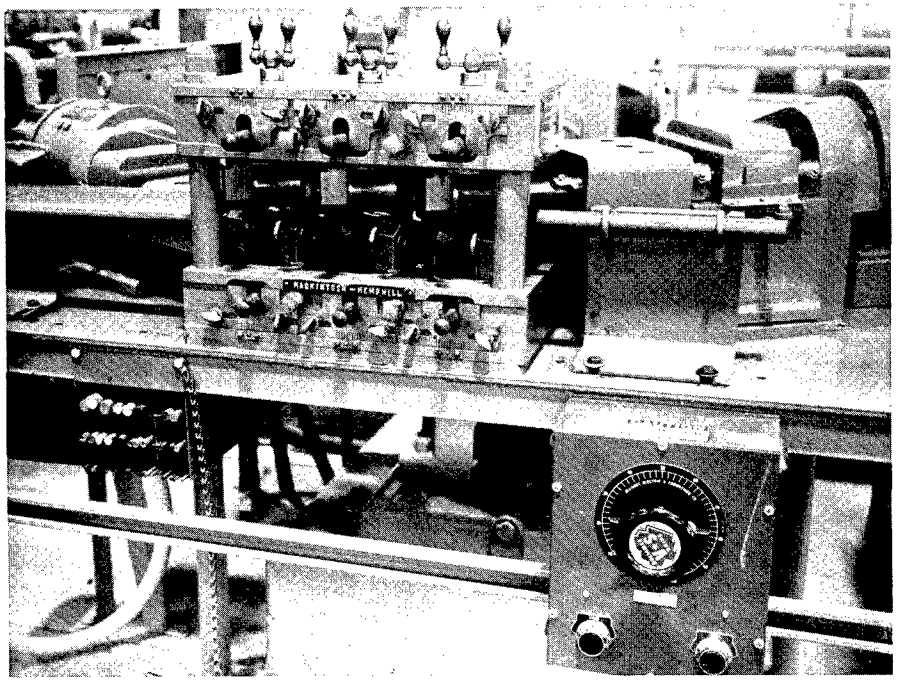

40248

Figure 23. Photograph of Six-skewed-roll Mackintosh-Hemphill Tube Straightener

TV-20 products were annealed or stress relieved in two furnaces, both of which were resistance-heated and capable of maintaining vacuums of 10^{-5} Torr at temperatures up to about 1100°C. The normal time to reach temperature after pump-down averaged about 1.5 hr for each furnace.

B. Cold Rolling of Bar, Rod, and Sheet

After removal of the stainless-steel jacket from a TV-20 ingot extrusion (Extrusion No. 290, see page 36), the heavily striated surface was removed by machining to a 3.3-cm (1.3-in.) diameter. One small piece of the machined bar was cold-rolled to a diameter of 2.62 cm (1.03 in.) (37% reduction in area) on the 23- x 41-cm (9- x 16-in.) mill. This bar was annealed for 1 hr at 900°C, nondestructively tested, and delivered to the requestor.

The balance of the machined bar stock was to be rolled and swaged to a diameter of 1.27 cm (0.50 in.), with an intermediate vacuum anneal at a diameter of 2.15 cm (0.85 in.) (57% reduction in area). The first piece rolled using this schedule split longitudinally before attaining the 2.15-cm diameter. The schedule was revised so that the material was rolled to a 2.54-cm (1.00-in.) diameter (41% reduction in area), vacuum-annealed, rolled to a 1.83-cm (0.72-in.) diameter (62% reduction in area), annealed, and finish-rolled to the final diameter of 1.37 cm (0.539 in.) (43% reduction in area). No cracking was encountered when this schedule was followed. The rolled rods were swaged to the final 1.27-cm (0.500-in.) diameter. The swaging also helped to make the rods round and straight. Finally, the material was cleaned, nondestructively tested, and given the required anneal before delivery.

An earlier extrusion (No. 262) was made available for conversion to rod stock. The starting diameter was 1.53 cm (0.6 in.), and the surface was such (owing to the use of the double-extrusion technique) that a light conditioning by belt-sanding was sufficient. The schedule called for conversion of the extruded and conditioned bar into a 0.75- and 0.55-cm (0.296- and 0.215-in.)-diameter rod.

After cold-rolling on the 23- x 41-cm (9- x 16-in.) mill to a 0.99-cm (0.382-in.) diameter, corresponding to a 59% reduction in area, the rod was sectioned, cleaned, and vacuum-annealed for 1 hr at 900°C. Rolling was continued on the same mill until the rod reached a diameter of 0.82 cm (0.323 in.). At this stage, the rod was swaged to a 0.75-cm (0.296-in.) diameter and the required length of material removed. The balance of the material was rolled to a 0.635-cm (0.260-in.) diameter on the small, 8- x 13-cm (3- x 5-in.), Stanat mill. After the final pass, the rods were swaged to a nominal diameter of 0.546 cm (0.215 in.). All rod stock was sectioned into suitable lengths, cleaned, and vacuum-annealed at 900°C for 1 hr. Annealed rods were nondestructively tested before delivery.

V-20w/oTi (TV-20) sheet of 0.15- and 0.04-cm (0.060- and 0.016-in.) thickness was requested for mechanical-property and corrosion test specimens. Starting material for sheet-rolling consisted of extruded sheet-bar produced by the double-extrusion technique described earlier (see page 37). The stainless-steel jacket was removed by mechanical peeling, and the TV-20 sheet-bar was lightly conditioned by belt-sanding. The microstructure of a typical as-extruded sheet-bar (Extrusion No. 281) is shown in Figure 24. The conditioned sheet-bar measured approximately 0.53 x 2.52 cm (0.210 x 0.990 in.), and the hardness was 215 DPH (94 R_B).

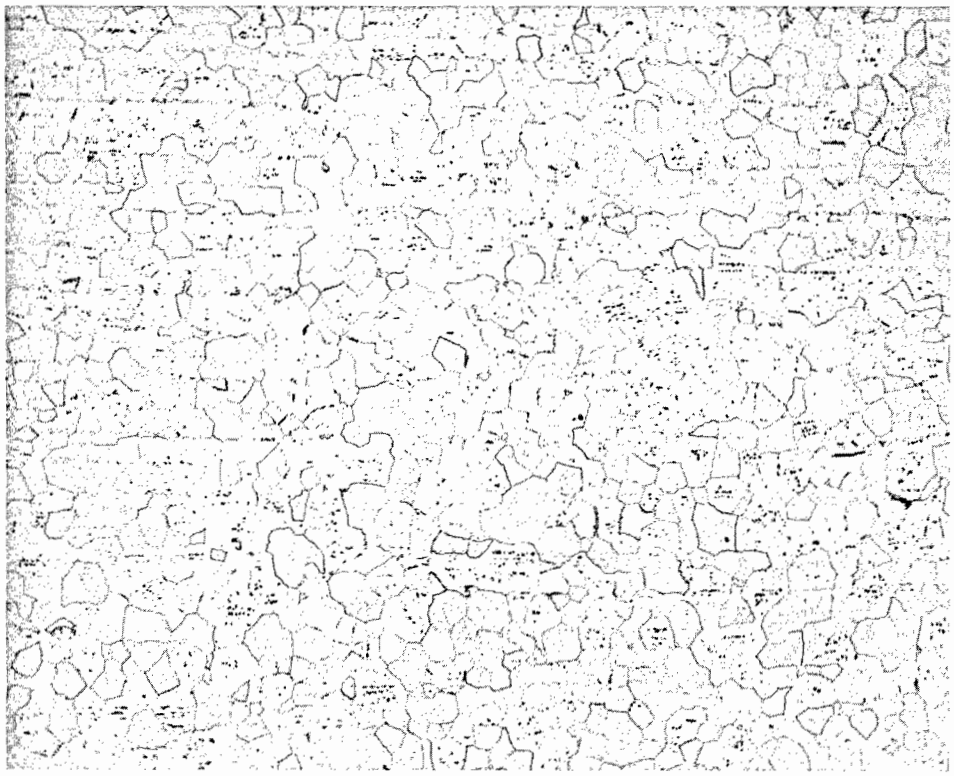

Micro 38952 150X

Etchant: 5% HF, 2% $AgNO_3$

Figure 24. Longitudinal Microstructure of V-20w/oTi Sheet-bar Extruded at 1200°C and a 13:1 Reduction Ratio (Extrusion No. 281)

The sheet-bar was sectioned into suitable lengths and long-rolled (i.e., rolled in the extruded direction) on the 43- x 61-cm (17- x 24-in.) United rolling mill. Reductions of approximately 5% per pass were used for the first few passes to level the bar, and then 10% reductions were used. The stock was rolled to a 0.25-cm (0.100-in.) thickness on this mill and finish-rolled to the desired 0.15-cm (0.060-in.) thickness (approximately 65% reduction in area) on the 15- x 36- x 30-cm (6- x 14- x 12-in.) Bliss four-high mill. The microstructure of the 0.15-cm cold-rolled sheet is shown in Figure 25a; the hardness was 289 DPH (28 R_C).

(a) 0.15-cm (0.060-in.) sheet, as rolled; 289 DPH (28 R_C)

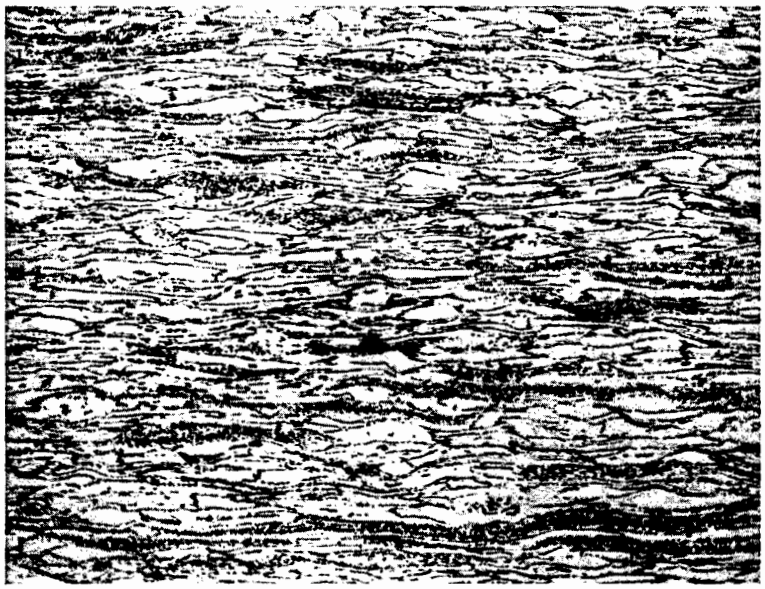

Micro 38953 150X

(b) Annealed for 1 hr at 900°C; 203 DPH (92 R_B)

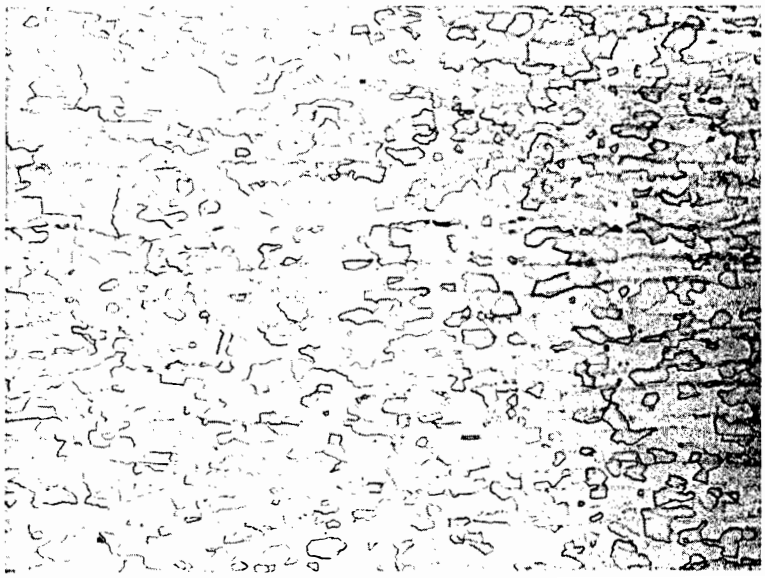

Micro 38954 150X

Figure 25. Longitudinal Microstructures of 0.15-cm (0.060-in.)-thick V-20w/oTi Sheet (a) after Rolling (~65% cold work) and (b) after Annealing for 1 hr at 900°C (Etchant: 2% HF, 5% $AgNO_3$)

A portion of the above cold-rolled sheet was stress-relieved for 1 hr at 700°C.* The resultant microstructure was identical to the as-rolled structure (Figure 25a). The stress-relieving treatment dropped the hardness to 222 DPH (95 R_B). Other sections of the cold-rolled material were vacuum-annealed for 1 hr at 900°C. The annealing produced the microstructure shown in Figure 25b and a DPH value of 203 (92 R_B). The stress-relieved sheet and a portion of the annealed sheet were nondestructively tested before delivery to the requestors.

The remainder of the annealed sheet was further long-rolled on the four-high mill to the final thickness of 0.04 cm (0.016 in.) (approximately 70% reduction in area). Reductions of 10 to 15% were used during this rolling sequence. The as-rolled hardness was 278 DPH (27 R_C), and the microstructure is shown in Figure 26a.

Half of this 0.04-cm sheet was stress-relieved for 1 hr at 700°C.* The stress-relieved hardness measured 195 DPH (91 R_B), and the microstructure is shown in Figure 26b. The structure indicates that recrystallization is well along, contrasted to the cold-worked structure of the stress-relieved 0.15-cm (0.060-in.) sheet. The remainder of the 0.04-cm sheet was vacuum-annealed for 1 hr at 900°C, with the annealed hardness measuring 191 DPH (90 R_B). The annealed microstructure is shown in Figure 26c.

In addition to the sheet mentioned above, an additional sheet, 0.15 and 0.04 cm (0.060 and 0.016 in.) thick, was rolled from material that had received a solution heat-treatment after extrusion. As will be described later in the report, this solution heat-treatment eliminated the "stringering" found in the as-extruded structure. The microstructure of extruded and solution heat-treated material is shown in Figure 27. This material was cold-rolled in much the same manner as sheet material already described. The major differences were that pass reductions were limited to 5% per pass during a major portion (to a 0.2-cm thickness) of the schedule to the 0.15-cm (0.060-in.) thickness, and the sheet was "double-passed" (i.e., twice through for each reduction). There appeared to be a greater tendency for this material to edge-crack and for these cracks to propagate into the body of the sheet. The microstructures of the solution heat-treated and rolled sheet after cold-rolling and after vacuum-annealing were identical to those shown earlier. There were no microstructural differences in finished products as a result of the solution heat-treatment.

In summary, no difficulties were encountered in cold-rolling extruded stock into bar and rod. The splitting that occurred in rolling the one section of the larger extruded bar may have been due to: (1) limitation of the amount

*Based on later heat-treatment studies discussed in Appendix C, the stress-relieving temperature of 700°C may be too high if the objective is to relieve internal stresses while avoiding any marked degree of recrystallization.

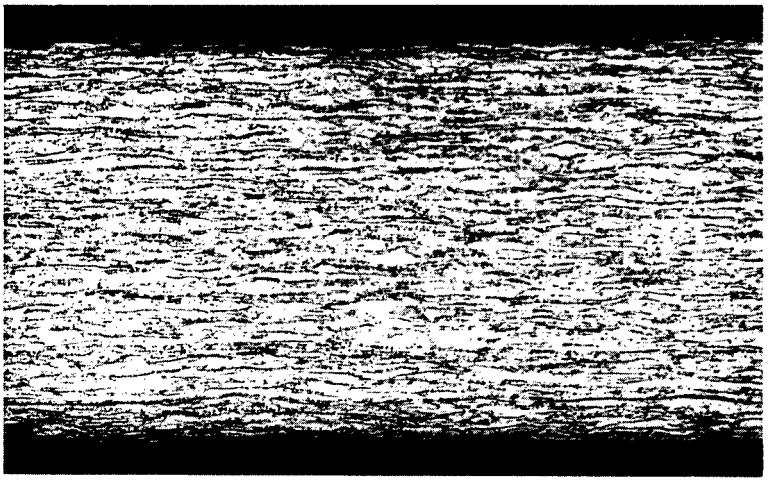

(a) 0.41-cm (0.016-in.) sheet, as-rolled; 278 DPH (27 R_C)

Micro 38955 150X

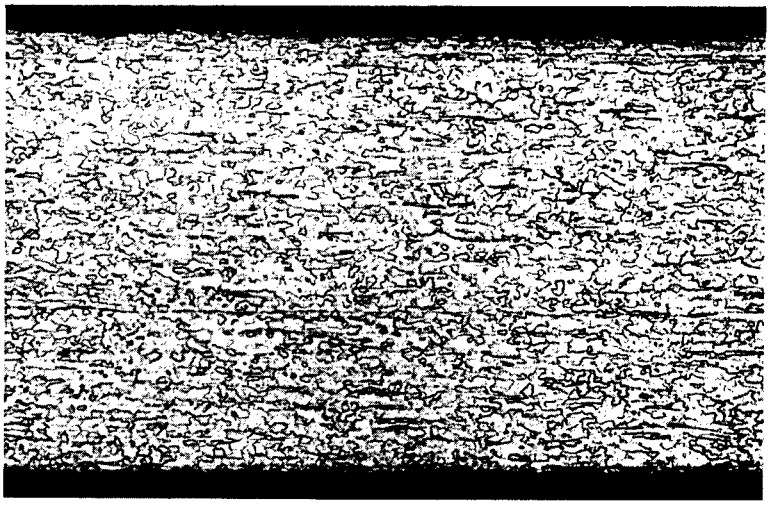

(b) Stress-relieved for 1 hr at 700°C; 195 DPH (91 R_B)

Micro 38964 150X

(c) Annealed for 1 hr at 900°C; 191 DPH (90 R_B)

Micro 38965 150X

Figure 26. Longitudinal Microstructures of 0.41-cm (0.016-in.)-thick V-20w/oTi Sheet (a) after Rolling (~70% cold work), (b) after Stress-relieving for 1 hr at 700°C, and (c) after Annealing for 1 hr at 900°C (Etchant: 2% HF, 5% $AgNO_3$)

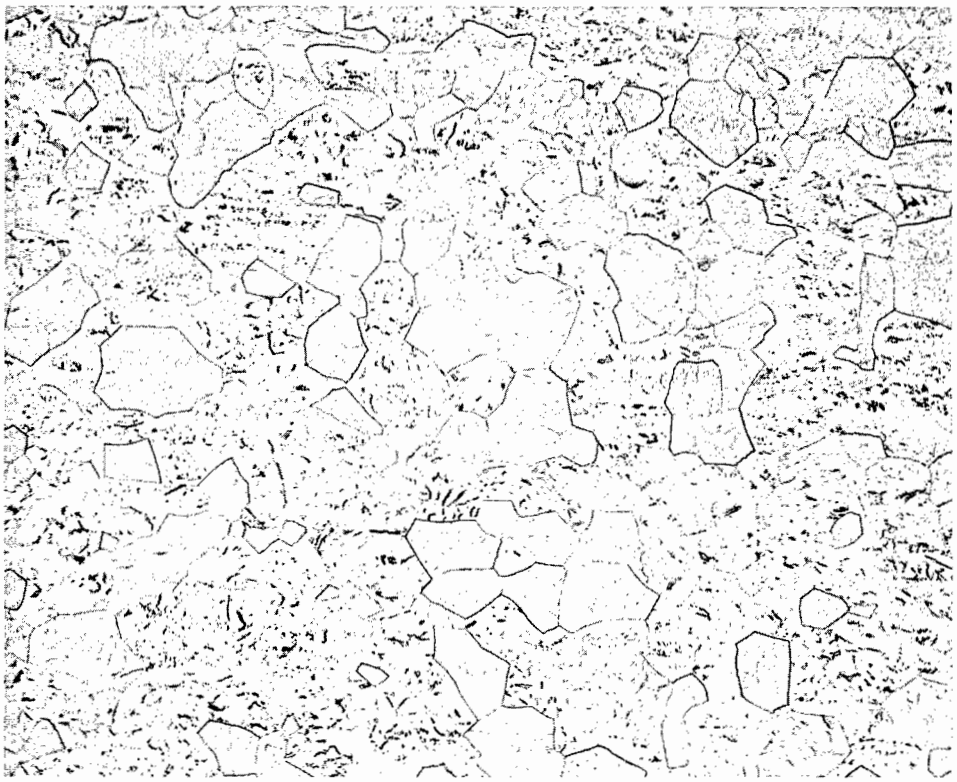

Micro 38550 150X

Etchant: 10% KOH, 10% $K_3Fe(CN)_6$

Figure 27. Longitudinal Microstructure of Extruded V-20w/oTi Sheet-bar after Solution Heat-treatment for 15 min at 1300°C

of hot-working by the scheduling of only one extrusion, (2) unduly high surface stresses caused by the use of a roll whose diameter was insufficient to work the large-diameter material to a sufficient depth, (3) the possible inability of large-diameter bars of the alloy to tolerate as much cold work before annealing as smaller-diameter rods. No defects such as center bursts or radial cracks were encountered. Surface quality after rolling was very good.

The flat rolling of extruded sheet-bar - both solution heat-treated and untreated - to 0.15- and 0.04-cm (0.060- and 0.016-in.) sheet was accomplished with no major difficulty. The material was given from 70 to 75% total reductions in area before annealing. Reductions of the order of 5 to 15% per pass were used. Some minor edge-cracking did occur.

C. Tubing Fabrication Development

Starting material for secondary fabrication of small-diameter, thin-wall tubing consisted of tube-blanks extruded by the technique described earlier (see page 37). The conversion of these blanks to the desired final tube sizes required the use of two different methods of fabrication, namely

swaging* and drawing. These techniques are reviewed in detail in the following paragraphs. Since there was no prior tubing fabrication history for the V-20w/oTi alloy, considerable development work was necessary to establish procedures that would guarantee a high-quality finished tube.

1. Swaging Procedures

The conversion of extruded tube-blanks required an initial swaging operation to true-up the wall, improve the surface finish, and obtain the proper D/t (OD-to-wall thickness) ratio before further drawing. (Swaging was also used at intermediate steps in the drawing operation for core and/or mandrel removal and readjustment of the D/t ratio as will be described later.)

Initially, extruded tube-blanks with no prior surface conditioning were swaged over a hard tool-steel mandrel through three passes to effect a total reduction in area of approximately 35 to 40%. After the third pass, the D/t ratio of the swaged tubes was approximately 10:1, which was the ratio desired for starting the ductile-core drawing operation. While the three-pass swaging was successfully accomplished, the quality of the swaged tubes left much to be desired. Although the dimensional control and surface finish were excellent, ultrasonic nondestructive examination of the swaged tubes indicated that serious longitudinal defects (and in some cases, radial defects) were present in almost all tubes. Because of these findings, and the resultant low yield of acceptable material for further processing, it became necessary to evaluate thoroughly the parameters of swaging extruded tube-blanks.

Accordingly, several tube-blanks were prepared as follows:

No. 1: As extruded

No. 2: Outer surface conditioned by belt sanding

No. 3: Inner and outer surfaces machined

No. 4: Conditioned outer surface (belt sanding); tube-blank annealed after each swage pass

No. 5: Conditioned outer surface (belt sanding), inner surface acid etched; outer surface re-etched and tube-blank annealed after each swage pass.

All the tube-blanks were ultrasonically inspected and found to be sound before swaging as outlined below:

*Swaging probably could be eliminated by tube reducing. A tube reducer is not available at ANL, but some progress has been made in tube reduction through industrial participation (see page 58).

a. Tube No. 1. The tube was swaged in one pass over a hardened-steel mandrel to an approximate 19% reduction in area. Ultrasonic examination indicated numerous longtiudinal cracks with depths ranging from 8 to 10% of the wall thickness.

b. Tube No. 2. The tube was swaged in one pass over a hardened tool-steel mandrel to a reduction of approximately 11%. Ultrasonic inspection indicated no defects initiated at this stage. The tube-blank was reswaged with an additional 19% reduction (total resultant reduction approximately 30%) and ultrasonically inspected. Inspection revealed longitudinal cracks approximately 4 to 7% of the tube-wall thickness in depth.

c. Tube No. 3. The tube was swaged in one pass on a hardened mandrel to a reduction of approximately 11%. Ultrasonic inspection indicated no defects were generated. The tube-blank was reswaged through the next die with a resulting reduction of approximately 22% (the total reduction at this stage being approximately 30%). Ultrasonic inspection detected no defects.

d. Tube No. 4. The tube was swaged in one pass over a hardened-steel mandrel, with area reduction being approximately 11%; no defects were noted. The tube was cleaned and vacuum-annealed for 1 hr at 900°C. The tube was then reswaged to a 19% reduction. Ultrasonic inspection revealed no gross defects, but indications of minor defects. After cleaning and reannealing at 900°C, the tube was further swaged with an additional 29% reduction in area. Ultrasonic examination indicated numerous shallow defects on the tube ID. A borescopic inspection of the inner surface indicated the presence of numerous longitudinal cracks, which appeared to be caused by metal lap-over during the swaging operation.

e. Tube No. 5. This tube was acid-etched on the inner surface with a 1:2 (by volume) HNO_3-H_2O solution before swaging. After etching, the tube was swaged over a hardened-steel mandrel to an approximate reduction of 11%. Ultrasonic inspection detected no defects. The tube was re-etched as before and vacuum-annealed for 1 hr at 900°C. After annealing, the tube was reduced an additional 22% by swaging, and inspection again revealed no defects. The tube was again re-etched and vacuum-annealed as before and given a final swage pass with reduction of approximately 11%. Inspection after this third pass indicated that the tube was sound and free of defects. A borescopic inspection of the inner surface revealed minor hair-line cracks and/or laps in random areas.

A later tube was worked in a manner similar to that of tube No. 5 but received a final swage pass of approximately 29% reduction in area. Sonic inspection of the tube indicated cracks to a depth of from 5 to 10% of the wall thickness.

The above evaluation showed that a relationship between the surface condition of the extruded tube-blank and the tendency to crack during swaging over a hardened mandrel did exist for this alloy. It was concluded that some conditioning of the tube-blank was necessary to assure final tube quality,* and that the conditioning could be best accomplished by belt-sanding of the outer surface and acid-etching of the inner surface. Etching between swage passes removed laps that had a tendency to be created in the prior pass. Maximum area reductions by swaging over a hardened mandrel should not exceed 25% before annealing if the material is to be sound and free of defects. Reductions of approximately 15 to 20% would be a safer reduction schedule with a probable higher yield of sound tubing.

2. Ductile-core Drawing

The mechanics of ductile-core drawing have been previously reported.[9] The process essentially permits the fabrication of pilot runs of high-quality tubing with a minimum of tooling while more conventional means are being investigated. Quality control results from the internal support of the inner surface, thereby preventing folds, laps, etc., that can occur in tube sinking and can definitely affect the quality of the final product. Early in the program, the decision was made that no deliberate sinking operations would be employed, in order to maximize tube quality.

Initial ductile-core drawing operations utilized either hard-drawn or annealed copper cores. The copper provided adequate support for the tube inner surface and essentially maintained the starting D/t ratio of the tube when carbide drawing dies were used. While Teflon (applied by an aerosol technique) proved to be a good lubricant, it was not entirely satisfactory. The TV-20 tubes tended to gall seriously unless the dies were kept spotlessly clean. Even with meticulous die care, it was difficult to obtain an adequate yield of tubing free of objectionable galling or surface striations.

Time did not permit a lengthy evaluation of drawing lubricants, so the galling problem was overcome by using aluminum-bronze dies (Dibronze No. 25) in combination with a heavy chlorinated-wax lubricant (Aldraw J-1). This combination of die material and lubricant resulted in a marked improvement of surface quality of the drawn tubes and was considered satisfactory for tubing production. The draw die design is shown in Figure 28. The entry angle is greater than that used on the carbide dies available at ANL.

The use of aluminum-bronze dies with their greater entry angle resulted in a decrease in the D/t ratio during the drawing operation. A

*As the program progressed, the surface quality of the tube-blanks improved to the point where minimum tube-blank conditioning was required.

change that was also made in the swaging procedure had the effect of lowering the D/t ratio going into drawing and resulted in a need for additional thinning of the tube wall during drawing. To compensate for the above effects, a core of cold-rolled steel was substituted for the copper core in the initial ductile-core drawing stage. Drawing of this composite resulted in a large amount of wall thinning and a corresponding increase in the D/t ratio during the draw. The attained D/t ratio was sufficient to allow the rest of the drawing to be done with cores of hard-drawn copper. Readjustment for any loss in D/t ratio during drawing with copper was readily achieved by plug drawing.

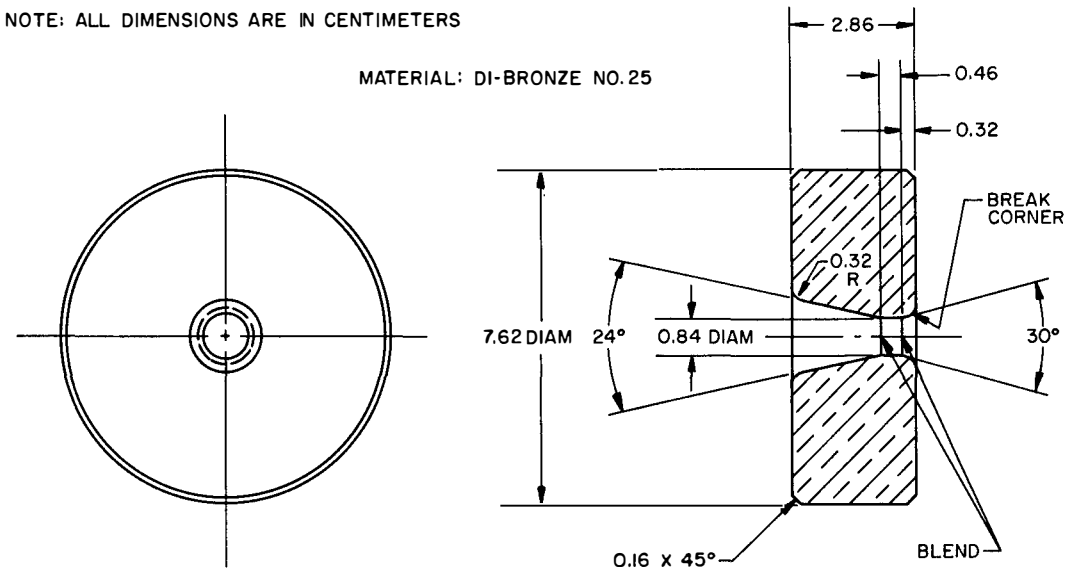

Figure 28. Typical Die Design for Ductile-core Drawing of V-20w/oTi Tubing

Initially, the core or mandrel was removed by swaging. A light reduction, combined with a slow feed and a number of passes through a die, was necessary to sufficiently loosen the core or mandrel. After swaging, the core or mandrel was extracted on a drawbench. Later, the core was removed by reeling on the Mackintosh-Hemphill skewed-roll tube-straightener. The roll setting essentially had no offset, and the contact area was at a minimum. Several passes of the composite tube and core through the straightener with use of moderate roll pressure was sufficient to expand the tube off the core. Rapid expansion (i.e., heavy roll pressure so expansion could be accomplished in one to three passes) and/or expansion of the tube beyond a 0.25-mm (0.010-in.)-diameter increase usually resulted in splitting or generation of ID defects. Expansions of the tube diameter from 0.12 to 0.25 mm (0.005 to 0.010 in.) was sufficient to permit easy removal of the core, yet insure quality tubing.

Initially, difficulty was experienced in removing the cores of copper and steel by reeling. The steel cores were the most difficult to

remove. It was apparent that bonding had occurred within some areas of the tube ID/core interface. This probelm was partially alleviated by cooling the composite bar (tube with core) in water after every draw to remove heat generated during drawing. Further aid was given by the use of a coating on the core before insertion in the tube for drawing. Several substances were tried with varying results. Dag 154 or Aqua Dag thinned with a solvent appeared to be most practical from the standpoint of coating retention, ease of application, and removal.

3. Plug Drawing

Initial problems in removing a mandrel-drawn* TV-20 tube from the mandrel, and the resultant scratches and poor finish on the internal surface of the tube, indicated that at the small finishing sizes of the tube, mandrel drawing would be difficult to control. Plug drawing was investigated as a possible substitute method which, if successful, would greatly facilitate tubing production.

Several plugs were made of aluminum-bronze to match existing carbide die sizes. Attempts to plug-draw intermediate-size tubes [0.94-cm (0.330-in.) OD tubes] were made, but resulted in failure. The apparent difficulty was in die design and in lubrication of the outer surface. Several dies were made of aluminum-bronze having an increased entry angle and shorter land length than the dies for ductile-core drawing. The plug-drawing die design is shown in Figure 29. Trial runs were made by using aluminum-bronze dies and plugs with the Aldraw J-1 drawing lubricant. These plug-draws were successful, but extreme wear of the aluminum-bronze plugs

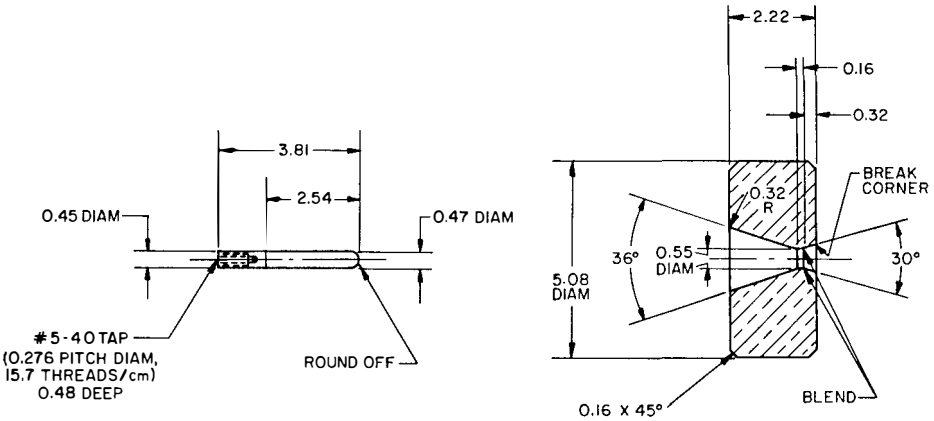

Figure 29. Typical Plug and Die Design for Plug Drawing of V-20w/oTi Tubing

*Mandrel drawing incorporates a free-moving hard mandrel that remains in the tube after the draw. The mandrel is removed by reeling or swaging the tube off the mandrel.

occurred. Plugs of the design shown in Figure 29 were made from Berylco-25 and heat-treated to a hardness of approximately 40 R_C. Using these plugs, together with aluminum-bronze dies and the Aldraw J-1 lubricant, resulted in plugs exhibiting acceptable wear resistance that would be suitable for the tubing production.

Wall-thickness reductions on the order of 20% were achieved in plug-draws in the intermediate sizes. Smaller reductions were necessary in the terminal sizes owing to strength limitations of the plug-holding mechanism and the tube size.

D. Typical Tubing Production Schedule

Approximately 45 meters of TV-20 tubing, measuring from 0.48 to 0.53 cm (0.188 to 0.208 in.) in OD, with a constant wall thickness of 0.04 cm (0.016 in.), were required for fuel-element irradiation testing. In addition, small amounts of tubing, measuring 0.81-cm OD x 0.04-cm wall thickness (0.32-in. OD x 0.016-in. wall) and 0.75-cm OD x 0.05-cm wall thickness (0.29-in. OD x 0.020-in. wall), were required for other tests. A detailed description of the production of a finished TV-20 tube to a size of 0.53-cm OD x 0.04-cm wall follows. A flow sheet of the operations is shown in Figure 30.

Extruded tube-blanks were cut into 30-cm (12-in.) sections and conditioned by belt-sanding the outer surface and then etching in a 35 v/o HNO_3-H_2O solution until the outer and inner surfaces had a uniform gray-blue appearance. The conditioned tube-blanks were approximately 1.80-cm OD x 0.28-cm wall thickness (0.710-in. OD x 0.110-in. wall). A hardened tool-steel mandrel, 1.21 cm (0.475 in.) in diameter, was coated with J-1 lubricant and inserted inside the tube-blank. The tube was swaged through in one direction to a diameter of 1.74 cm (0.685 in.). The tube was slipped off the mandrel and degreased, the resulting tube measuring 1.74-cm OD x 0.26-cm wall thickness (0.685-in. OD x 0.102-in. wall). This first swage operation essentially trued up the tube. The cross-sectional area was reduced approximately 9%, while the wall thickness was reduced approximately 7%.

The tube was acid-etched as before, cleaned, and vacuum-annealed for 1 hr at 900°C. After annealing, the 1.21-cm (0.475-in.) mandrel was recoated and reinserted in the tube, and the assembly was reswaged to a diameter of 1.64 cm (0.645 in.). The cross-sectional reduction for this pass was 22%, the wall thickness being reduced 20%. The tube was again conditioned by re-etching and reannealed for 1 hr at 900°C in vacuum.

The third and final swage utilized a 1.14-cm (0.450-in.)-diameter hardened mandrel. The assembly was swaged to a diameter of 1.55 cm (0.610 in.), the swaged tube measuring 1.55-cm OD x 0.20-cm wall

thickness (0.610-in. OD x 0.079-in. wall). The cross-sectional area reduction of the tube was 12%, whereas the wall-thickness reduction was approximately 6%. Again the tube was conditioned by etching and vacuum-annealed before drawing.

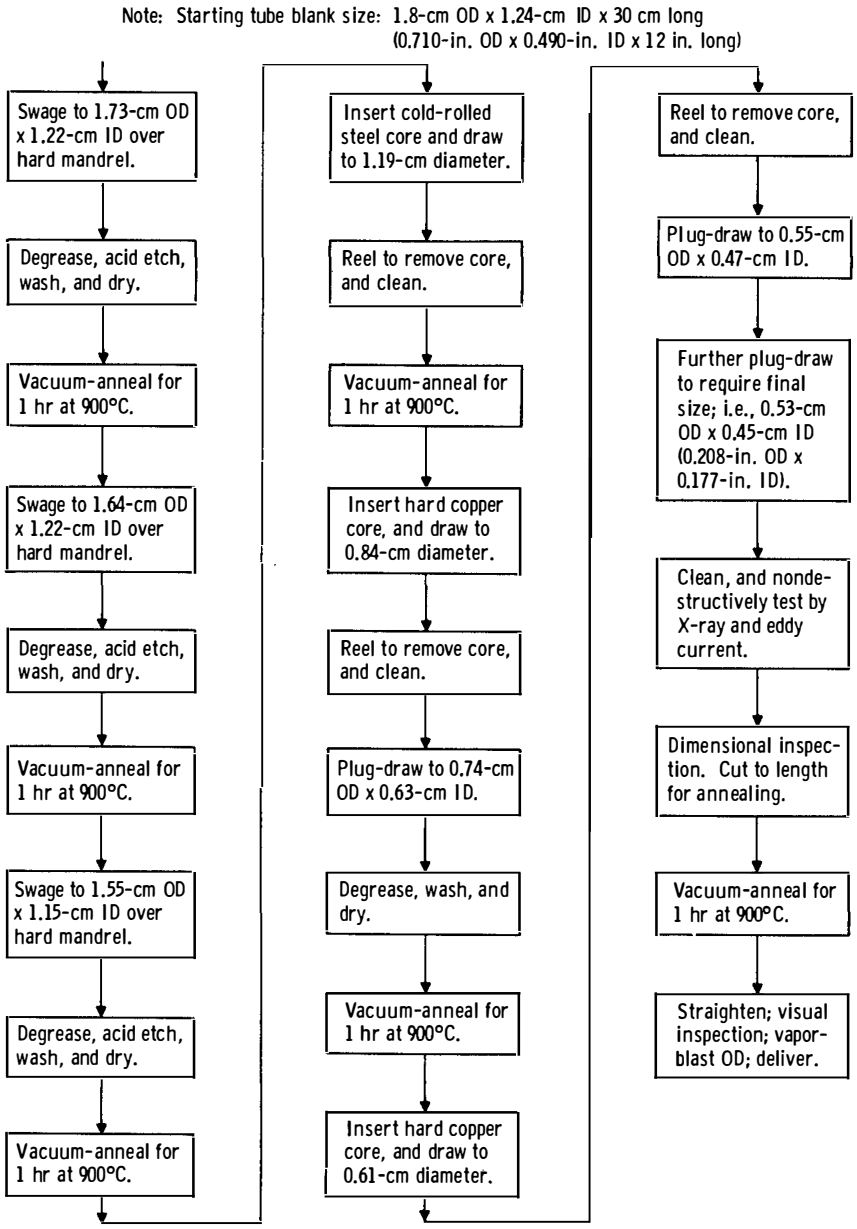

Figure 30. Flow Sheet for Secondary Fabrication of V-20w/oTi (TV-20) Tubing

A cold-rolled steel rod, measuring approximately 1.14-cm (0.450-in.) diameter was coated with Dag-154 (Aqua Dag, thinned with methyl alcohol, was used as an alternate), dried, and inserted in the swaged TV-20 tube. The composite was then swage-pointed and drawn in accordance with the schedule in Table VIII. A commercial lubricant (Aldraw J-1)

Table VIII

DIE SIZES USED IN DRAWING V-20w/oTi TUBING

Die Size, cm (in.)	Remarks
A. Initial ductile core draw with cold-rolled steel core. Starting tube size: 1.55-cm OD x 1.16-cm ID (0.610-in. OD x 0.455-in. ID).	
1.40 (0.550) 1.33 (0.525) 1.27 (0.500) 1.22 (0.470)	After reeling to remove core, tube measures 1.22-cm OD x 0.99-cm ID (0.470-in. OD x 0.390-in. ID). Cross-section reduction = 58%; wall reduction = 49%.
B. Intermediate draw with copper core. Starting tube size: 1.22-cm OD x 0.99-cm ID (0.470-in. OD x 0.390-in. ID).	
1.13 (0.445) 1.07 (0.420) 1.00 (0.394) 0.93 (0.366) 0.88 (0.345) 0.84 (0.330) 0.80 (0.315) 0.74 (0.292)	Reeled to remove copper core. Used in conjunction with a 0.66-cm (0.261-in.)-diameter plug. Used in conjunction with a 0.63-cm (0.249-in.)-diameter plug. Cross-section reduction = 66%; wall reduction = 46%.
C. Final draw with copper core. Starting tube size: 0.74-cm OD x 0.63-cm ID (0.292-in. OD x 0.249-in. ID).	
0.71 (0.281) 0.68 (0.266) 0.65 (0.256) 0.61 (0.241) 0.58 (0.228) 0.55 (0.218)	Reeled to remove copper core. Used in conjunction with a 0.49-cm (0.193-in.)-diameter plug. Used in conjunction with a 0.47-cm (0.186-in.)-diameter plug.

was used during all drawing procedures. It was necessary to cool the composite rod after each draw to prevent bonding and later difficulty in core removal. After the initial ductile-core drawing, the tube size measured 1.19-cm OD x 0.99-cm ID (0.470-in. OD x 0.390-in. ID). The total cross-sectional reduction of the tube was 58%, while the tube-wall thickness was reduced 49%. After completion of the drawing schedule, the tube was lifted off the cold-rolled steel core by reeling on the six-roll straightener. The OD of the tube was expanded a maximum of 0.025 cm (0.010 in.), and the core was withdrawn by hand or with the aid of the drawbench. The tube

was sectioned into 56-cm (22-in.) lengths, cleaned thoroughly, and vacuum-annealed for 1 hr at 900°C. After annealing, the tube was again fitted with a ductile core of hard-drawn copper, as previously described. The composite was drawn in accordance with schedule in Table VIII. Upon completion of drawing to a diameter of 0.84 cm (0.330 in.), the composite was reeled and the core removed. The tube was then cleaned and plug-drawn to adjust the wall thickness. The tube size upon completion of plug drawing was 0.74-cm OD x 0.63-cm ID (0.292-in. OD x 0.249-in. ID). Total reduction for the draw schedule was 66%, whereas wall-thickness reduction was approximately 46%. The tube was sectioned, cleaned, and vacuum-annealed.

After annealing, the tube was fitted with a new core of hard-drawn copper, and drawn in accordance with the schedule in Table VIII. The copper core was removed after drawing the composite to a 0.61-cm (0.240-in.) diameter. The resultant tube had a wall thickness of 0.051 cm (0.020 in.), and it was necessary to plug-draw to reduce the wall thickness. Accordingly, the tube was plug-drawn with aluminum-bronze dies and beryllium copper plugs to a 0.55-cm OD x 0.47-cm ID (0.218-in. OD x 0.186-in. ID). Finally, a sizing draw was made to the finish size of 0.53-cm OD x 0.04-cm wall thickness (0.208-in. OD x 0.016-in. wall). A plug was used during this draw mainly to support the tube ID, as essentially no wall thinning occurred.

After the final sizing plug-draw, the swaged point of the tube was cropped off and the tube cleaned and hand-straightened. Integrity of the tube was evaluated by a nondestructive eddy-current technique to a defect level of less than 10% of the wall thickness. Following a dimensional inspection (micrometer on OD, Sheffield air gauge internally), the tube was cut into required lengths, cleaned, and vacuum-annealed for 1 hr at 900°C. After annealing, the tube was straightened and the outer surface given a light vapor blast before delivery.*

The microstructure of as-drawn tubing of a typical finished size is shown in Figure 31. The as-drawn hardness measured 238 DPH (98 R_B). After annealing, the microstructure showed a uniform, fine-grained, recrystallized structure as shown in Figure 32. Annealed tubing had a hardness of approximately 194 DPH (90 R_B). Figure 33 shows a series of tubes of V-20w/oTi produced at Argonne National Laboratory.

E. Commercial Tubing Fabrication

In addition to tubing produced at Argonne National Laboratory for evaluation and irradiation testing, extruded tube-blanks of V-20w/o Ti have been sent to commercial tube fabricators. The objective is to establish the feasibility of commercial availability of the alloy in tubing form and to

*In the early development period, the tubes were eddy-current inspected both before and after annealing. Annealing was not found to cause any tube defects.

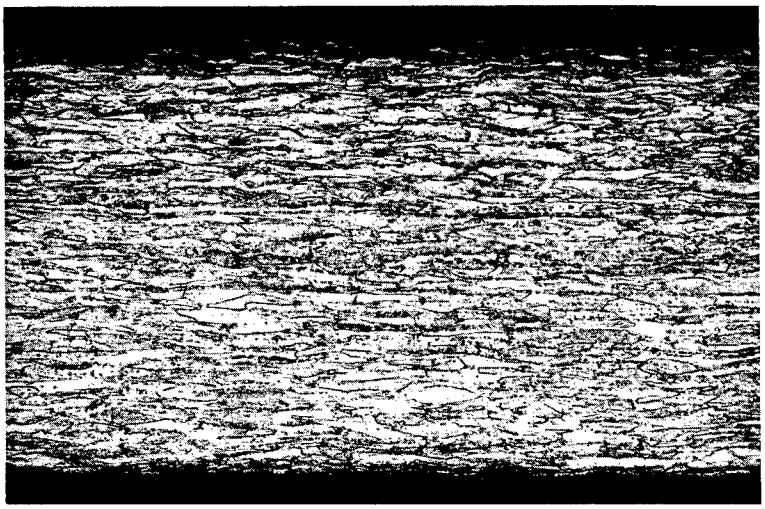

Micro 38747 150X

Etchant: 10% KOH, 10% $K_3Fe(CN)_6$

Micro 38748 500X

Etchant: 10% KOH, 10% $K_3Fe(CN)_6$

Figure 31. Longitudinal Microstructure of As-drawn 0.48-cm OD x 0.04-cm Wall (0.190-in. OD x 0.016-in. wall) V-20w/oTi Tubing, Cold-worked Approximately 67% from Last In-process Anneal

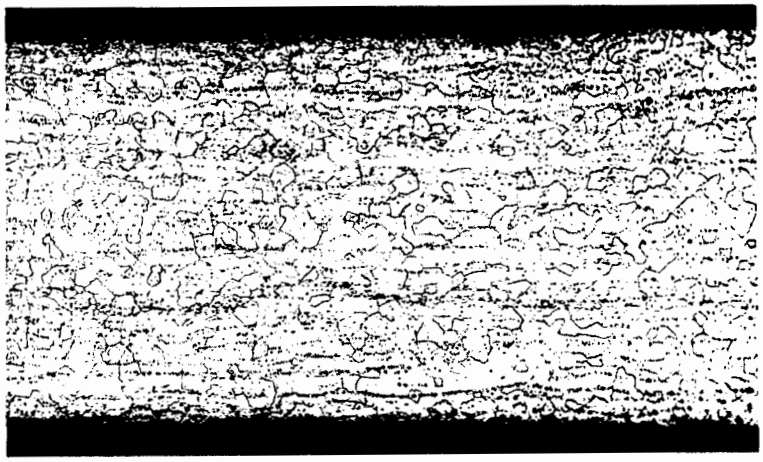

Micro 38896 150X

Etchant: 5% HF, 2% $AgNO_3$

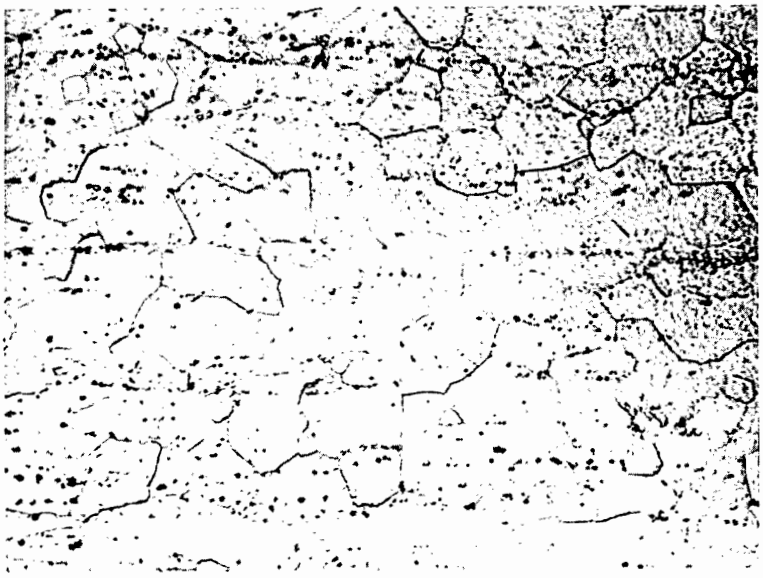

Micro 38895 500X

Figure 32. Longitudinal Microstrucutre of 0.48-cm OD x 0.04-cm Wall (0.192-in. OD x 0.016-in. wall) V-20w/oTi Tubing, Vacuum-annealed for 1 hr at 900°C

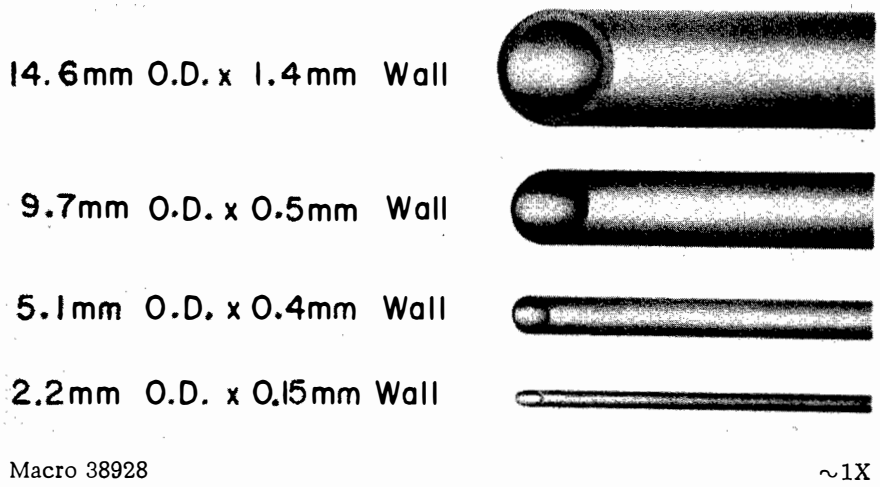

Figure 33. Photograph of Variety of V-20w/oTi (TV-20) Tube Size Produced at Argonne National Laboratory

evaluate tubing produced by commercial techniques. Tube-blanks measuring 1.91-cm OD x 1.27-cm ID (0.750-in. OD x 0.500-in. ID) have been shipped to the Superior Tube Company, Wolverine Tube Company, and Fansteel Metallurgical Corporation. The target size for finished tubing is 0.53-cm OD x 0.04-cm wall (0.208-in. OD x 0.016-in. wall).

While tubing fabrication is only about 50% complete at the time of writing, the vendors have indicated that the material is working successfully so far. Tube reduction has been attempted and appears feasible. Drawing with carbide dies may be successful if a proprietary lubricant is used.

The success of commercial tube fabrication remains to be verified, however, by a rigorous evaluation of finished tubing.

VI. DISCUSSION

The integrated fabrication technology described in the previous sections has produced moderate quantities of high-quality bar, rod, sheet, and small-diameter, thin-wall tubing of V-20w/oTi (TV-20). The developed methods were determined to be the best or most fruitful for this type of pilot or limited-production run with the available facilities. The methods employed are by no means the only ones that could be utilized - certainly other approaches might be used equally well. The procedures to be used by others will depend upon equipment available, size and shape of raw material, etc. An understanding of practices employed at ANL and a discussion of some of the problem areas should prove highly beneficial to others having a potential interest in the alloy.

In ingot consolidation, alloy homogeneity is improved by remelting. Which melting technique (EB or arc) should precede the other, or whether the same method can be used for both melts, will require further study. The porosity found in all single-melted EB-ingots of TV-20 dictated the subsequent arc-melt for ingot soundness. While porosity could be tolerated in a semifinished ingot scheduled for remelting, it would be highly undesirable in a final cast product. Arc-melting also produced a finer grain size and better surface quality - the latter reducing material losses in conditioning. Further development might indicate that other possible consolidation routes would produce ingots of acceptable quality; however, melting once in each type of furnace affords the advantages of both. Perhaps other more economical means of drip-rod preparation can be devised, but any gains should not be at the expense of final ingot homogeneity or quality.

Although the alloy can be easily cold-worked, TV-20 extruded tube-blanks cannot be sized by swaging over a hard mandrel with other than light passes and frequent intermediate anneals. While this problem may be partially overcome by an evaluation of other swaging die designs, tube-reducing would be a much more satisfactory approach.

The tendency for the TV-20 alloy to gall when being drawn through carbide dies should direct further emphasis to the selection of satisfactory lubricants. A conversion coating technique, in conjunction with a suitable lubricant, may be required. The galling problem was overcome at ANL by using aluminum-bronze dies and a chlorinated-wax lubricant, such as Aldraw J-1. Plug-drawing was shown to be feasible and was accomplished in small-diameter tubing by using an aluminum-bronze die and a beryllium-copper plug. Problems such as wear of the beryllium-copper plug may be alleviated by use of a more sophisticated die and plug design. Carbide tooling may prove feasible if a suitable lubricant is developed.

Ductile-core drawing probably would be unnecessary if a complete plug/die tooling inventory were available; this would be a prerequisite for a sizeable tube production campaign. One word of caution is in order, however: the tube-sinking characteristics of TV-20 were not investigated at ANL. Tube sinking was avoided in an effort to prevent ID imperfections that often result from such an operation. Ductile-core drawing assisted in this direction. The only sinking that occurred throughout the process was the small amount necessary to seat the tube on the mandrel, ductile-core, or plug, as the case may be.

Plug-drawing is highly recommended for the close tolerance requirements and integrity of nuclear tubing of this type. Smooth outer and inner surfaces are mandatory when eddy-current nondestructive means are used in searching for wall defects. A defect equal to 10% of the wall thickness is only about 0.041 mm (0.0016 in.) in depth, assuming a 0.4-mm (0.016-in.) tube wall. If both the outer and inner surfaces are rough, it will be difficult to sort out minor defects from the background that may result from such surfaces.

Even under the best-established conditions, extreme care is still required to produce high-quality tubing - particularly small-diameter, thin-wall tubing.

The mechanical properties of the alloy will be subject to the degree of purity (i.e., to interstitial element content) of the starting material. As suggested by the results of solution heat-treatments, precipitates normally found in the alloy may possibly be retained in the solution by a high-temperature heat treatment and water quench. A controlled reprecipitation may be produced in a subsequent lower-temperature aging treatment. The identification of such precipitates, their control, and influence on properties need further study.

VII. CONCLUSIONS

This report has established that the V-20w/oTi (TV-20) alloy can be successfully consolidated and fabricated into various products. High-quality, small-diameter, thin-wall tubing for use as a potential fuel-element jacket material for fast reactors can be produced if care is exercised in selection and control of fabrication techniques. No particular problems are involved in the fabrication of bar, rod, or sheet products.

Industrial participation in the TV-20 fabrication program has been encouraged, and early results appear cause for optimism. Ingot stock is commercially available. While the tubing fabricators have not completed their analysis, the consensus would indicate that little real difficulty is anticipated in this area of fabrication technology.

APPENDIX A

Purification of Vanadium by Electron-beam (EB) Melting

This brief study was concerned with the effect of EB melting on removal of the interstitial elements (C, O, N, and H) from vanadium. The resultant purity of an EB-melted vanadium ingot depends primarily on the following variables: (1) melt rate (time), (2) power input (temperature), (3) vacuum (pressure), and perhaps to some extent (4) the degree of agitation of the molten pool. Since it is difficult to vary the pressure or degree of agitation, and the power level was fixed, the melt rate is left as the independent variable in the purification study. The high vacuums (or low pressures) of 10^{-5} to 10^{-7} Torr provide a driving force for the removal of gaseous impurities and/or elements with high vapor pressures.

The charge material consisted of vanadium chips procured from the Vanadium Corp. of America. Analyses for interstitial elements are reported in Table IX. The chips were Syntron-fed into the molten pool of vanadium maintained by the electron beam. The resulting 3.8-cm (1.5-in.)-diameter ingot (EB3) was remelted at the same melt rate of 30 g/min into the same size mold to yield ingot EB4. This ingot (EB4) was then sectioned into three parts, each part being remelted at successively lower melt rates at the same power setting of approximately 12 kW. In all, five castings were made from the initial charge material.

Table IX

INFLUENCE OF ELECTRON-BEAM MELTING ON INTERSTITIAL CONTENT OF VANADIUM

Melt No.	Material	Carbon (ppm)	Oxygen (ppm)	Nitrogen (ppm)	Hydrogen (ppm)	Total (ppm)	Remarks[1]
	Chips (Vanadium Corp.)	400	1300	390	50	2140	Syntron-fed to yield EB3.
1	Ingot EB3	230	1070	342	13	1655	Melt-rate: 30 g/min
2	Ingot EB4 (Remelt of EB3)	129	820	380	18	1347	Melt-rate: 30 g/min
3	Ingot EB22(a) (Remelt of EB4)	110	450	465	8	1033	Melt-rate: 15.5 g/min
4	Ingot EB22(b) (Remelt of EB4)	68	290	470	3	831	Melt-rate: 7.7 g/min
5	Ingot EB22(c) (Remelt of EB4)	80	85	461	1	637	Melt-rate: 5.2 g/min

[1]Melt numbers 1 through 5 used constant power setting of approximately 12 kW.

The analysis results of Table IX indicate significant reduction in all interstitial elements, except nitrogen. The nitrogen is probably present in the form of a nitride of vanadium that is relatively stable under the existing pressure-temperature conditions. The reduction in carbon content most likely results from a carbon deoxidation reaction.

Overall, each remelt resulted in additional purification with diminishing returns as the purity level increased. As expected, reducing melt-rates increases the parent metal loss. A total loss of 25% of the initial charge weight was experienced in the production of EB22 on using the three different melt-rates (a, b, and c).

Alloy purification by EB melting would prove difficult if the alloy base metals had widely different melting points and vapor-pressure characteristics. In the vanadium-titanium system, it would be expected that titanium would be lost at a faster rate than vanadium during EB melting, other factors being equal. Accordingly, close control of the titanium content would be difficult to achieve if a series of EB melting operations was performed on the alloy.

APPENDIX B

TV-20 Interstitial Analysis Methods and Results

Discrepancies have occasionally occurred between values reported by other investigators and those reported by ANL. Examples are shown in Table X for TV-20 ingots procured from Union Carbide. There is rather wide variation in certain instances for the first three groups of analyses obtained on the Union Carbide ingots.

Table X

COMPARATIVE RESULTS OF INTERSTITIAL ANALYSIS BY ANL AND UNION CARBIDE

Material	Source of Analysis	Interstitial Content (ppm)				
		Carbon	Oxygen	Nitrogen	Hydrogen	Total
Union Carbide Ingot 761-1	Union Carbide[1]	480	358	138	13	989
	ANL[2]	330	400	450	35	1215
Union Carbide Ingot 761-2	Union Carbide[1]	370	525	230	5	1130
	ANL[2]	490	390	390	60	1330
Union Carbide Ingot 761-3	Union Carbide[1]	360	508	82	21	971
	ANL[2]	480	480	430	140	1530
ANL Extrusion No. 289[4]	Union Carbide[1]	450	405	126	40	1021
	ANL[2]	480	540	271	90	1381
	ANL[2](R1)	-	325	180	-	
	ANL[3](R2)	-	420	330	-	

[1]Carbon by combustion manometric; oxygen, nitrogen, and hydrogen by vacuum fusion.

[2]Carbon by combustion manometric; oxygen by inert gas fusion; nitrogen by Kjeldahl; hydrogen by hot extraction.

[3]Oxygen and nitrogen by inert gas fusion.

[4]ANL Extrusion No. 289 reduced Union Carbide ingot No. 761-3 to bar stock. See Table V for details.

In an effort to resolve these discrepancies, a 5.1-cm (2-in.)-diameter x 2.5-cm (1-in.)-thick cross section was removed from Extrusion No. 289 (ingot material from UC761-3) for analysis. The slice was cut into two semicylindrical halves, and one half was sent to Union Carbide; the other half was cut into smaller pieces for analysis at ANL. The results are indicated in the fourth group of values in Table X.

Carbon values agree quite closely, but oxygen, nitrogen, and hydrogen show wide variations. Contamination could have been introduced at ANL during cutting of the samples; thus, an additional set of samples was taken from

the same material for oxygen and nitrogen analyses. Care was taken to remove the outer surface layer from all pieces to be analyzed to reduce the probability of error from this source. Values reported for the rerun analyses (R1), as shown in Table X, were somewhat lower in oxygen and nitrogen content.

Another rerun (R2) was carried out at ANL by the same method for oxygen analysis, but by a different method for nitrogen analysis. The results indicated considerably different values than those obtained in the two previous attempts.

There may be some difference in values depending on the method employed. Another possibility is that a real difference exists in interstitial content from one unit volume to another in a given slice of TV-20. Further, when samples are more carefully cleaned before analysis (to eliminate the surface contamination error) it would seem reasonable to expect more representative and accurate values. These variables may, or may not, explain why the analytical results obtained by Union Carbide and ANL are not in closer agreement. Further study will be necessary to determine the causes of analytical disagreement.

APPENDIX C

Heat Treatment Studies

1. Annealing Studies

To establish the parameters of "in-process" annealing, a series of samples was prepared with various degrees of cold reduction and was subsequently heat-treated for 1 hr at 700 to 950°C in 50° increments. Vacuum-annealing was done in a resistance-heated furnace, the heating time being approximately 1.5 hr to temperature, and the dynamic vacuum during annealing being maintained at 10^{-5} Torr or better. After annealing, the samples were mounted and machined to provide a longitudinal surface through the center of the rod for metallographic examination and hardness measurements. Sections of as-rolled material were prepared in the same manner for similar examination. The samples were evaluated by using three techniques: (1) diamond-pyramid-hardness (DPH) measurements with a 10-kg load, (2) microhardness measurements on individual grains with a Tukon diamond-pyramid-hardness tester and a 5-g load, and (3) metallographic examination.

The macrohardness (DPH vs temperatures) data are presented in Figure 34. In general, the samples representing increasing amounts of cold work showed decreasing hardness values for annealing at a given temperature. Based upon these measurements, the full recrystallization annealing temperature would be approximately 900°C where hardness is near minimum.

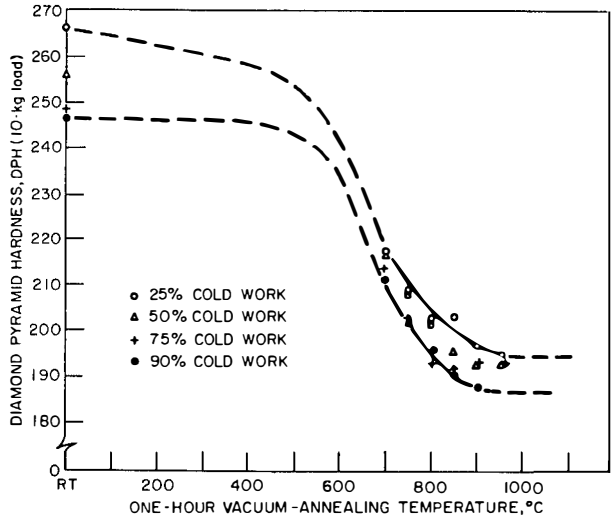

Figure 34

Diamond-pyramid-hardness Data on Heat-treated V-20w/oTi Having Various Amounts of Cold Work

The metallographic results are shown in Figures 35, 36, 37, and 38, representing the annealing of material with 25%, 50%, 75%, and 90% cold work, respectively. A worked structure was not evident until approximately 50% cold work was attained. Material that was cold-worked 25% and annealed at various temperatures exhibited no definite temperature at which

As Rolled; 25% Cold Work

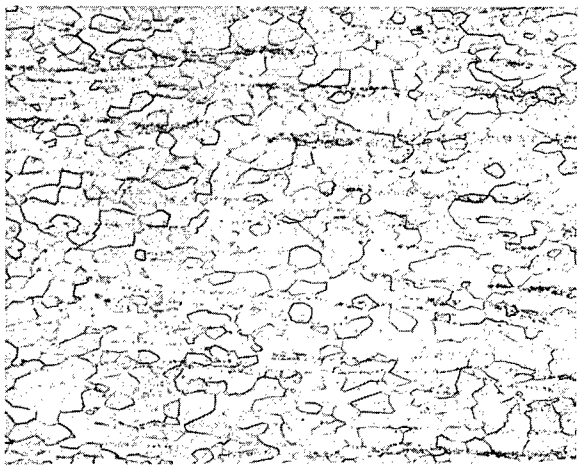

Micro 39375 150X

After 1 hr at 750°C

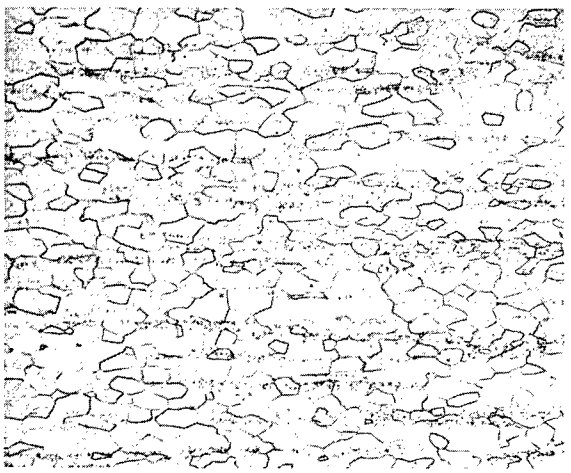

Micro 39383 150X

After 1 hr at 800°C

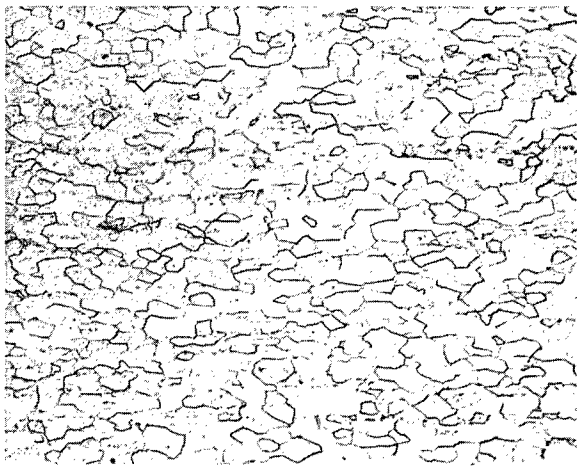

Micro 39536 150X

After 1 hr at 850°C

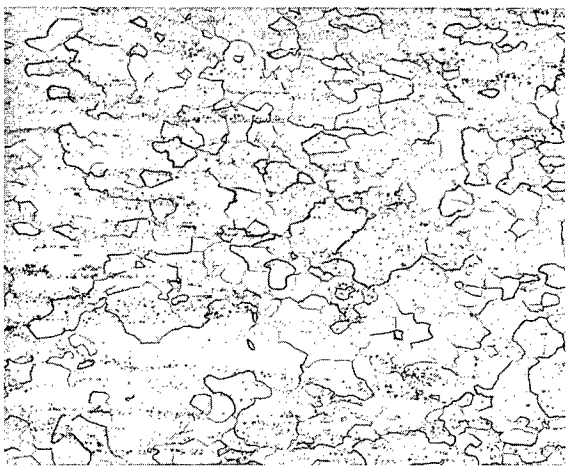

Micro 39421 150X

After 1 hr at 900°C

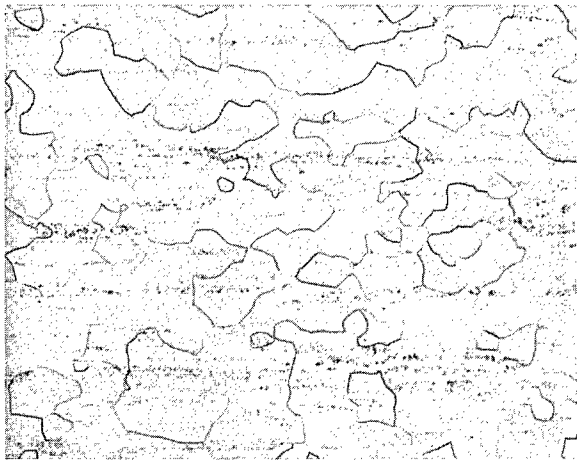

Micro 39387 150X

After 1 hr at 950°C

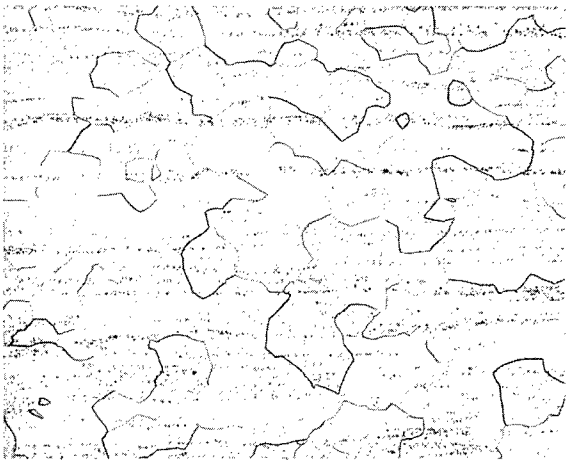

Micro 39540 150X

Figure 35. Longitudinal Microstructure of V-20w/oTi Cold-worked 25% and Vacuum-annealed for 1 hr at Various Temperatures (Etchant: 5% HF, 2% $AgNO_3$)

As Rolled; 50% Cold Work

Micro 39376 150X

After 1 hr at 750°C

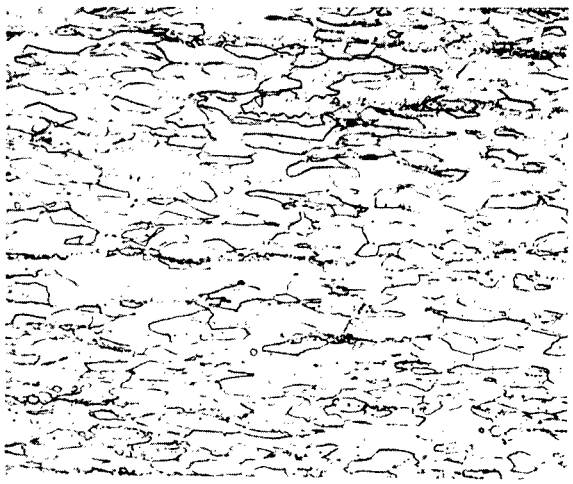

Micro 39384 150X

After 1 hr at 800°C

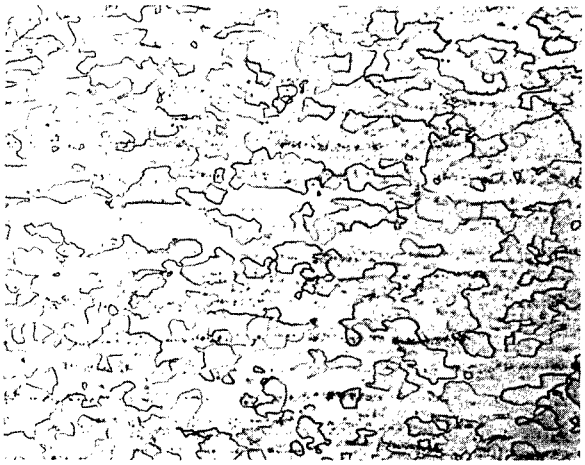

Micro 39537 150X

After 1 hr at 850°C

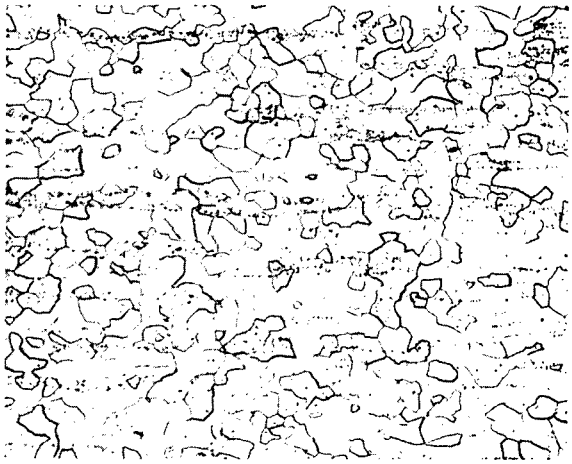

Micro 39422 150X

After 1 hr at 900°C

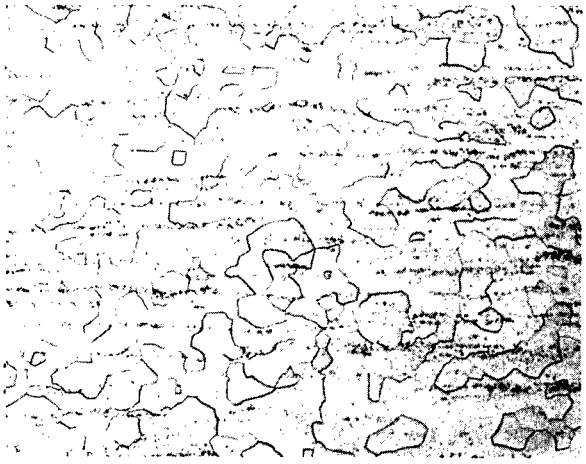

Micro 39388 150X

After 1 hr at 950°C

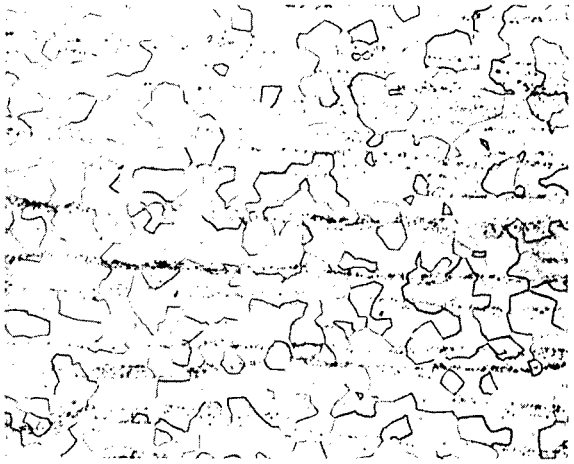

Micro 39541 150X

Figure 36. Longitudinal Microstructure of V-20w/oTi Cold-worked 50% and Vacuum-annealed for 1 hr at Various Temperatures (Etchant: 5% HF, 2% $AgNO_3$)

As Rolled; 75% Cold Work

Micro 39377 150X

After 1 hr at 700°C

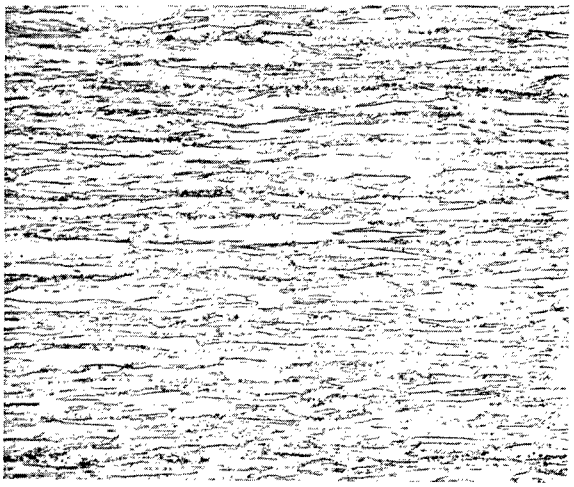

Micro 39381 150X

After 1 hr at 750°C

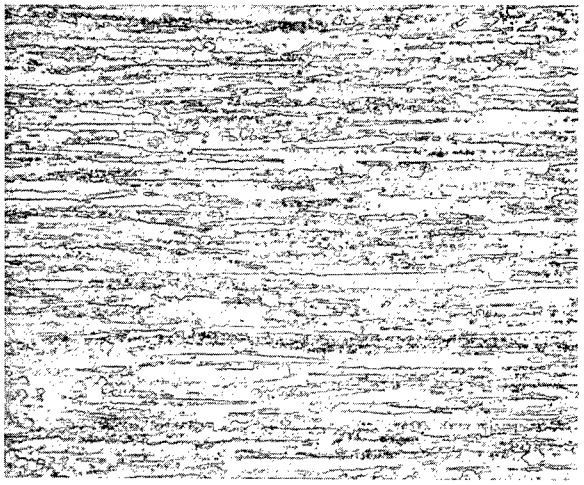

Micro 39385 150X

After 1 hr at 800°C

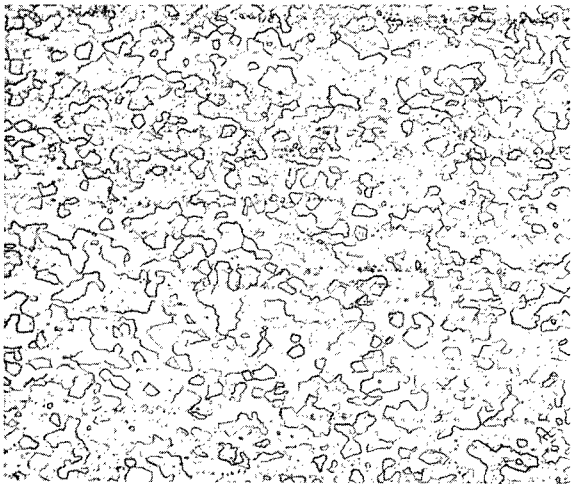

Micro 39538 150X

After 1 hr at 850°C

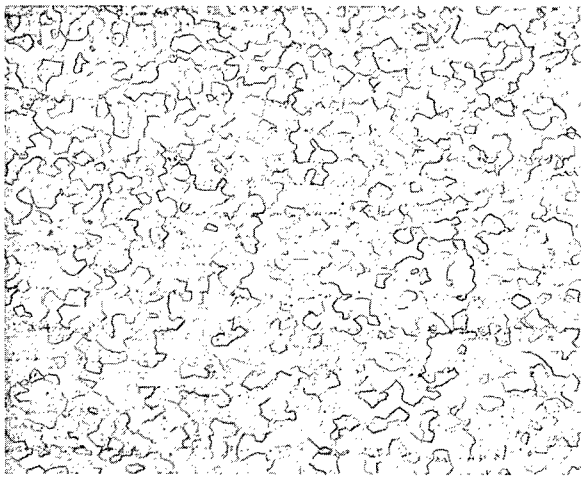

Micro 39423 150X

After 1 hr at 900°C

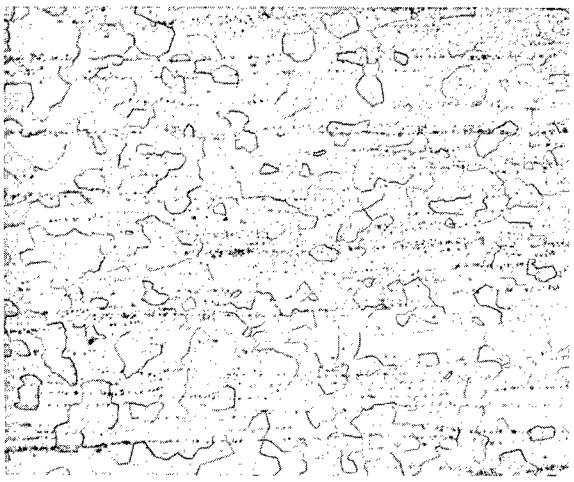

Micro 39389 150X

Figure 37. Longitudinal Microstructure of V-20w/oTi Cold-worked 75% and Vacuum-annealed for 1 hr at Various Temperatures (Etchant: 5% HF, 2% $AgNO_3$)

As Rolled; 90% Cold Work

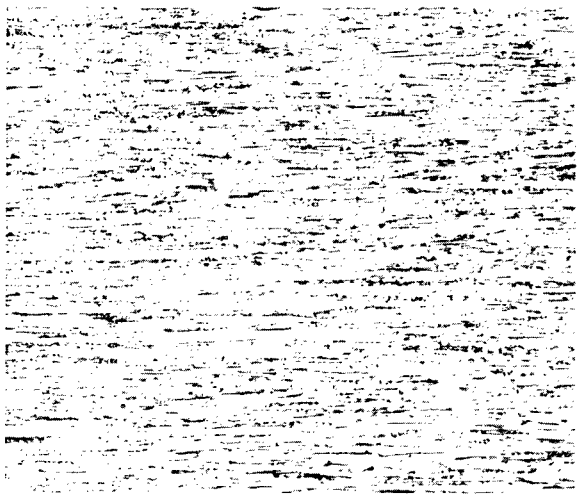

Micro 39378 150X

After 1 hr at 700°C

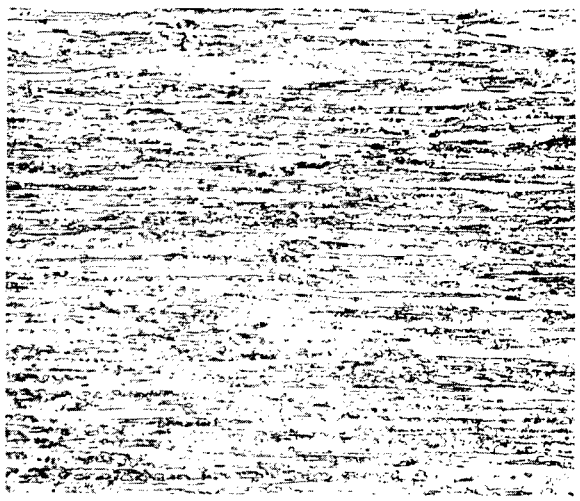

Micro 39382 150X

After 1 hr at 750°C

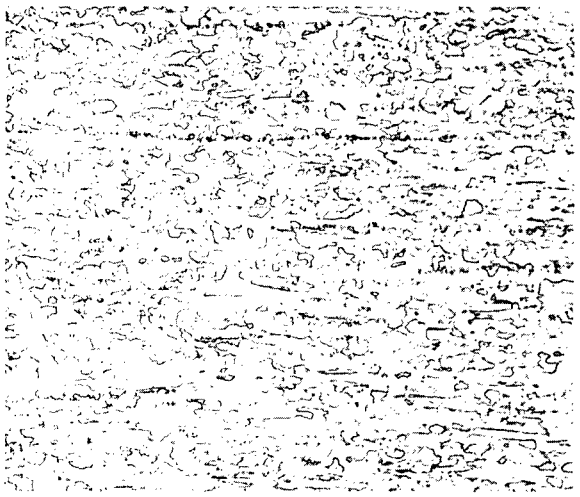

Micro 39386 150X

After 1 hr at 800°C

Micro 39539 150X

After 1 hr at 850°C

Micro 39424 150X

After 1 hr at 900°C

Micro 39390 150X

Figure 38. Longitudinal Microstructure of V-20w/oTi Cold-worked 90% and Vacuum-annealed for 1 hr at Various Temperatures (Etchant: 5% HF, 2% $AgNO_3$)

recrystallization began because of the nature of the as-worked structure. However, at 850°C, grain growth began to appear; and at 900°C, grain growth became rapid. Material that was worked 50% exhibited evidence of recrystallization at 750°C, and of complete recrystallization at 800°C. No large grain growth was observed, even at 950°C. Material cold-worked 75% exhibited a slight amount of recrystallization at 700°C, the degree of recrystallization increasing until complete recrystallization was observed at 800°C. Material cold-worked 90% showed recrystallization being initiated at 700°C, with further recrystallization evident at 750°C, and full recrystallization at 800°C. Grain growth was evident at 900°C. No sample was available for heat treatment at 950°C. At 900°C, all samples exhibited complete recrystallization with a uniform grain size. In general, the metallographic examination reveals that, as would be expected, recrystallization is initiated at lower temperatures with increasing amounts of cold work. Based on metallography, a fully recrystallized structure is realized by heat treating for 1 hr at 850°C, as contrasted with the 900°C treatment necessary for minimum hardness as determined by the macrohardness test.

To determine more fully the recrystallization behavior of the V-20w/oTi alloy, a series of microhardness readings was taken on a sample, the readings being measured on individual grains. A frequency distribution of the grain hardnesses yielded a plot used to determine the percent recrystallization as a function of annealing temperature.[10] A typical plot is shown in Figure 39. In general, materials that exhibited partial recrystallization showed two distributions of hardness values, with the distributions representing recrystallized grains and worked grains. Approximately 40 to 70 readings per sample were taken. The microhardness values were rounded off to the nearest whole number divisable by five (in some cases to numbers divisable by other integers) and plotted as a frequency distribution. The percent recrystallization was determined by the number of readings in the respective areas, i.e., recrystallized or work-hardened. As the annealing temperature increased, the bimodal distribution would be shifted towards a single-mode distribution grouped around an average hardness representing recrystallized material. The results of this study are shown in Figure 40 in which the percent recrystallization is plotted as a function of annealing temperature for the various degrees of cold work. In contrast to the data shown by the macrohardness examination and metallographic observations, all materials exhibited a pronounced degree of

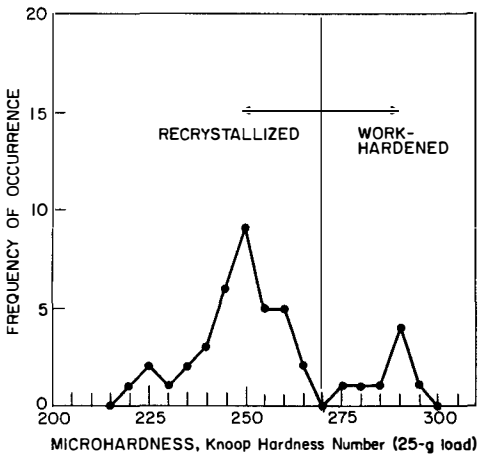

Figure 39

Frequency Distribution of Microhardness Measurements on Individual Grains in a Sample of V-20w/oTi Cold-rolled 75% and Vacuum-annealed for 1 hr at 750°C

recrystallization, even at 700°C, with the greater amount of recrystallization corresponding to the material having the greater amount of cold work. While all samples exhibited at least 90% recrystallization at an annealing temperature of 850°C, only the material worked 90% exhibited 100% recrystallization at 900°C.

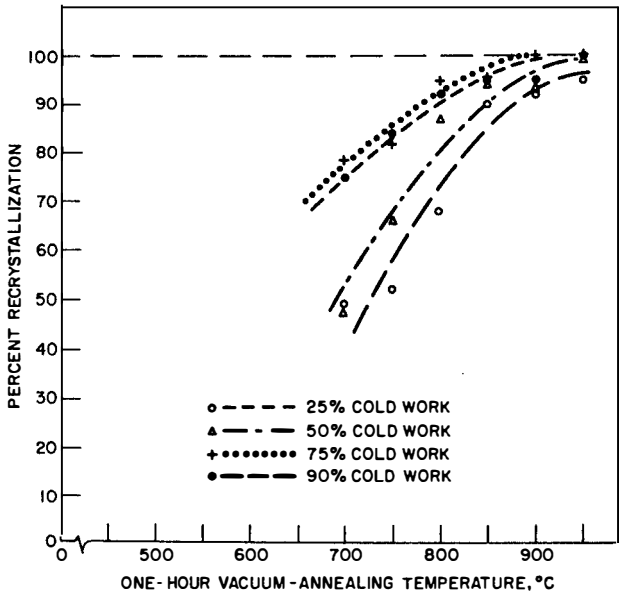

Figure 40

Study of Recrystallization Behavior of V-20w/oTi as Function of Annealing Temperature by Distribution of Individual Grain Hardnesses

Based on the above observations, an annealing treatment of 1 hr at 900°C would seem to be adequate from a practical annealing standpoint for material that had received approximately 50% or more cold work. Temperatures of 950°C or higher, while insuring complete recrystallization, might result in excessive grain growth of the annealed product. The stress-relief heat treatment of 1 hr at 700°C employed for stress-relieving of rolled sheet was selected before the study on individual grain hardnesses was made. In retrospect, this temperature of 700°C could be too high since it results in approximately 50% or more recrystallization for material that has received a minimum of 50% cold work, while the objective was to remove residual stresses without incurring appreciable recrystallization. Based on metallographic examination, however, this degree of recrystallization is not apparent after the stress-relieving heat treatment. Unfortunately, sufficient material was not available for heat treatments at temperatures below 700°C to further evaluate the hardness as a function of annealing temperature, thereby enabling better selection of an adequate stress-relief temperature.

2. Solution Annealing

Initial metallographic examination of extruded V-20w/oTi (TV-20) showed a precipitate appearing in the matrix grains, along with a series of stringers or "streaks" aligned in the longitudinal direction (i.e., the extrusion direction) and consisting of fine particles (see Figure 21). While

the particles comprising the stringers were not identified, it was thought that perhaps they might be oxide inclusions in the original cast ingot that were stringered in the process of extrusion. The precipitate within the grains was not identified until a later time but was thought to be a carbide or nitride of titanium, or possibly a complex also involving vanadium. It was thought that these stringers (and possibly the precipitate) might cause difficulty in fabrication of tubing. In addition, the presence of these stringers and/or precipitate might also affect properties of the final product. It was felt, therefore, that a suitable solution heat treatment might take the various items into solution thereby producing a "clean" structure. On this assumption, a series of solution heat treatments were carried out.

Small samples of 0.5-cm (0.2-in.)-thick, as-extruded sheet-bar, with the microstructure shown in Figure 24, were induction-heated to 1250, 1300, 1350, 1450, or 1500°C. After holding at temperature for approximately 3 min, the samples were either helium-cooled or water-quenched. Metallographic results are shown in Figures 41 and 42. Microstructural examination of the heat-treated samples indicated that at 1250°C the streaks or stringers were completely taken into solution in samples that were helium-cooled and almost completely into solution in samples that were water-quenched. In addition to elimination of the streaks or stringers, additional precipitate can be seen within the grains. At the higher solution heat-treat temperatures, grain growth occurred, growth being more pronounced in samples that were water-quenched. The amount of precipitate diminished as the solution heat-treat temperature increased. This was more pronounced for material water-quenched after the heat-treat than for material cooled in the helium gas stream. One sample of extruded sheet bar was heated for approximately 3 min at 1500°C and water-quenched. The resultant microstructure is shown in Figure 42. While the grain size is extremely large, contrasted to that of samples heated at the lower temperatures, the microstructure shows the matrix of the grains to be extremely clean with little evidence of precipitate present. Hardness measurements on the sample, water-quenched from 1500°C, averaged 249 DPH (22 R_C), contrasted with a hardness of 216 DPH (94 R_B) on material heat-treated at 1250°C and water-quenched. In general, the hardness of the heat-treated and water-quenched material increased with increasing solution heat-treat temperatures. This gradual hardness increase was not observed for materials that were helium-cooled after heat-treating, as all hardnesses fell within a range of 215 to 220 DPH. Based on hardness and microstructural evidence, there is a possibility that the TV-20 alloy (of the purity used for these tests) can be subjected to a precipitation-hardening phenonema. A high-temperature heat-treatment, followed by a rapid quench, would produce a structure in which the precipitate was retained in solution. A low-temperature aging treatment may cause reprecipitation, the amount being dependent upon the time and temperature of the aging treatment. The feasibility of this type of treatment remains to be established. The high heat-treat temperature may result in an abnormally large grain size, even though a water quench is employed. This may preclude the use of a solution heat-treatment and aging technique for improving mechanical properties.

1250°C, Helium Cool; 215 DPH (94 R_B)

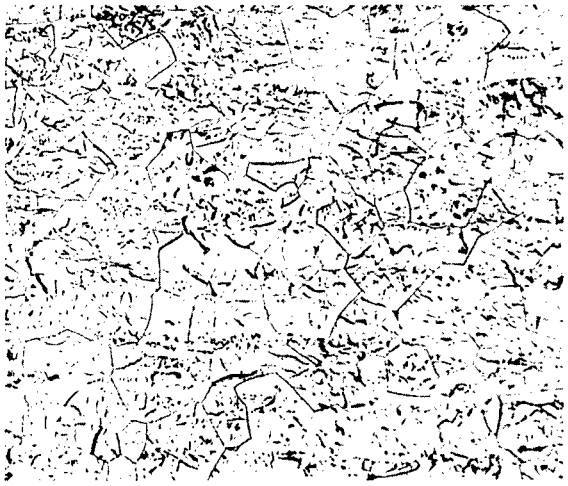

Micro 38548 150X

1250°C, Water Quench; 216 DPH (94 R_B)

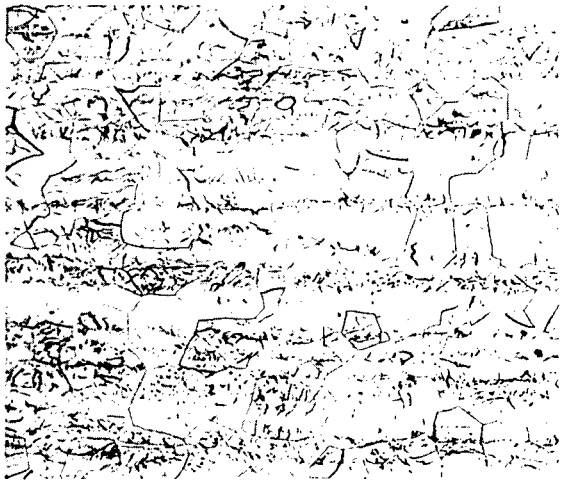

Micro 38549 150X

1350°C, Helium Cool; 222 DPH (95 R_B)

Micro 38553 150X

1350°C, Water Quench; 233 DPH (97 R_B)

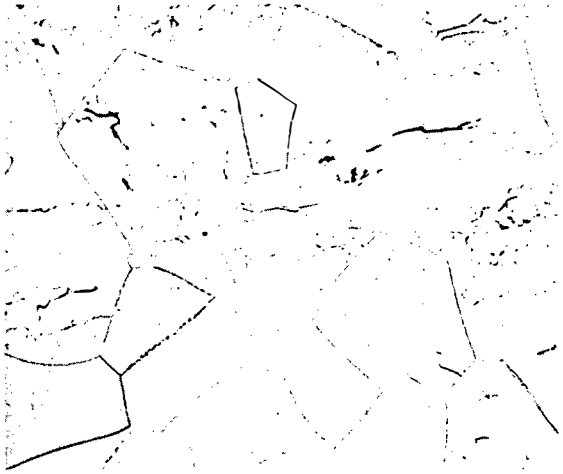

Micro 38554 150X

1450°C, Helium Cool; 218 DPH (95 R_B)

Micro 38555 150X

1450°C, Water Quench, 233 DPH (97 R_B)

Micro 38556 150X

Figure 41. Longitudinal Microstructures of As-extruded V-20w/oTi Sheet-bar after Solution Heat Treatment at Various Temperatures with Helium Cool or Water Quench (Etchant: 10% KOH, 10% $K_3Fe(CN)_6$)

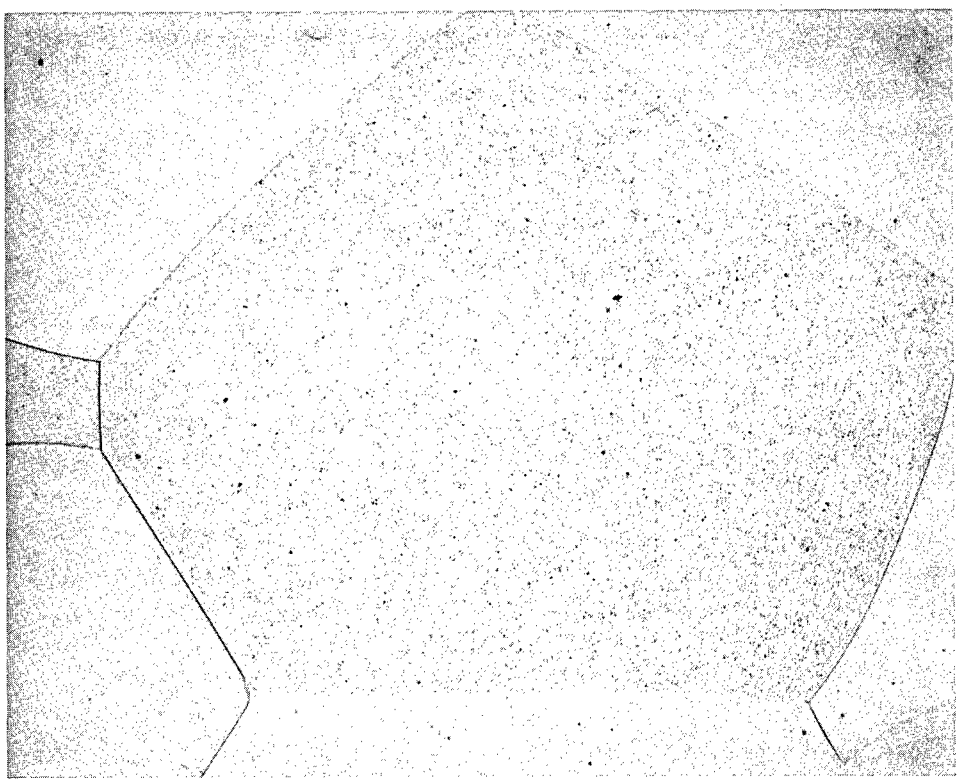

Micro 38545 150X

Etchant: 10% KOH, 10% $K_3Fe(CN)_6$

Figure 42. Microstructure of As-extruded V-20w/oTi Sheet-bar after Solution Heat Treatment for 3 min at 1500°C Followed by Water Quench; Hardness Measures 249 DPH (22 R_C)

Because of the results of the solution heat-treat study and the desire to eliminate the streaks present in the as-extruded structure, sections of sheet-bar were solution heat-treated before being rolled into finished sheet. The heat treatment was done in vacuum and consisted of a 15-min hold at 1300°C, followed by a furnace cool. The resultant microstructure has been previously shown in Figure 27. As expected, the streaks disappeared, and an increased amount of precipitate was present in the matrix grains. The resultant grain size was only slightly larger than that of as-extruded sheet-bar (see Figure 24).

This solution heat-treatment was dropped from the fabrication procedure for subsequent sheet and tubing as the material appeared to be slightly more difficult to fabricate due to greater edge cracking and surface flaking. No change in mechanical properties was observed for sheet that had received the solution anneal before fabrication.

3. Precipitate Identification

An attempt was made to identify the precipitate observed in both cast and wrought V-20w/oTi (TV-20) materials. A knowledge of the

composition should aid in controlling the quantity (and perhaps the distribution) of the precipitate, which was shown earlier to affect the hardness and microstructure of the alloy.

A heat treatment was employed to increase the amount of precipitate present in the test sample in order to aid extraction and analysis. The heat treatment consisted of heating to 1500°C (in vacuo), holding for 3 hr, and slow-cooling at a rate of about 100°C every 15 min. The microstructure resulting from this heat treatment is shown in Figure 43. Heat-treated specimens were dissolved in a bromine-methanol solution, and the residue (precipitate) was carefully recovered and subjected to several analytical methods for possible identification of the constituents.

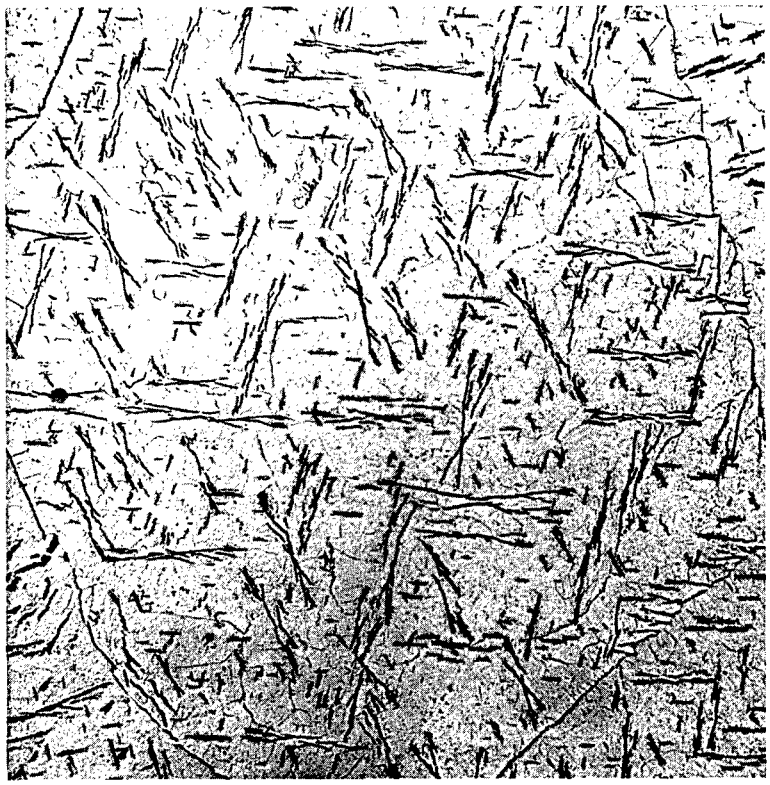

Micro 38674 100X

Etchant: 5% HF, 2% $AgNO_3$

Figure 43. Typical Microstructure of V-20w/oTi after a 3-hr Heat Treatment at 1500°C and Very Slow Cool (100°C every 15 min)

X-ray diffraction results on two different precipitate samples yielded a_0 values of 4.26 to 4.27 and 4.25, and a reportedly fcc (face-centered cubic) structure. An a_0 value of 4.27 was obtained by Union Carbide on precipitate extracted from TV-20 by a different means.[11] It is somewhat difficult to obtain useful information from the diffraction pattern without some knowledge of the constituents actually present. Neutron diffraction would be considerably more diagnostic in this instance but a larger

sample size (approximately 5 g) was required. Collecting this much precipitate by the above-described dissolution method was considered prohibitive and was not attempted.

Neutron activation analysis indicated that carbon was present in sizeable quantities. The activation tests could not clearly indicate the presence of nitrogen and oxygen; either could be overshadowed by carbon to the extent that detection would be impossible. Spectrographic samples were prepared, and the test results indicated the presence of very little vanadium but an abundance of titanium. At this point, the precipitate appeared to be a Ti(V) C(N) compound, with the nitrogen and carbon being essentially interchangeable.

Later, sufficient material was collected so that chemical analysis could be carried out. Milligram (mg) quantities were analyzed giving the following:

Titanium:	75.0 w/o;	Oxygen:	7.7 w/o;
Vanadium:	6.8 w/o;	Nitrogen:	3.4 w/o;
Carbon:	4.4 w/o;	Hydrogen:	not analyzed.

(Fair confidence in reported values can be assumed, except in the case of oxygen. Air drying of the precipitate for analytical purposes may have resulted in atmospheric contamination.)

More work will be necessary to complete the identification, if for no reason other than academic interest. Time has not been made available due to the pressures of fulfilling the demands for TV-20 fabricated products. However, the above analysis confirmed the early concern over the amount of interstitials that can be tolerated. Generally, it may be concluded that titanium serves as a scavenger in this alloy, precipitating (under certain conditions) a fcc second phase consisting largely of titanium combined in some form with carbon, nitrogen, and possibly oxygen. It is interesting to note the concentration of all of these elements in the precipitate, from the nominal TV-20 composition: titanium, 20 w/o; carbon, ~0.04 w/o; oxygen, ~0.04 w/o; nitrogen, ~0.03 w/o.

It should be expected (as was indicated for vanadium in Appendix A) that the quantity of the precipitate can be controlled by controlling the purity of the charge material and the product. (Distribution control by heat treatment has been previously demonstrated; see Sec. 2 of this appendix.) This is the course (purity control) that was followed throughout the TV-20 consolidation and fabrication processes.

APPENDIX D

Mechanical-property Tests

During the course of fabricating sheet and tubing, some mechanical-property tests were performed to determine if the stringers present in extruded material would affect mechanical properties of the alloy or if directional properties might result from fabrication. Initial tests were run on 0.15-cm (0.060-in.)-thick V-20w/oTi (TV-20) sheet. Two types of material were used for the testing, the first being material extruded and long-rolled to the final thickness and annealed, the second type being extruded material that was cross-rolled to a 0.46-cm (0.180-in.) thickness, followed by long-rolling to the final 0.15-cm (0.060-in.) thickness, and annealed. The tensile test data, shown in Table XI, indicated that the transverse strength (perpendicular to the long-rolling direction) was equivalent to the longitudinal strength (parallel to the long-rolling direction); thus, no directionality was evident. In addition, incorporating cross-rolling operations at the beginning of sheet fabrication did not affect the tensile properties. On this basis, it was concluded that the presence of stringers elongated in the rolling direction did not markedly affect the properties of the alloy, or contribute directionality to the properties of the sheet itself.

Table XI

RESULTS OF ROOM-TEMPERATURE TENSILE TESTS
ON 0.15-cm (0.060-in.)-THICK V-20 w/o Ti (TV-20) SHEET

Material History	Average Ultimate Tensile Strength,[1] kg/mm^2 (psi x 10^{-3})	
	Longitudinal (Parallel to Long-rolling Direction)	Transverse (Perpendicular to Long-rolling Direction)
Extruded to 0.55 cm (0.215 in.); long-rolled to 0.15 cm (0.060 in.); annealed 1 hr at 900°C	65.7 (93.2)	67.2 (95.3)
Extruded to 0.55 cm (0.215 in.); cross-rolled to 0.46 cm (0.180 in.); long-rolled to 0.15 cm (0.060 in.); annealed 1 hr at 900°C	66.4 (94.2)	66.6 (94.5)

[1]Average of three tests.

To evaluate further the strength of the alloy, small sections of tubing were tested in a conventional tensile test. In addition, tubing of Type 304 stainless steel and Nb-1Zr was also tested to provide comparative data with the TV-20 alloy. Tubing measuring 0.40-cm ID x 0.04-cm wall thickness (0.156-in. ID x 0.017-in. wall) was tested in the annealed condition for all three materials. In addition, TV-20 tubing was tested in the as-drawn and stress-relieved (one hour at 700°C) condition, Type 304 SS was tested in the as-drawn condition, and Nb-1Zr was tested in the

stress-relieved (2 hr at 1200°C) condition. The results of the tensile tests are shown in Table XII. Both Type 304 SS and the TV-20 alloy showed marked improvement in strength over Nb-1Zr in an annealed condition, the TV-20 alloy being slightly stronger than the Type 304 SS. As drawn, however, Type 304 SS showed a slightly higher strength than TV-20. Stress-relieved TV-20 exhibited half again the strength of Nb-1Zr in the stress-relieved condition. From this data, the TV-20 alloy appears attractive for use as fuel-element cladding material in that the alloy was at least as strong as Type 304 SS in the annealed condition and markedly stronger than Nb-1Zr, which had been considered until ruled out by sodium corrosion behavior.

Table XII

RESULTS OF ROOM-TEMPERATURE TENSILE TESTS ON 0.40-cm ID x 0.04-cm WALL (0.156-in. ID x 0.017-in. WALL) TUBING

Material	Average Ultimate Tensile Strength,[1] kg/mm^2 (psi x 10^{-3})		
	As drawn	Stress-relieved	Annealed
304 SS	92.9 (131.8)	-	59.9 (85.0)
Nb-1w/oZr	-	44.2 (62.7)	32.7 (46.4)
V-20w/oTi	88.7 (125.8)	67.4 (95.6)	62.4 (88.5)

[1]Average of three tests on V-20w/oTi and Nb-1w/oZr.
Average of two tests on 304 SS.

In addition to the tensile tests, room-temperature tube-burst tests were conducted on annealed tubing of Type 304 SS, Nb-1Zr, and TV-20. The results of the tests are shown in Table XIII. Here again, both the Type 304 SS and TV-20 tubing exhibited a marked improvement over the Nb-1Zr alloy, the TV-20 tubing being weaker than the stainless steel. While the data for the Type 304 SS and Nb-1Zr showed little scatter around the average burst pressure, data for TV-20 showed much greater scatter. The reason for this is not fully known, although tubing for this test was taken from material produced early in the tube fabrication program before tube fabrication procedures were fully developed. This tubing is undoubtedly inferior to later tubing produced after establishment of a proper fabrication sequence and delivered for actual irradiation testing.

Table XIII

HYDRAULIC TUBE BURST TEST RESULTS
FOR FULLY ANNEALED TUBING

Tubing Material	Tube Size, cm		Burst Pressure, kg/cm^2	Calculated[1] Hoop Stress, kg/cm^2
	ID	Wall		
304 SS	0.40	0.02	568	5,140
304 SS	0.40	0.02	574	5,170
304 SS	0.40	0.02	576	5,225
			Avg. 573	Avg. 5,180
Nb-1w/oZr	0.40	0.02	277	2,535
Nb-1w/oZr	0.40	0.02	273	2,540
Nb-1w/oZr	0.40	0.02	286	2,615
			Avg. 279	Avg. 2,565
V-20w/oTi (TV-20)	0.40	0.02	566	5,020
V-20w/oTi (TV-20)	0.40	0.02	464	4,070
V-20w/oTi (TV-20)	0.40	0.02	508	4,535
V-20w/oTi (TV-20)	0.40	0.02	474	4,040
V-20w/oTi (TV-20)	0.40	0.02	631	5,375
			Avg. 529	Avg. 4,610
V-20w/oTi (TV-20)	0.40	0.04	1,020	5,380
V-20w/oTi (TV-20)	0.40	0.04	1,058*	5,790*

*Tube did not fail at maximum test capability.
[1]Calculated from thick-wall tube formula.

The scatter in burst pressure may be real, but there remains a question as to the correlation between burst pressure and tube defects less than 10% of the wall thickness that constitutes minimum tube-quality standards.

While these tests were rather preliminary in nature and, more importantly, were not conducted at proposed reactor operation temperatures or after exposure to reactor environments (irradiation and sodium coolant corrosion effects), they provided additional data for determining the feasibility of the alloy as a potential cladding material.

More sophisticated tests are being conducted on the alloy, including elevated-temperature strength and creep data.

ACKNOWLEDGMENTS

The authors gratefully acknowledge the help of the following individuals: F. G. Foote and R. E. Macherey for their guidance and encouragement of the overall work; R. W. Bane, R. E. Telford, B. D. Holt, and J. P. Faris for analytical work on the alloy; J. Wing for neutron activation analysis on the precipitate; H. W. Knott and D. D. Zauberis for X-ray diffraction studies on the precipitate; and the technicians of the Foundry and Fabrication Group for their major efforts in the successful fabrication of the TV-20 alloy into the product form desired.

BIBLIOGRAPHY

1. W. P. Chernock, R. M. Mayfield, and J. Weir, Cladding Materials for Nuclear Fuels, 1964 Geneva Conference Paper A/Conf, 28/P/255, p. 7 (May 1964).
2. K. F. Smith and R. J. Van Thyne, Selected Properties of Vanadium Alloys for Reactor Application, ANL-5661 (May 1957).
3. D. Okrent, Nuclear Considerations in the Selection of Materials for Fast Power Reactors, Nuclear Metallurgy (AIME) 9, 1-56 (Nov 1963). See also - D. Okrent, Neutron Physics Considerations in Large Fast Reactors, Power Reactor Technology 7(2), 128-133 (Spring 1964).
4. H. A. Levin and S. Greenberg, Corrosion of Refractory Metal Alloys in Sodium (Unpublished report, 1963).
5. C. M. Walter and J. A. Lahti, Compatibility of U-Pu-Fz Fuel Alloys with Vanadium and Vanadium-Titanium Alloys, Trans. ANS 7(2), 406-407 (Nov 1964).
6. F. L. Yaggee and E. R. Gilbert, High-temperature Mechanical Properties of Refractory Metals (Unpublished report, 1963).
7. F. J. Karasek, Techniques for the Fabrication of Ultra Thin Metallic Foils, Nucl. Sci. Eng. 17, 365-370 (Nov 1963).
8. R. W. Fraser and J. A. Lund, Effect of Titanium Additions on the Low Temperature Behavior of Vanadium, Canadian Metallurgical Quarterly 1(1), 1-11 (July-Sept 1962).
9. J. E. Flinn, Jr., and R. M. Mayfield, Evaluation of New Fabrication Techniques for High Quality Refractory Metal Tubing, Tech. Conference on Applied Aspects of Refractory Metals (AIME), Dec. 9-10, 1963, Los Angeles, Calif. (To be published in Refractory Metals and Alloys III, Gordon and Breach Science Publishers.)
10. Paul Gordon, Microcalorimetric Investigation of Recrystallization of Copper, Trans. AIME 203, 1043 (1955).
11. Private communication: Union Carbide Corp. letter of July 16, 1964, to R. M. Mayfield, ANL.